MEASUREMENT OF CURRENT IN PULSED ELECTRON BEAMS

STEVEN N. ANASTASION
DONALD W. SENCENBAUGH

Library
U. S. Naval Postgraduate School
Monterey, California

Plant 158
8854

January 16, 1948.

Professor J. S. Newell,
Secretary of the Faculty,
Massachusetts Institute of Technology,
Cambridge, Massachusetts.

Dear Sir:

In accordance with the requirements for the Degree of Master of Science, we submit herewith a thesis entitled, "Measurement of Current in Pulsed Electron Beams".

Respectfully,

Steven N. Anastasion,
Lieutenant, U.S.N.

Donald W. Sencenbaugh,
Lieutenant, U.S.N.

Library
U. S. Naval Postgraduate School
Annapolis, Md.

January 15, 1948.

Professor J. E. Merrill,
Secretary of the Faculty,
Massachusetts Institute of Technology,
Cambridge, Massachusetts.

Dear Sir:

In accordance with the requirements for the Degree of Master of Science, we submit herewith a thesis entitled, "Measurement of Current in Pulsed Electron Beams".

Respectfully,

Steven N. Anastasion,
Lieutenant, U.S.N.

Donald W. Zeneseugh,
Lieutenant, U.S.N.

Library
U. S. Naval Postgraduate School
Annapolis, Md.

MEASUREMENT OF CURRENT IN PULSED ELECTRON BEAMS

by

Lieutenant Steven N. Anastasion, U.S.N.
B. S., U. S. Naval Academy, 1942
and
Lieutenant Donald W. Sencenbaugh, U.S.N.
B. S., U. S. Naval Academy, 1942

Submitted in partial fulfillment of the

requirements for the degree of

Master of Science

in

Electrical Engineering

at the

Massachusetts Institute of Technology

1948

Signatures of Authors: _____

_____

Department of Electrical Engineering, January, 1948.

Signature of Thesis Supervisor: _____

Signature of Chairman of
Department Committee on
Graduate Students: _____

Thesis
A44

DEMONSTRATION OF CONSTANT-K FILTERS ELECTRICAL ANALOG

by

Lieutenant Steven E. Anderson, U.S.N.
B. S., U. S. Naval Academy, 1962
and
Lieutenant Donald E. Sandenbergh, U.S.N.
B. S., U. S. Naval Academy, 1962

Submitted in Partial Fulfillment of the

Requirements for the Degree of

Master of Science

in

Electrical Engineering

at the

Massachusetts Institute of Technology

1964

Signatures of Authors:

_____

_____

Department of Electrical Engineering, January, 1964.

Signature of Thesis Supervisor: _____

Signature of Chairman of
Department Committee on
Graduate Students:

_____

TABLE OF CONTENTS

	Page
Title Page	i
Acknowledgment	ii
Abstract	iii
Table of Contents	iv
CHAPTER I	
Introduction	1
CHAPTER II	
Design and Construction	4
2. Requirements of the Linear System	5
3. The Accelerating Tube	6
4. Power Supply	9
5. Detector Housing	12
6. Detector Unit	13
7. Collector Plate and Glass Separator	15
8. Accelerating Voltage Supply and Associated Networks	16
9. Final Preparation	18
10. Review of Approximations	23
11. Recommendations for Future Work	25
CHAPTER III	
Associated Testing Apparatus	29
2. Radio Receiving Equipment	30
3. 50-Megacycle Oscillator	34
4. Receiver Calibration Oscillator	36
5. Receiver Calibration	38
References	40
Appendix I Theoretical Analysis of the Problem	41
Appendix II Constructional Drawings of the Detector Housing and Collector Plate	70
Appendix III Schematic Drawings of the Accelerating System together with the Circuit Details	78

TABLE OF CONTENTS

Page

Title Page 1

Acknowledgement ii

Abstract iii

Table of Contents. iv

CHAPTER I

Introduction 1

CHAPTER II

Basics and Construction 4

2. Magnetrons of the Linear Styrap . . . .
3. The Accelerating Tube 9
4. Power Supply 12
5. Deflector Housing. 12
6. Detector Unit 13
7. Collector Plate and Glass Separator . . . 15
8. Accelerating Voltage Supply and Associated Network 16
9. Final Preparation 20
10. Tuning of Klystrons. 23
11. Recommendations for Future Work 25

CHAPTER III

Associated Testing Procedure 29

2. Radio Receiving Equipment 30
3. 70-Megacycle Oscillator 34
4. Receiver Calibration Oscillator 36
5. Receiver Calibration. 38

Bibliography 40

Appendix I
Theoretical Analysis of the Problem 41

Appendix II
Construction Drawings of the Detector
Housing and Collector Plate 70

Appendix III
Schematic Drawings of the Associated
System together with the Circuit Details. . 78

TABLE OF CONTENTS
(Cont'd)

	Page
Appendix IV Photographs of the System	86
Appendix V Activation Schedule	91
Appendix VI Characteristics of Eveready Battery #493. . .	98

TABLE OF CONTENTS
(cont'd)

Page

Appendix IV
Functional Description of the System 36

Appendix V
Activation Schedule 91

Appendix VI
Characteristics of Tropical Battery Cell . . . 98

ACKNOWLEDGMENT

The authors of this thesis wish to express their sincere appreciation to Dr. Ivan A. Getting, Dr. J. E. Thomas, and Mr. J. S. Clark for their assistance and constructive criticism in conducting this work.

Acknowledgment

The authors of this thesis wish to express their sincere appreciation to Dr. Evan A. Swilling, Dr. W. E. Thomas, and Dr. J. S. Clark for their assistance and constructive criticism in conducting this work.

ABSTRACT

The basic problem under consideration was the investigation of the possibility of measuring the current and wave shape of the beam being accelerated in the M.I.T. synchrotron. To approximate the synchrotron conditions, a linear accelerator and detector system were designed and constructed. A pulsed beam was formed at the electron-gun end of the accelerator by driving the grid at 50 megacycles with a TBY-8 transmitter. The maximum acceleration possible with the system is 75,000 volts.

The accelerated pulsed beam was led through a cylindrical detector. The signal induced by the beam on the detector was led to an RDO receiver. The receiver output was calibrated to convert input to microvolts.

While the induced signals were observed on the receiver, they could not be used in a comparison with the theoretical analysis of the problem. The r-f radiations from the entire system to the receiver and detector were of such magnitude as to overdrive the receiver. Hence, there are some shielding problems to be considered before the system can be used to advantage.

ABSTRACT

CHAPTER I

INTRODUCTION

The concept of cross sections in the modern theory of nuclear physics and engineering is basic in the fundamental relations which form the foundations of this relatively new branch of science. Cross section may be considered analogous to the probability of an event occurring when a nuclear target is bombarded by a stream of high energy particles. More explicitly, it is defined as the fraction of particles in one square centimeter of the incident beam which causes a particular type event to occur within the target. For a given target material there will be values of cross section for the many types of events that may occur (absorption, capture, scattering, fission, various reaction processes), and for each material and each event there will be values of cross section over the entire range of energies to which it is possible to accelerate the bombarding particles.

The values of these various cross sections are determined largely by conducting numerous experiments. By examining the reactions which occur when a target is bombarded by a stream of nuclear particles of a definite energy, and also by examining the composition of the incident beam, it is possible to compute the value of cross section for the event being observed.

This method is convenient for particle accelerators whose beam is continuous and directed toward the target as it emerges

CHAPTER I

INTRODUCTION

at high energy from the accelerator. In the standard cyclotron, for example, the positive ions which are accelerated to 16 million electron volts are stopped and collected by a moderate thickness of metal and the beam is thus easily analyzed.

In the synchrotron, however, the particles are accelerated in bunches, each cycle of operation accelerating one bunch. Furthermore, the high energy bunch of electrons does not emerge from the synchrotron toward an external target. Rather, the bunch is directed toward a target within the accelerating tube. The result is a beam of high energy x-rays traveling in the direction of the incident electrons. These x-rays are directed toward a target placed external to the synchrotron for the investigation of nuclear phenomena.

Since the electrons are accelerated to 300 million electron volts in the MIT synchrotron, it would be impractical to attempt to analyze the beam by any method which would involve collection of the electrons. A suitable metallic collector to stop all the electrons at 300 mev would, of necessity, be at least several feet in thickness. However, the fact that the electrons are accelerated in bunches makes possible measurement by induction methods which are impossible with continuous beam accelerators.

In order to compute cross sections from synchrotron electron induced reactions, it is necessary to know the number of electrons being accelerated in each bunch and the dis-

ber of electrons being accelerated in each bunch and the dis-
ejection induced reactions, it is necessary to know the num-

In order to compute cross sections from ejection
measurement by interaction methods which are incompatible with
the ejections are accelerated in numbers extra possible
at least several feet in thickness. However, the fact that
to stop all the ejections at 300 mev would, of necessity, be
collection of the ejections. A suitable material collector
attempt to analyze the beam by any method which would involve
tron volts in the MIT synchrotron, it would be impractical to
synchrotron for the investigation of nuclear phenomena.

Since the ejections are accelerated to 300 million elec-
x-rays are directed toward a target placed external to the
traveling in the direction of the incident electrons. These
celerating tube. The result is a beam of high energy x-rays
farther, the beam is directed toward a target within the ac-
not emerge from the synchrotron toward an external target.
mum. Furthermore, the high energy beam of electrons does
ated in pancakes, each cycle of operation accelerating one
In the synchrotron, however, the particles are accelera-

mplexed.
modynamic phenomena of metal and the beam is then readily
to 16 million electron volts are stopped and collected by a
tron, for example, the positive ions which are accelerated
et high energy from the accelerator. In the standard cyclo-

tribution of the electrons in the bunch before it strikes the internal target. This, then, is the basic problem under consideration.

For this thesis, the problem undertaken was the construction of a system which would approximate the beam conditions of the synchrotron and which would make possible the determination of the pulse characteristics by suitable measurements. A system was designed which would make possible the measurement of the various harmonic components of the effect of a pulsed electron beam passing through a cylindrical detector. By a Fourier synthesis of these components, the pulse characteristics of the beam can be reconstructed.

CHAPTER II

DESIGN AND CONSTRUCTION

Before considering the design of the apparatus which was constructed to approximate the synchrotron beam conditions, it will be necessary to examine the phases of synchrotron operation which were considered in the design and which reveal the degree of approximation.

In the synchrotron, the electron bunches being accelerated are caused to travel in circular orbits in a doughnut-shaped tube by the presence of a strong magnetic field. The acceleration is accomplished by the action of a radio-frequency electric field applied at a point in the orbit. Each time the bunch passes through the field, an increment of energy is added to the total energy of the bunch until, as in the MIT synchrotron, for example, the total energy reaches 300 million electron volts. At this time, the magnetic field is disturbed and the electron bunch is directed toward the internal target.

By increasing the magnetic field in such a manner that the electron bunch is driven in synchronism with the accelerating field, the angular velocity of the bunch maintains a value fixed by the frequency of the accelerating voltage. Thus, the period at which the electrons pass a fixed point in the orbit is constant. Because of this, the radius of the orbit will increase in proportion to the linear velocity of the bunch. But synchrotron acceleration begins only after the bunch has been accelerated to 2 million electron volts, about 98 percent

MOTION AND CONSERVATION

of the speed of light, by the betatron principle of induction acceleration. During the remaining acceleration to 300 million electron-volts, at which energy the bunch will be traveling almost at the speed of light, the increase in radius will be only 2 percent. Thus, it may be assumed that the linear velocity of the bunch, and hence the radius of the orbit, remain fairly constant.

Under these conditions, then, a detector viewing the synchrotron bunch in rotation will be unable to distinguish it from a separate beam of electrons pulsed at a frequency corresponding to the angular velocity of the rotating bunch and led past the detector in the path of the bunch.

Since the radius of the synchrotron orbit is about 100 cm in the case of the MIT model, it will be possible to replace a 10 cm arc section at the orbit by a straight section of the same length. Now, the arrangement which will satisfy the conditions of the problem can be a linear one which eliminates the use of a large magnet to bend the electrons into a circular path.

2. Requirements of the Linear System.

The requirements for such a linear system may now be formulated. This system must provide for:

(1) Formation of a beam of electrons pulsed at a rate corresponding to the angular velocity of the electron bunches in the synchrotron. This corresponds to 50 megacycles in the case of the MIT synchrotron.

(2) Equal acceleration of the pulses through an accurately known voltage.

constantly known voltage.

(3) Total acceleration of the pulses through an
of the MIT klystron.

This corresponds to 30 megacycles in the beam
of the electron beam in the klystron.

[illegible] at the point corresponding to the highest velocity
electron-volts, at which velocity the beam will be traveling al-
most at the speed of light, the impulses in traces will be
only 6 percent. Thus, it may be assumed that the finest velo-
city of the group, and hence the profile of the output, remain
nearly constant.

Under these conditions, then, a detector viewing the
electrostatic beams in rotation will be unable to distinguish
it from a separate beam of electrons pulsed at a frequency
corresponding to the angular velocity of the rotating beam
and not past the detector in the path of the beams.

Since the radius of the electrostatic orbit is about 100 cm
in the case of the MIT model, it will be possible to replace a
10 cm section at the ends by a straight section of the same
length. Now, the arrangement which partially the monitors
of the protons can be a linear one which eliminates the use of
a large magnet to bend the electrons into a circular path.

2. Requirements of the linear system.

The requirements for such a linear system may come be
formulated. This system must involve four:

(1) Formation of a beam of electrons pulsed at
a rate corresponding to the highest natural
of the electron beams in the synchrotron.

(2) Total acceleration of the pulses through an
of the MIT klystron.

(3) A detector which can transmit the effect of the field of the pulsed beam to a receiver capable of separating the various components of the effect.

(4) A collector plate where the beam will terminate and from which it will be possible to determine the total charge flowing in the beam.

The remainder of this chapter describes the apparatus and associated components which were designed and constructed to meet the requirements set forth in this section.

3. The Accelerating Tube.

To form the electron beam, it was decided to use a modified 5RP DuMont cathode-ray tube. The type 5RP is a high-voltage tube incorporating very high overall accelerating voltages in several steps. The standard 5RP tube has three accelerating rings spaced along the main cylindrical surface of the tube between the electron gun and the fluorescent screen. It is designed for a maximum accelerating voltage of about 20,000 volts. Since it was desired to design the system for an accelerating voltage of at least 75,000 volts, it was necessary that the tube be lengthened somewhat and that more accelerating rings be added. In a conference with the Head of the Tube Engineering Department at the DuMont Laboratories in New Jersey, the problem was discussed and final plans were drawn for the tube. As constructed by DuMont under

(3) A detector which can transmit the effect of the field of the pulsed beam to a receiver capable of separating the various components of the effect.

(4) A collector plate where the beam will terminate and from which it will be possible to determine the total charge flowing in the beam.

The remainder of this chapter describes the apparatus and associated components which were designed and constructed to meet the requirements set forth in this section.

3. The Accelerating Tube.

To form the electron beam, it was decided to use a modified 5UP vacuum cathode-ray tube. The type 5UP is a high-voltage tube incorporating very high overall accelerating voltages in several steps. The standard 5UP tube has three accelerating rings spaced along the main cylindrical surface of the tube between the electron gun and the fluorescent screen. It is designed for a maximum accelerating voltage of about 20,000 volts. Since it was desired to design the system for an accelerating voltage of at least 75,000 volts, it was necessary that the tube be lengthened somewhat and that more accelerating rings be added. In a conference with the Head of the Tube Engineering Department at the General Laboratories in New Jersey, the problem was discussed and final plans were drawn for the tube. In construction all pieces under

the title "Synchrotron Tube", the length was increased from 17 inches to 27 inches and the number of accelerating rings was increased to six. While the 5-inch main body diameter was unchanged, the fluorescent screen at the end of the tube was left off to allow a wax seal connection of the tube to the rest of the system.

Since wax seals are used to interconnect all parts of the apparatus, a vacuum pump unit providing continuous evacuation was used (Drawing C-1052-I, Appendix 5). For this reason, the gun end of the tube was not closed off with the normal plug base. Instead, it was wax sealed with a glass cap to facilitate replacement of the filament and cathode. Replacement of these elements would be necessary if they were exposed to the atmosphere after activation in vacuum. The leads for the electrodes were brought out through the wax seal.

During the activation process, which will be given in detail later, it was found that the arrangement with the leads coming out through the wax seal was unsatisfactory. The first step of the activation process is to heat the gun to a very high temperature, by induction, in order to outgas the metallic electrodes. When this was done, it was found that there was sufficient heat conduction through the leads to melt the wax in the seal, destroying the vacuum which had been established. This difficulty could not be eliminated by water cooling, air cooling, or by liquid nitrogen cooling

Since wax seals are used to interconnect all parts of the apparatus, a vacuum pump unit providing continuous evacuation was used (Drawing E-1093-1, Appendix 3). For this reason, the gun end of the tube was not closed off with the normal glass bead. Instead, it was sealed with a glass cap to facilitate replacement of the filament and cathode. Replacement of these elements would be necessary if they were exposed to the atmosphere after activation in vacuum. The leads for the electrodes were brought out through the wax seal.

During the activation process, which will be given in detail later, it was found that the arrangement with the inside coating cut through the wax seal was unsatisfactory. The first step of the activation process is to heat the gun to a very high temperature, by ionization, in order to outgas the metallic electrodes. When this was done, it was found that there was sufficient heat conduction through the inside to melt the wax in the seal, destroying the vacuum which had been established. This difficulty could not be eliminated by water cooling, air cooling, or by liquid nitrogen cooling

the title "Speedotron Tube", the length was increased from 17 inches to 27 inches and the number of accelerating rings was increased to six. While the 9-inch main body diameter was unchanged, the flat-screen at the end of the tube was left off to allow a wax seal connection of the tube to the rest of the system.

applied outside of the tube. It was decided to alter the form of the glass cap to eliminate the necessity of having the leads come through the wax. The form of this new cap can be seen in Figure 1a. Figure 1b is a sketch of the original glass cap. With the new arrangement, no further difficulty was experienced during the activation process.

The form of the accelerating tube can be seen in the photographs of Appendix 6 and in the drawings of Appendix 5.

4. Power Supply (Drawing C-1052-C, Appendix 3).

In establishing the accelerating voltage over the entire system, there were two possibilities available since a center-tap-grounded accelerating voltage was to be used. If the positive half were used, the electron gun and power supply could be maintained at ground level. However, the entire system beyond the last accelerating ring would have to be maintained at the high positive accelerating voltage. The vacuum system, detector housing, receiver and collector plate would have to be operated well above ground, requiring an isolation transformer of considerable size. On the other hand, by using the negative half of the accelerating voltage source, as was done for this thesis, these units are operated at ground level while the electron gun and its power supply are maintained at the negative accelerating voltage with respect to ground (Figure 2). Since a suitable isolation transformer was not available for the power supply, a battery arrangement floated at the negative cathode potential was used.

applied outside of the room. It was desired to alter the
form of the flyer only to eliminate the possibility of having
the leads come through the wall. The form of this new cap
can be seen in Figure 7a. Figure 7b is a sketch of the
original flyer cap. With the new arrangement, no electro-
difficulty was experienced during the motivation problems.

The form of the repulsor-ring can be seen in the
photographs of Appendix C and in the drawings of Appendix D.

4. Power Supply (Drawing D-1054-C, Appendix D).

In reestablishing the accelerating voltage over the entire
system, there were two possibilities which arose: a double-
ended-grounded accelerating voltage was to be used. If the
positive half were used, the electron gun and power supply
could be maintained at ground level. However, the entire sys-
tem below the last accelerating ring would have to be main-
tained at the high positive accelerating voltage. The vacuum
system, detector mounting, secondary and deflector plate would
have to be operated well above ground, requiring an insulation
breakdown of considerable size. On the other hand, by using
the negative half of the accelerating voltage source, no new
problems would arise. The only problem encountered was that
(Figure 2). Since a suitable insulation transformer was not
available for the power supply, a Variac-transformer fluated
at the negative accelerating potential was used.

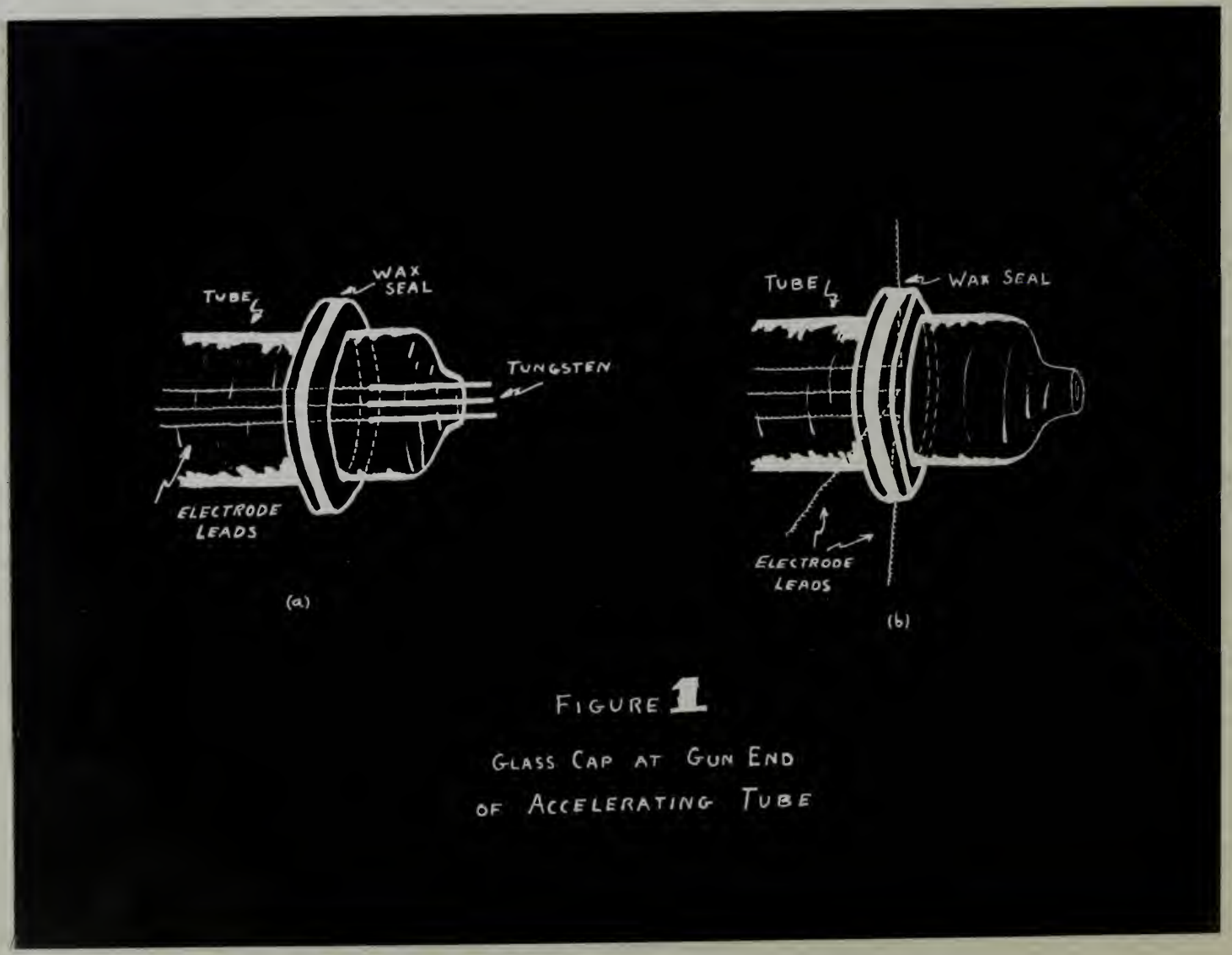

FIGURE 1

GLASS CAP AT GUN END OF ACCELERATING TUBE

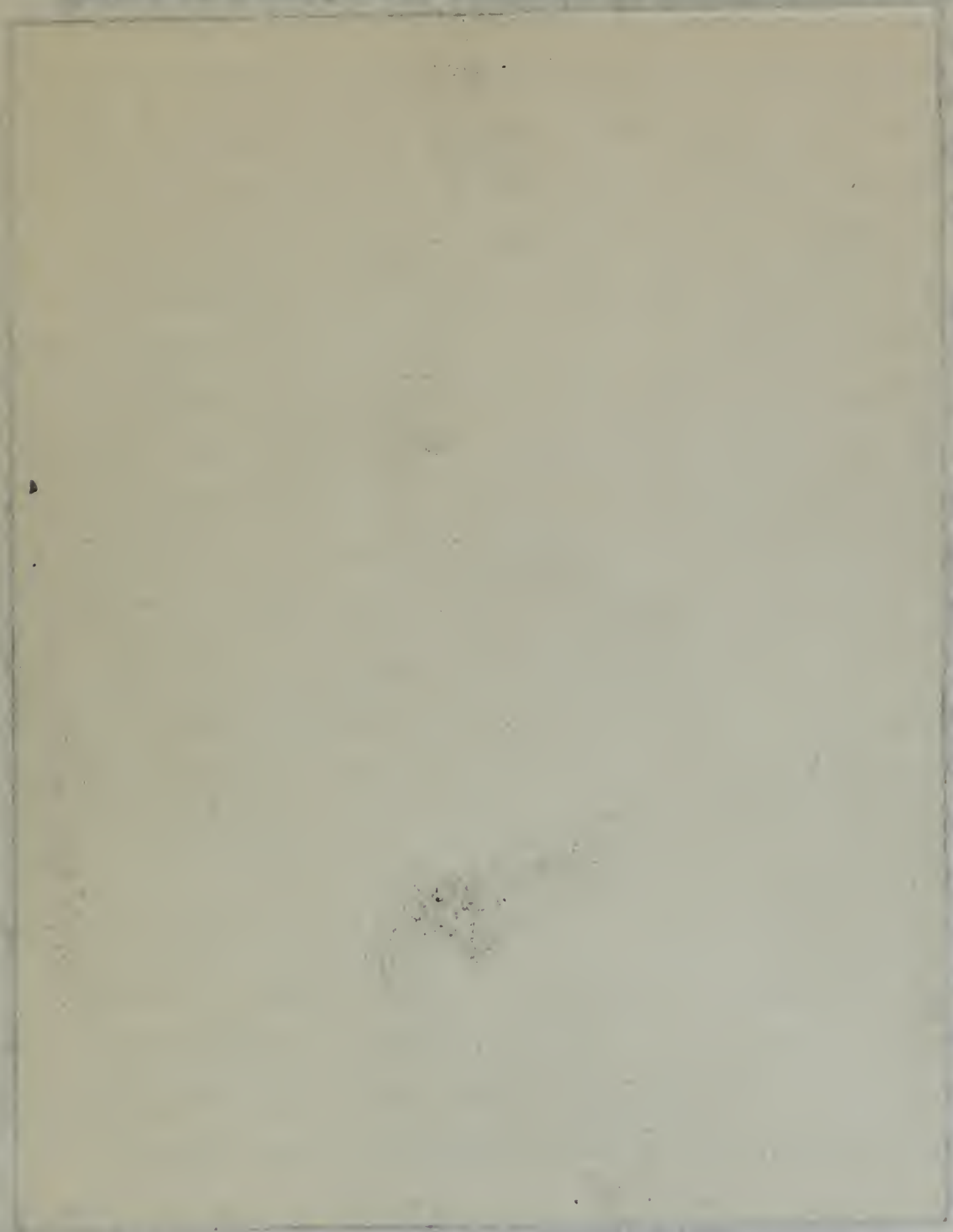

A voltage of about 2000 volts in conventional dry-cell batteries would result in a fairly large unit. Fortunately, a newly-developed and small 300-volt battery (Eveready 493) was available. Since these batteries are designed for very low current drain, the resistance network associated with the power supply was designed for a maximum current drain of about 40 microamperes. The resistance potentiometers used were those available and best suited to meet the conflicting requirements of maximum voltage variation of electrode potentials, minimum battery current drain, and small size of power supply. The characteristics of the Eveready 493 battery have been included as Appendix 6.

The overall design of the power supply is conventional. The voltage from the cathode to the deflection plates is 1800 volts. The grid bias available is 150 volts. Investigation of the typical grid drive characteristics of the tube shows that this voltage is more than sufficient to carry the electron gun into its cut-off region.

The condensers used between the electrodes serve to smooth the burst of current which would be drawn from the batteries if the beam current should hit the electrodes. Further, these condensers will also by-pass any radio-frequency current developed in the battery system by such contact.

Since the cathode is to be maintained at a large negative voltage, it was necessary to use an input condenser to the

a voltage of about 2000 volts is conventional tip-seal
instrument would result in a fairly large unit. Fortunately,
a nearly-developed and small 300-volt battery (Eveready 493)
was available. Since these batteries are designed for very
low current drain, the resistance network associated with the
power supply was designed for a maximum current drain of
about 40 microamperes. The resistance potentiometers used
were those available and best suited to meet the qualifying
requirements of maximum voltage variation of electronic pertinacity, minimum battery current drain, and small size of power
supply. The characteristics of the Eveready 493 battery have
been included as Appendix B.

The overall design of the power supply is conventional.
The voltage from the cathode to the deflection plates is
1800 volts. The grid bias available is 150 volts. Investigation of the typical grid drive characteristics of the type
shows that this voltage is more than sufficient to carry the
electron gun into its cut-off region.

The condensers used between the electrodes serve to
smooth the burst of current which would be drawn from the
batteries if the beam current should hit the electrodes.
Further, these condensers will also by-pass any radio-frequency
current developed in the battery system by sweep contact.

Since the cathode is to be maintained at a large negative voltage, it was necessary to use an input capacitor to the

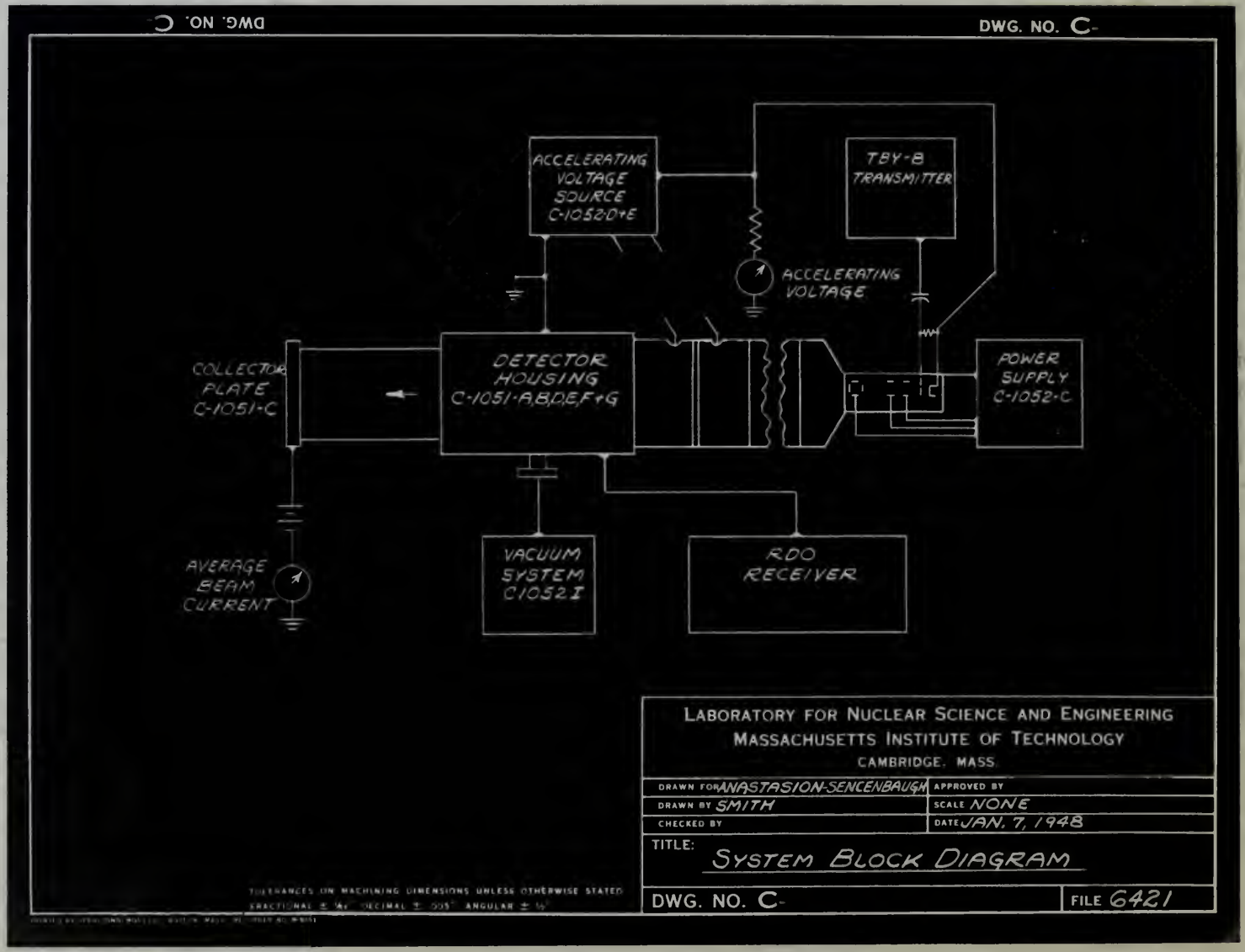
DWG. NO. C-
DWG. NO. C-
ACCELERATING VOLTAGE SOURCE C-10520-E
TBY-B TRANSMITTER
ACCELERATING VOLTAGE
COLLECTOR PLATE C-1051-C
DETECTOR HOUSING C-1051-A,B,D,E,F+G
POWER SUPPLY C-1052-C
AVERAGE BEAM CURRENT
VACUUM SYSTEM C1052I
RDO RECEIVER
LABORATORY FOR NUCLEAR SCIENCE AND ENGINEERING
MASSACHUSETTS INSTITUTE OF TECHNOLOGY
CAMBRIDGE, MASS.
DRAWN FOR ANASTASION-SENCENBAUGH
APPROVED BY
DRAWN BY SMITH
SCALE NONE
CHECKED BY
DATE JAN. 7, 1948
TITLE: SYSTEM BLOCK DIAGRAM
DWG. NO. C-
FILE 6421
TOLERANCES ON MACHINING DIMENSIONS UNLESS OTHERWISE STATED
FRACTIONAL ± 1/64" DECIMAL ± .005" ANGULAR ± 1/2°

Fig. 2.

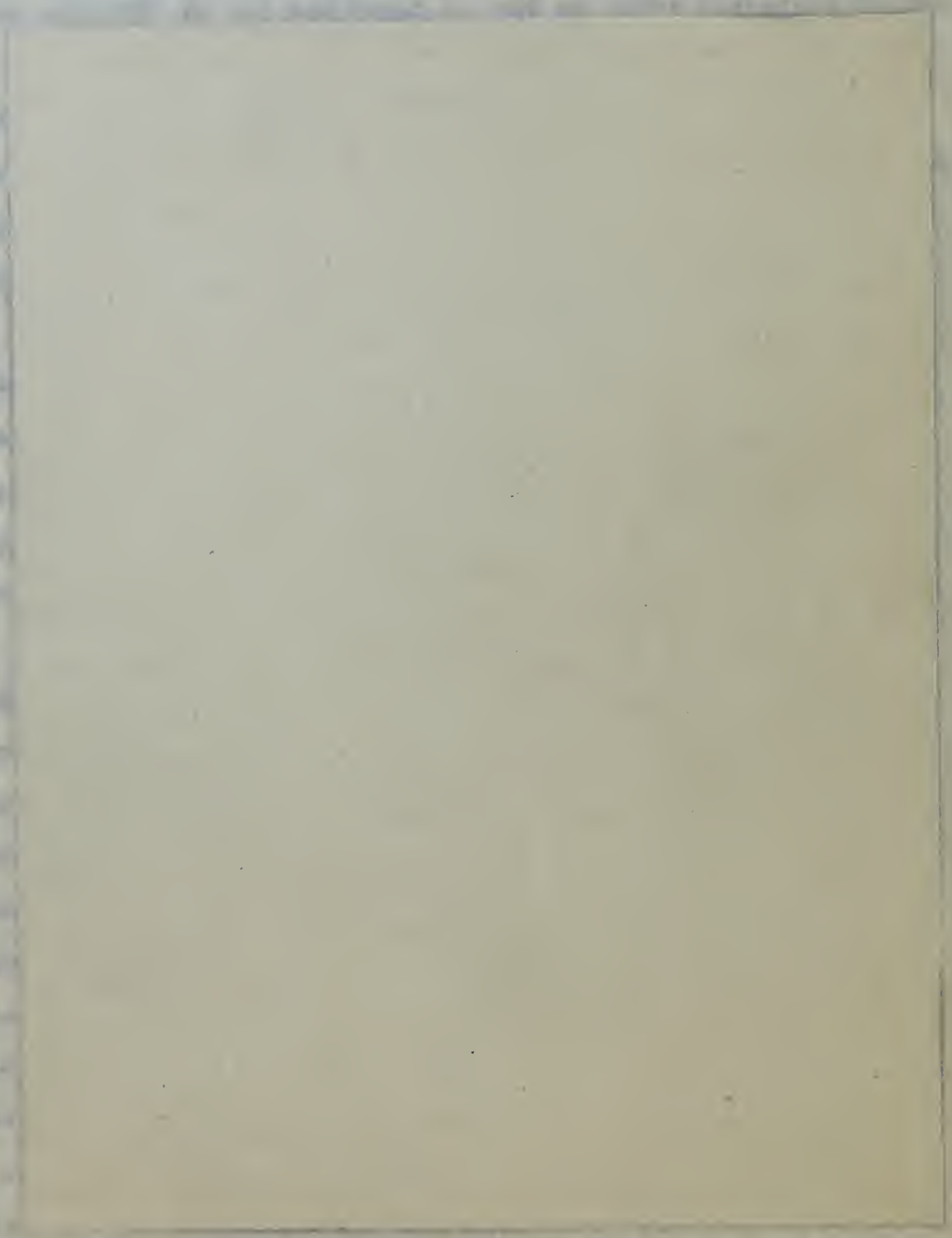

grid. By using four large condensers in series, a voltage rating of 80,000 volts was obtained with a capacity of 125 micromicrofarads. This rating is satisfactory for the highest accelerating voltage which may be applied to the system.

The filament supply for the electron gun was furnished by the x-ray apparatus, which also furnished the main accelerating voltage and will be described with that unit.

In order to prevent arcing over of the power supply at high voltages, a cylindrical corona shield was built to surround the supply unit. The open end of the corona shield extends over the gun end of the accelerating tube to cover the electrode leads. The shield is mounted on insulating porcelain blocks. In order to provide protection for the operating personnel, it is placed in position behind a metallic ground plane. The construction of these parts may be seen from the photographs in Appendix 4. The potentiometers controlling the electrode potentials are insulated by 12-inch bakelite rods. These rods are led out through the corona shield and ground plane for control by the operators.

5. Detector Housing.

The detector housing, as constructed, serves many purposes. Since the housing is maintained at ground potential, the electrons become completely accelerated as they enter the housing. The accelerating tube is connected to one end of

mounting. The accelerating tube is connected to one end of the aluminum housing which is maintained at ground potential, since the housing is maintained at ground potential, the aluminum becomes completely accelerated as they enter the tube. By using four large condensers in series, a voltage drop of 80,000 volts was obtained with a capacity of 1/5 microfarads. This rating is satisfactory for the highest accelerating voltage which may be applied to the system.

The filament supply for the electron gun was furnished by the X-ray apparatus, which also furnished the main accelerating voltage and will be described with that unit.

In order to prevent arcing over of the power supply at high voltages, a cylindrical corona shield was built to surround the supply unit. The open end of the corona shield extends over the gun end of the accelerating tube to cover the electrode leads. The shield is mounted on insulating porcelain blocks. In order to provide protection for the operating personnel, it is placed in operation behind a metallic ground plane. The construction of these parts may be seen from the photographs in Appendix A. The potentiometer controlling the electrode potentials are insulated by 12-inch bakelite rods. These rods are led out through the corona shield and ground plane for control by the operator.

5. Deflector Housing.

The deflector housing, as constructed, serves many purposes. Since the housing is maintained at ground potential,

the housing by a wax joint. In order to eliminate the possibility of shorting one of the accelerating rings to ground through the thin wax seal, the last ring was also connected to ground. As can be seen from the photographs in Appendix 4, the housing also supports the ionization gauge for determining the vacuum of the system. On the other end of the housing, the glass separator is also supported by a wax joint. Within the housing is contained the cylindrical detector itself, as shown in the sketch (Drawing C-1052-G, Appendix 3). In the walls of the housing are two kovar terminals placed diametrically opposite each other. One is connected to the detector itself and provides the signal input to the receiver from the voltage induced by the passing electron pulses. The other terminal is attached to the guard rings on each end of the detector. Through this terminal will pass the current of the electron beam should the electron beam be sufficiently off center to hit the guard rings.

6. Detector Unit.

The detector was made of cylindrical form, as seen in Drawings C-1052-F and G, Appendix 3. As stated in the previous section, the detector is connected to one of the kovar seals in the housing.

The theoretical analysis of this problem assumes that the detector under consideration is a section of an infinite cylinder. To approximate this condition in the physical

cylinder. To maximize this condition in the physical
the detector under consideration is a section of an infinite

The theoretical analysis of this problem assumes that
seals in the housing.

alone section, the detector is connected to one of the hoses
Dewetron D-102B-T and C, Appendix 3. As stated in the pre-

3. Detector Unit.

The detector was made of Pyrex tube, as shown in

the electron beam be sufficiently off center to hit the guard
ring.

terminal will pass the current of the electrons once should
the guard rings on each end of the detector. Through this
passing input to the receiver from the voltage induced by the
one is connected to the detector itself and provides the
passing electron pulses. The other terminal is attached to
lower terminals placed diametrically opposite each other.
D-102B-C, Appendix 3). In the wall of the housing are two
cylindrical detector itself, as shown in the sketch (Drawing
covered by a rea joint. Within the housing is contained the
either end of the housing, the glass separator is also sur-
flange for centering the ends of the system. On the
in Appendix C, the housing also supports the insulation
observed to rotate. As can be seen from the photographs
Second through the thin wax seal, the inal tube was also
possibility of shorting one of the counclecting rings to
the housing by a wax joint. In order to eliminate the

problem, a guard ring is placed at each end of the detector and maintained at a potential very nearly that of the detector itself.

The guard rings are held in position on each end by two snug-fitting cylindrical glass sections. In order to support and position the detector unit so that its axis coincides with the axis of the accelerating tube and the detector housing, two metal cradles were made. The cradles were made to fit the inside diameter of the housing and the outside diameter of the glass connectors. The cradles were soldered inside the housing with a separation such that the detector unit is supported at the glass cylinders.

The guard ring closest to the accelerating tube was made with a flange reducing the circular opening through the detector. The diameter of the opening was made such that the electron beam would pass completely through the detector unit, or if offset, would strike this ring rather than any part of the unit. The arrangement is shown in Figure 3.

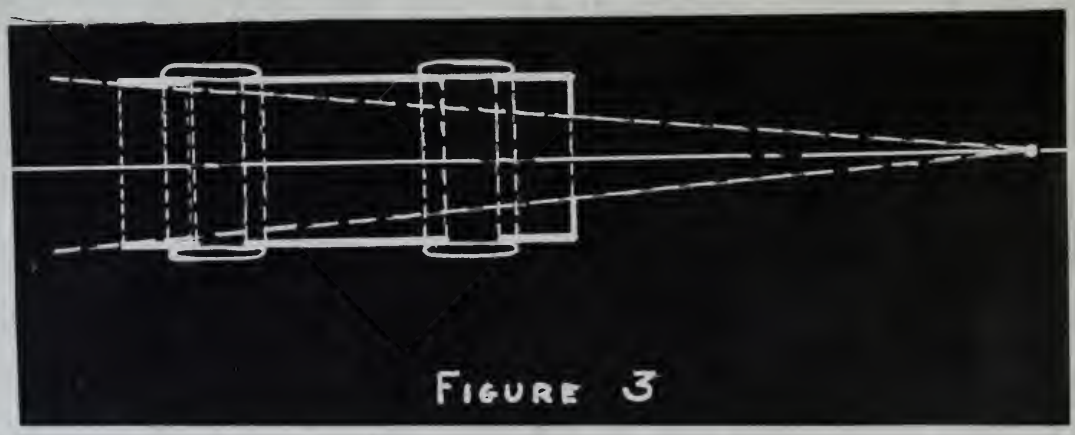

FIGURE 3

11254

Figure 3.

A microammeter has been placed in the guard ring circuit (Drawing C-1052-M, Appendix 3). By noting the magnitude of current which is flowing through this meter, it is possible to make rough corrections on the focus and deflection controls of the power supply in order that the beam be properly positioned through the detector.

7. Collector Plate and Glass Separator.

The electron beam which is formed in the accelerating tube, and which is being investigated, is terminated at a brass collector plate. The collector plate is insulated from the detector housing by a glass separator. The separator is connected to both metal parts by a wax joint. Since the electrons strike the plate with very high energies, there are secondary electrons emitted from the plate. To insure that these electrons will be recaptured by the collector, the plate is maintained 180 volts above the detector housing. Thus, the average current indicated by the ammeter in the collector circuit will actually be the average beam current unaffected by the secondary electrons. This average indication will serve to establish the absolute area under the pulse which is synthesized by adding the various harmonic components of the beam as measured by the receiver.

11254

The high energy beam striking the brass plate will produce x-rays traveling in the direction of the beam. For this reason, the collector end of the accelerating system was surrounded by a lead box. According to reference (4), 75 kilovolt

7. Collector Plate and Glass Chamber.

The electron beam which is formed in the accelerating tube, and which is being investigated at a given collector plate. The collector plate is insulated from the detector housing by a glass separator. The separator is connected to both metal parts by a wax joint. Since the electrons strike the plate with very high energies, there are secondary electrons emitted from the plate. To insure that these electrons will be recaptured by the collector, the plate is maintained 180 volts above the detector housing. Thus, the average current indicated by the ammeter in the collector circuit will actually be the average beam current modified by the secondary electrons. This average location will serve to establish the absolute zero under the pulse which is established by adding the various increments of the beam as measured by the precision.

The high energy beam striking the brass plate will produce x-rays traveling in this direction at the beam. For this reason, the collector and of the accelerating system are surrounded by a lead box. According to reference (4), 75 kilovolt

x-rays will be reduced to 5% of their original strength after passing through a lead wall of 0.0394 inches. To provide a suitable safety factor, the lead box walls were made 0.125 inches thick.

The collector plate was coated with a thin layer of zinc ortho-silicate which fluoresces, at the point of incidence of the electron beam. Since the collector plate can be viewed through the glass separator, there exists now a very efficient method of positioning the electron beam.

The details of the collector plate and collector end assembly can be seen from Drawing C-1051-C in Appendix 2, and Drawing C-1052-H in Appendix 3.

8. Accelerating Voltage Supply and Associated Networks.

The voltage used to accelerate the electron bunches is obtained from a 150 kilovolt Westinghouse X-Ray unit. As stated previously, the unit presents a center-tapped output, of which only the negative half is used. The negative voltage is applied to the cathode via the corona shield, and the detector housing is maintained at ground. Accelerating voltages from 15 to 75 kilovolts are available.

The open circuit voltage of the x-ray apparatus is half-wave rectified at sixty cycles, and as such it is unsuitable for continuous acceleration. To provide a direct voltage for acceleration, the output was applied to the system across an RC network providing a time constant of

system without an HV network providing a time constant of
voltage for observation. The output was applied to the
multiple rate operation. To provide a direct-
half-wave rectified AC static system, but is most if is un-
X-rays will be reduced to 1/e of their original strength after
passing through a lead wall of 0.034 inches. To provide a
minimum safety factor, the lead wall were made 0.125
inches thick.

The collector plate was coated with a thin layer of
zinc orthosilicate which fluoresced, at the point of inci-
dence of the electron beam. Since the collector plate can
be viewed through the glass envelope, there exists now a
very efficient method of positioning the electron beam.

The details of the collector plate and collector and
assembly can be seen from Drawing C-1091-C in Appendix B, and
drawing D-1092-A in Appendix B.

8. Accelerating Voltage Supply and Associated Networks.

The voltage used to modulate the electron beams
is obtained from a 150 kilovolt Cockcroft-Walton unit. As
stated previously, the unit presents a center-tapped output,
of which only the negative unit is used. The negative
voltage is applied to the cathode via the coarse shield, and
the detector housing is maintained at ground. Accelerating
voltages from 15 to 75 kilovolts are available.

The open circuit voltage of the X-ray machine is
half-wave rectified AC static types, but is most if is un-
suitable for continuous modulation. To provide a direct-

4.18 seconds, sufficient to smooth out the sixty cycle rectified voltage.

Included in this RC network is a calibrated resistance of 60 megohms in series with an ammeter. This branch is shunted across the entire system to enable an accurate measurement of the accelerating voltage.

A simplified wiring diagram of the x-ray apparatus is given in Drawing C-1052-D, Appendix 3. The accelerating system schematic is given in Drawing C-1052-E, Appendix 3.

Use was made of the filament transformer of the inoperative x-ray tube to provide filament voltage for the accelerating tube at the negative potential level of the cathode. An ordinary variac was used at the input to this transformer, as can be seen in Drawing C-1052-D, Appendix 3.

9. Final Preparation.

The complete system in various stages of assembly can be seen in the photographs of Appendix 4. Copper tubing instead of wire lead was used at the high-potential levels as a precaution against corona.

With the assembly complete, the accelerating voltage was turned on at 15 kilovolts and gradually increased to 60 kilovolts. No corona was evident anywhere in the accelerating system proper. At 30 kilovolts and higher, however, some corona was observed at the output terminal of the x-ray apparatus. Its effect was checked on the receiver and found to be negligible after the initial turning-on transient had subsided.

Radio-frequency radiations from the grid-input condensers had considerable effect on the receiver indications. To eliminate this condition, the condensers were placed in a large grounded metal box. The signal was then led to the grid from the condensers via a coaxial cable whose shield was maintained at the cathode potential. In addition, an r-f path to ground from the corona shield was provided through a 0.0009 microfarad condenser. This condenser was also placed in the metal box. Since the radio-frequency by-pass condenser will shunt the accelerating voltage bleeder, the time constant of that network will now be increased over the value previously given, thereby serving to smooth out further the accelerating voltage.

9. Final Procedure.

The complete system in various stages of assembly can be seen in the photographs of Appendix A. Copper shield instead of wire lead was used at the high-potential leads as a precaution against corona.

When the assembly complete, the accelerating voltage was turned on at 15 kilovolts and gradually increased to 60 kilovolts. No corona was evident anywhere in the accelerating system proper. At 50 kilovolts some light, however, some corona was observed at the output terminal of the 3-kV eliminator. Its effect was checked on the Tricolvac and found to be negligible after the initial bursting-on transient had subsided.

Radio-frequency radiation from the high-input condenser had considerable effect on the receiver indications. To eliminate this condition, the condenser was placed in a large grounded metal box. The signal was then led to the grid from the condenser via a coaxial cable whose shield was maintained at the cathode potential. In addition, an F-7 path to ground from the corona shield was provided through a 0.005 microfarad condenser. This condenser was also placed in the metal box. Since the radio-frequency by-pass condenser will annul the accelerating voltage ripple, the time constant of that network will not be increased over the value originally given, thereby serving to smooth out further the accelerating voltage.

In providing this shield, the first available box was used. The physical dimensions of this box and the condensers within now restrict the maximum accelerating voltage which can be applied to the system to about 30 kilovolts. Hence, if it is desired to work with the system at itx maximum voltage rating, the shield for the input condensers must be modified.

Before the accelerating tube could be used, it was necessary to activate the cathode unit of the electron gun. A complete activation schedule was forwarded by DuMont for placing the tube into operation. Also forwarded was a circuit for providing the proper grid potential during the activation period. Since continuous evacuation was used with this system, it was not necessary to use a getter or to "tip off" the tube. The instructions forwarded by DuMont, together with the activation schedule used and the circuit of the positive grid activation unit as simplified, have been included as Appendix 5.

Since no induction furnace was immediately available for bombarding the metallic components of the gun, an activation was tried without bombarding. Although the schedule was carried through twice, the attempt to produce an electron beam was unsuccessful. Although it was believed at that time that the cathode might have been poisoned by the oil vapor from the oil diffusion pump, another activation was tried, this time with the aid of a "bombarder" borrowed

In providing this shield, the first available box was used. The physical dimensions of this box and the coverage were within new restraint the maximum accelerating voltage which can be applied to the system to about 30 kilovolts; hence, if it is desired to work with the system at its maximum voltage rating, the shield for the input condensers must be modified.

Before the accelerating tube could be used, it was necessary to activate the cathode unit of the electron gun. A complete activation schedule was forwarded by Dumont for placing the tube into operation. Also forwarded was a circuit for providing the proper grid potential during the activation period. Since continuous evacuation was used with this system, it was not necessary to use a getter or to "zip off" the tube. The instructions forwarded by Dumont, together with the activation schedule used and the circuit of the positive grid modification unit as simplified, have been included as Appendix 3.

Since no induction furnace was immediately available for boosting the metallic components of the gun, an activation was tried without boosting. Although the schedule was carried through twice, the attempt to produce an electron beam was unsuccessful. Although it was believed at that time that the cathode might have been poisoned by the oil vapor from the oil diffusion pump, another activation was tried, this time with the aid of a "booster" borrowed

from the M.I.T. Research Laboratory of Electronics. The first few attempts at bombarding proved that the original glass cap and wax seal at the end of the tube were unsatisfactory, as has been stated previously. When the new cap was used, the bombardment was carried out without difficulty.

Upon completion of this activation, the power supply was installed to form the electron beam. Even with 15,000 volts applied to the system, there appeared to be no emission from the cathode. This cathode was removed and was found to have a small portion of its emission surface remaining. The remaining oxide-coated surface was black, due to the oil which had diffused throughout the system.

Another cathode and filament were installed and the activation repeated. This time, some emission was observed during the activation process, but no beam could be formed with the power supply and accelerating voltage applied. This cathode was also removed and upon examination was found to have a small dark spot over the emission surface, about the size of the grid hole.

The entire system was dismantled and thoroughly cleaned. Each part was washed in CCl_4, alcohol, and ether. An oil trap was installed between the diffusion pump and the overflow tank and the system was reassembled. This trap is not shown in Drawing C-1052-I, Appendix 3. Another cathode was installed in the gun and the activation repeated. Now, an emission current of 28.5 milliamperes was noted on the posi-

from the M.I.T. Research Laboratory of Electronics. The first few attempts at manipulating proved that the original plans for mounting the switch on the panel were poor, the mechanism was carried too strongly. Once the new location was fixed on the rear of the inner aperture panel, as the case turned previously. Once the new design was used, the mechanism worked perfectly.

Upon completion of this operation, the power supply was installed to furnish the ejection surge. Less than 15,000 volts applied to the system, tests indicated it to be adequate for the purpose. This capacity was reduced and was found to have a small portion of its radiation multiple voltage. The resulting glow-coated surface was black, due to the oil which had filtered through the glass.

Another defense was finally carried out the activation temperature. This time, some moisture was observed during the activation process, but no harm occurred as long as the high vacuum was maintained with this above. This operation was also repeated and some condensation was found to have a small dark spot over the emission surface, about the size of the grid mode.

The entire system was dismantled and thoroughly cleaned. Each part was washed in CCl$_4$, alcohol, and ether. An oil free was installed between the diffusion pump and the manifold. This was the system was reassembled. This can is not shown in Drawing C-1333-I, Assembly 3. Another antenna was installed in the rear and the activation repeated. Now, no moisture current of 10^{-7} milliamperes was noted on the pos-

tive grid activation unit. When the power supply and accelerating voltage (15,000 volts) were applied, a beam was detected on the fluorescent coating. The current in the beam, however, was so small that it could not be detected on a 0-100 microammeter. It was centered fairly well by the deflection plates but could not be focused properly. Since the best focus was obtained with the focus voltage low, the entire focus assembly in the power supply was moved 300 volts closer to the cathode. This change is not shown in the power supply circuit diagram.

While the beam could be obtained with the high accelerating voltage applied, no beam could be formed with the power supply alone, even though an emission of 2.2 milliamperes was observed with the grid maintained at 45 volts positive. In an attempt to produce the beam with the power supply alone, an auxiliary power supply was inserted between electrodes A1 and A2. Although the DuMont catalogue gave a maximum voltage to A2 of 4000 volts, there was a breakdown of insulation between A1 and A2 at 3000 volts on A2.

In a telephone conversation with the tube engineers at the DuMont Laboratories in New Jersey, it was learned that the activation schedule which they had sent was in error in that there should have been no bombardment or heating of the gun structure included.

Fortunately, a tube quite similar to the "Synchrotron" tube had been built by DuMont for Dr. W. H. Bostick at the

tube had been built by Dumont for Dr. V. K. Zworykin at the Princeton laboratories in New Jersey, it was learned that the activation schedule which they had been in error in that tube should have been no departure or inserting of the rom structure involved.

Fortunately, a tube quite similar to the "Iconoscope" was available, and when the power supply was adjusted for the rated voltage (12,000 volts) were applied, a beam was detected on the fluorescent coating. The current in the beam, however, was so small that it could not be detected on a D-C0 electrometer. It was ascertained fairly well by the deflection plates but could not be focused properly. Since the best focus was obtained with the focus voltage low, the anodic focus assembly in the level supply was moved 500 volts closer to the cathode. This change is not shown in the power supply circuit diagram.

While the beam could be obtained with the high accelerating voltage applied, no beam could be formed with the power supply alone, when through an emission of 2.5 milliamperes was observed with the grid maintained at 45 volts positive. In an attempt to produce the beam with the power supply alone, an auxiliary power supply was inserted between electrodes G1 and G2. Although the Dumont oscilloscope have a maximum voltage to G2 of 4000 volts, there was a breakdown of insulation between G1 and G2 at 3000 volts on G2.

In a telephone conversation with the tube engineers at the Dumont laboratories in New Jersey, it was learned that tubes should have been de-gassed or heated of the activation schedule which they had been in error in that tube.

Research Laboratory of Electronics. With his consent, this tube was modified to fit the designed accelerating apparatus. The activation schedule was carried through on this tube. The emission readings for this activation were the best obtained and have been included in Appendix 5.

The power supply and accelerating voltage (15,000 volts) were applied and the filament voltage was set at 8 volts. An electron beam of 45 microamperes at zero grid bias was measured on the collector plate. The deflection plates, focusing control and guard rings were quite effective in producing a fairly sharp beam.

With the transmitter turned on, the induced effects from the detector were observed on the receiver. However, the receiver was being overdriven by radiations from the accelerating system and the observations were not significant.

There still remains some work on shielding before accurate measurements can be taken. Since considerable pick-up was observed on the receiver even with no direct input, it is necessary that the receiver itself be very carefully shielded. Also, it is necessary that the detector housing be modified to shield the detector from radiations from the grid.

Research Laboratory of Electronics. With this document, this tube was modified to fit the desired accelerating potentials. The modulation schedule was carried through on this tube. The radiation readings for this modification were the best obtained and have been included in Appendix J.

The power supply and accelerating voltage (12,000 volts) were applied and the filament voltage was set at 8 volts. An aperture plate of 45 microseconds at zero grid bias was measured on the oscilloscope plate. The deflection plates, focusing control and guard rings were quite effective in producing a fairly sharp beam.

With the transmitter turned on, the impulse pulses from the detector were observed on the receiver. However, the receiver was being overdriven by reflections from the associated system and the observations were not satisfactory.

There still remains some work on matching before accurate measurements can be taken. Since equivalent pick-up was observed on the receiver when with no direct input, it is necessary that the receiver itself be very carefully shielded. Also, it is necessary that the detector crystal be modified to match the characteristics from the grid

10. Review of Approximations.

In reviewing the results obtained by this system, the many approximations which were made should be kept in mind. It was pointed out earlier that the synchrotron acceleration began with the electrons already traveling at a speed of about 97 percent of the speed of light and at a corresponding energy of 2 million electron volts. Thus, the main relativistic change which occurs in the subsequent acceleration to 300 million electron volts is in the mass of the electrons. In the adaptation of a similar system directly to the synchrotron, the effects of increasing orbit radius, increasing linear velocity, and changing pulse shape with acceleration will be small.

It is possible to minimize these effects so that the linear measurements taken will more closely fit the conditions of the synchrotron. This can be done by substituting for the right circular cylindrical detector used in this case, one which has the form of a section of the accelerating tube, as shown in Figure 4.

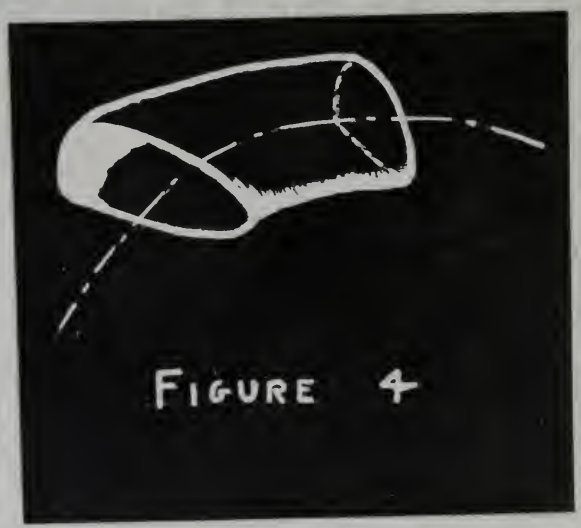

FIGURE 4

10. Design of accelerators.

In designing the results obtained by this system, the many considerations which must be made should be kept in mind. It was pointed out earlier that the synchronous acceleration began with the electrons already traveling at a speed of about 97 percent of the speed of light and at a corresponding energy of 2 million electron volts. Thus, the main relativistic change which occurs in the subsequent acceleration to 200 million electron volts is in the mass of the electrons. In the adaptation of a similar system directly to the synchrotron, the effects of increasing orbit radius, increasing linear velocity, and changing pulse shape with acceleration will be small.

It is possible to minimize these effects so that the linear accelerator taken will more closely fit the conditions of the synchrotron. This can be done by substituting for the right circular cylindrical detector used in this case, one which has the form of a section of the accelerating tube, as shown in Figure 9.

With this detector, any radial movement of the bunch caused by an increase in the velocity of the bunch would be compensated for by an increase in the path of travel of the bunch through the detector, thus keeping constant the time of travel of the bunch within the detector.

Although the system has been designed for a maximum pulse acceleration of only 75,000 volts, there will be sufficient evidence of the relativistic variation of the field shape even at this relatively low voltage to enable one to confirm the effects predicted by theory at much higher energies.

One characteristic of the bunch in rotation in the synchrotron has been completely neglected in this analysis since it occurs only in a system which accelerates the electrons in a circular path. It has been found that electrons traveling in circular paths at velocities close to the speed of light radiate as electromagnetic waves some of the energy which they are given during acceleration. At 300 million electron volts, the final energy of the electrons in the MIT synchrotron, the velocity of the bunch will be almost exactly that of the speed of light. Hence, it is quite certain that these radiations will occur, and that they will have an effect on the detector indications. It is not possible to predict the effect of such radiations by any measurements taken with the linear system. Investigations of this radiation must be made at the synchrotron when it has been completed.

plated.

tion must be made of the characteristics it has been com-
taken with the linear system. Corresponding of data must-
predict the effect of such conditions by any measurements
fect on the focusing functions. It is not possible to
there predictions will occur, and thus they will have an ef-
that of the speed of light. Hence, it is quite certain that
chronotron, the velocity of the bunch will be almost exactly
eleven volts, the final energy of the electrons in the KEW
which they are given during acceleration. At 300 million
of light particle as electromagnetic waves some of the energy
traveling in circular paths at velocities close to the speed
tered in a circular path. It has been found that electrons
tion it occurs only in a system which accelerates the elec-
chamber has been completely neglected in this analysis
ergies.

One characteristic of the bunch in motion in the
conflict the effects predicted by theory at such highest
ficient evidence of the relativistic variation of the field
sible even at this relatively low voltage to modify and to
pulse acceleration of only 75,000 volts, there will be suf-
Although the system has been designed for a maximum

travel of the bunch within the betatron.

through the betatron, thus keeping constant the time of
ated for by an increase in the path of travel of the bunch
by an increase in the velocity of the bunch would be accompan-
ction path dynamics, any radial movement of the bunch caused

11. Recommendations for Future Work.

It might be well to consider some modifications and additions to the apparatus which would facilitate future work. As stated previously, the battery type power supply for the accelerating tube was used to take advantage of the material immediately at hand, and to expedite construction. While satisfactory as a power supply, it is inconvenient in several respects. Since the batteries are designed for very small drain at an intermittent use of two hours per day, the research time per day will be small unless many of these batteries are available. Use of other batteries with more suitable drain characteristics, and with the same total voltage, would result in a much larger power supply. A more suitable arrangement would be to procure a suitable step-up transformer to be used in conjunction with the x-ray tube filament isolation transformer. Using this transformer with suitable electric circuit elements to provide the proper direct voltages would eliminate the necessity of entering the corona shield to disconnect each part of the power supply to reduce current drain through the batteries during delays in operation.

Some thought might be given to the application of a suitable oscilloscope to the collector plate. If a sufficiently fast sweep could be found, it would be possible actually to see the shape of the pulse which passes through the detector.

the motor.

especially to use the piston motion because changing electric lead wires would be tiresome. It would be possible to have a multiple position switch in the circuit. If a multiple position switch is used, some thought ought to be given to the application of a resistance in the circuit to reduce current drain through the potentiometer during delays in operation.

The power supply should be rated at the power requirements of the motor. Since the potentiometer is a power multiplier, it is recommended to maximum sensitivity immediately at hand, and to eliminate construction. While operation is not a power multiplier, it is recommended to maximum sensitivity. Since the potentiometer is

Also, a receiver would be useful at the collector plate. By using as its input the voltage developed by the beam current across a suitable impedance, the actual Fourier components of the beam current could be measured and compared directly to the induced detector indications.

However, with the system as thus constructed, it is possible to adapt the equipment for the investigation of many problems. For the problem of electron induced cross sections, for example, the possible advantage of using other types of detectors in the determination of pulse characteristics can easily be investigated merely by replacing the cylinder in the housing by any other type detector.

Closely allied with this problem are the many classical academic problems dealing with moving charges through and past suitable detectors. The analytic results of all such problems may be confirmed experimentally. As before, any type detector may be used with any type beam which can be produced by suitable modulation of the grid of the accelerating tube.

The most important recommendation for future work with this equipment, beyond that of investigating the pulse characteristics, is that which deals with a possible modification of synchrotron operation. If the relations which determine the action of a charged particle in the synchrotron are investigated, they will reveal the fact that the ratio of the magnetic field to the electric field frequency must

of the magnetic field to the electric field fluctuating most are interesting, they will prevent the fact that the ratio deteriorates the action of a detector particularly in the admittance characteristics, in that which deals with a possible modification of electronic operation. If the variations which exist between a multiple impedance, the actual functional ones of the beam current should be measured and compared directly to the induced detector impedance.

However, with the system as thus constructed, it is possible to adapt the equipment for the investigation of many problems. For the purpose of electron induced grain emissions, for example, the possible advantage of using either types of detectors in the determination of pulse characteristics can easily be investigated merely by replacing the collector in the housing by any other type detector.

Closely allied with this problem are the many physical semiconductor problems dealing with scoring discharge and heat sensible detectors. The analytic complete of all such problems may be continued indefinitely. In brief, any type detector may be used with any type beam which can be produced by suitable modification of the grid of the accelerating tube.

The most important recommendation for future work with this equipment, beyond that of investigating the pulse characteristics, in that which deals with a possible modification of electronic operation. If the variations which

bear a definite relation to the product of the radius of the particle orbit and the relativistic mass of the particle. In the electron synchrotron, the electric field is maintained at a constant value while the magnetic field is increased in such a manner as to balance the relativistic increase in the mass of the particle with acceleration, while the orbit radius increases in proportion to the velocity of the particle, and the angular velocity of the particle remains in phase with the electric field frequency. Since synchrotron acceleration of the electron bunch begins at 2 million electron volts (0.97 x velocity of light), there is little overall increase in orbit radius during the subsequent acceleration to 300 million electron-volts. In the case of the proton synchrotron which is being considered at Brookhaven, the case is somewhat different, due to the fact that the rest mass of the proton is some 1800 times as large as the rest mass of the electron. Thus, even if accelerated to an energy of 1100 million electron-volts, the protons will possess a velocity of only one-half of the speed of light. During the acceleration of the protons to the proposed 10 billion electron-volts, therefore, there would be considerable increase in orbit radius, requiring a larger magnet than for a corresponding electron synchrotron. The radius, however, can be maintained at a fixed value throughout the entire accelerating cycle by varying both the magnetic field and the electric field frequency. Since the relation between these quantities

beer a definite relation to the product of the motion of the particle orbit and the relativistic mass of the particle. In the electron synchrotron, the electric field is maintained at a constant value while the magnetic field is increased in such a manner as to balance the relativistic increase in mass of the particle with acceleration, while the orbit radius increases in proportion to the velocity of the particle, and the angular velocity of the particle remains in phase with the electric field frequency. Since synchrotron acceleration of the electron begins at 2 million electron volts (0.97 x velocity of light), there is little material increase in orbit radius during the subsequent acceleration to 300 million electron-volts. In the case of the proton synchrotron which is being considered at BROOKHAVEN, the case is somewhat different, due to the fact that the rest mass of the proton is some 1800 times as large as the rest mass of the electron. Thus, even if accelerated to an energy of 1100 million electron-volts, the proton will possess a velocity of only one-half of the speed of light. During the acceleration of the protons to the proposed 10 million electron-volts, therefore, there would be considerable increase in orbit radius, requiring a larger magnet than for a synchronizing electron synchrotron. The result, however, can be obtained at a fixed value throughout the entire accelerating cycle by varying both the magnetic field and the electric field frequency. Since the relation between these quantities

must be maintained for proper acceleration, some means of synchronizing their variation must be found. Such synchronizing action is possible if the deviation of the proton bunch from the chosen orbit can be readily detected.

One method of locating accurately an electron beam offset by the deflection plates of the tube requires a reconstruction of the collector plate. By reconstructing the plate so that it holds many terminals distributed over the plate, the beam can be located by detecting it on one of these terminals. The detector in its housing can then be used to compare the signal obtained from the offset beam with the signal from the beam which was sent down the centerline of the tube. Again, in this problem as in the first, it is simple to adapt the apparatus for the investigation of the optimum offset indication by use of many types of detectors.

types of deflection.

Portion of the optimum effect introduction by use of many first, it is simple to adapt the apparatus for the investigation of the tube. Again, in this problem as in the with the signal from the beam which was sent down the used to compare the signal obtained from the offset beam these instruments. The detector in its housing can then be plate, the beam was located by detecting it on one of plate so that it holds only terminals distributed over the combination of the collector plate. By rearranging the others by the deflection plates of the tube requires a re-

One method of locating accurately an electron beam through from the chosen orbit may be readily detected. relative motion is possible if the certation of the proper synchronizing their variation must be found. Such electro- must be maintained for proper acceleration, some source of

CHAPTER III

ASSOCIATED TESTING APPARATUS

The problem under investigation is the measurement of current in a pulsed electron beam. The number of coulombs in a bunch of electrons passing through a cylindrical detector on its axis is to be deduced from the voltage induced on the detector.

Hence, measurements will be made of small induced voltages having a frequency of 50 megacycles, and harmonics of that frequency. The reason for making measurements at these selected frequencies is that 50 megacycles corresponds to the angular frequency of the electrons in the synchrotron when they are undergoing synchronous acceleration.

Measurements of the Fourier components of the induced detector voltage permit synthesis of its wave shape. Then, knowing the impedance the detector circuit presents to the electron beam, the induced charge on the detector as a function of time may be determined. This induced charge function must be related in some manner to the linear charge density of the electron beam as determined by experiment. Or, if only the total charge in each bunch of electrons in the beam is known (by collecting all the electrons in the beam), this total charge must be related to the integral of the induced charge function.

CHAPTER III

ASSOCIATED TESTING APPARATUS

The problem under investigation is the measurement of current in a pulsed electron beam. The number of coulombs in a bunch of electrons passing through a cylindrical detector on its axis is to be deduced from the voltage induced on the detector.

Hence, measurements will be made of small induced voltages having a frequency of 30 megacycles, and harmonics of that frequency. The reason for making measurements at these selected frequencies is that 30 megacycles corresponds to the angular frequency of the electrons in the synchrotron when they are undergoing synchronous acceleration.

Measurements of the Fourier components of the induced detector voltage permit synthesis of its wave shape. Then, knowing the impedance the detector circuit presents to the electron beam, the induced charge on the detector as a function of time may be determined. This induced charge function must be related in some manner to the linear charge density of the electron beam as determined by experiment. Or, if only the total charge in each bunch of electrons in the beam is known (by collecting all the electrons in the beam), this total charge must be related to the integral of the induced charge function.

2. Radio Receiving Equipment.

An important unit of the measurement apparatus is a frequency-sensitive micro-voltmeter. A calibrated radio receiver Model RDO, manufactured by the E. H. Scott Radio Laboratories, Inc., performs this function. The particular receiver used in this thesis was borrowed from the U. S. Navy Radar School located at the Harbor Building, Boston, Massachusetts. "RDO Radio Receiving Equipment is a search receiver designed to measure the frequency of radar or radio signals within its frequency range. It is a superheterodyne type receiver, complete in itself, but may be used with radio spectrum scanning and pulse analyzer equipment not furnished as part of the Model RDO equipment." (Reference 5).

This equipment covers a frequency range from 40 to 1000 mcps. Three plug-in tuning units are used with the receiver, and have frequency ranges as follows:

Tuning Unit TN-1B/APR1
40 - 105 mcps.

Tuning Unit TN-2B/APR1
75 - 300 mcps.

Tuning Unit TN-3B/APR1
300 - 1000 mcps.

The conventional type of electrical circuit is used in this receiver. The input signal is detected and converted by means of a high-frequency oscillator to an intermediate frequency of 30 mcps. After 5 stages of intermediate-frequency amplification, the signal is again detected. Normally, the signal would then be led through: a stage of audio-amplifica-

3. Radio Receiving Equipment.

An important unit of the measurement apparatus is a frequency-sensitive micro-voltmeter. A calibrated radio receiver model MRO, manufactured by the S. H. Scott Radio Laboratories, Inc., performs this function. The particular receiver used in this thesis was borrowed from the U. S. Navy Under Seaol located at the Harbor Building, Boston, Massachusetts. "MRO Radio Receiving Equipment is a master receiver designed to measure the frequency of radar or radio signals within its frequency range. It is a superheterodyne type receiver, complete in itself, but may be used with radio spectrum scanning and pulse analyzer equipment not furnished as part of the model MRO equipment." (Reference 5).

This equipment covers a frequency range from 40 to 1000 mcps. Three plug-in tuning units are used with the receiver, and have frequency ranges as follows:

Tuning Unit TM-1D\ARR1
40 - 105 mcps.

Tuning Unit TM-2D\ARR1
75 - 300 mcps.

Tuning Unit TM-3D\ARR1
300 - 1000 mcps.

The conventional type of electrical circuit is used in this receiver. The input signal is detected and converted by means of a high-frequency oscillator to an intermediate frequency of 30 mcps. After 3 stages of intermediate-frequency amplification, the signal is again detected. Normally, the signal would then be led through a stage of audio-amplifica-

tion; a band-pass filter; a silencer amplifier, a second stage of audio-amplification; and an audio-frequency power output stage. However, since the signals to be measured will be unmodulated, the output of the second detector will be a constant current, and the audio-amplification circuit will be inactive. Hence, the audio circuits were disregarded, and a micro-ammeter was installed in the second detector diode circuit to provide relative measurements of the input radio-frequency voltages. The micro-ammeter reading was calibrated with a standard ultra-high-frequency signal generator to be described later.

In the RDO receiver, the radio-frequency input is made through a 50-ohm concentric line to the tuning unit. The antenna input circuit is unbalanced to ground and is designed to terminate a 50-ohm transmission line. Thus, the induced signal from the cylindrical detector will be modified by the 50-ohm cable impedance in parallel with the capacity-to-ground of the cylindrical detector. If the time constant of this circuit is comparable with the duration of the electron pulse (about .01 micro-second), the induced charge as a function of time will be altered by decreasing exponential functions as detector capacity is charged through a resistance of 50 ohms.

The capacity of the cylindrical detector to ground was measured with a Boonton "Q" meter at a frequency of 50 mega-cycles to be 15 micromicrofarads. This capacity is very easily calculated, as the geometry of the detector and its housing is

The capacity of the cylindrical detector to ground was measured with a Boonton "Q" meter at a frequency of 30 megacycles to be 35 micromicrofarads. This capacity is very easily calculated, as the geometry of the detector and its housing is

one of concentric cylinders. The capacity per unit length of two concentric cylinders is given by:

$$C = 2\pi\varepsilon_0 \left(\ln \frac{b}{a}\right)^{-1} \quad \text{farad/meter} \qquad (1)$$

where ε_0 is the inductive capacitance of free space, b the radius of the outer cylinder, and a the radius of the inner cylinder, all given in the MKS rationalized system of units. Substituting the proper dimensions in the above formula, the capacity of the cylindrical detector is found to be:

$$C = (2\pi/4\pi)\times 10^{-9}\left(\ln \frac{.0605}{.01985}\right)^{-1} \quad \text{farad/meter}$$

$$= 49.7 \text{ micromicrofarad/meter.}$$

As the cylindrical detector was 10 centimeters in length, its capacity to ground is 4.97 micromicrofarads. The distributed capacity of the leads exterior to the detector must be approximately 10 micromicrofarads. The time constant of the total capacity in parallel with 50 ohms is 750 micro-micro-seconds. Since this time constant is much less than the length of a single pulse of the electron beam, it becomes necessary to parallel the detector with an additional capacity to increase the time constant. As the duration of a charge pulse on the cylinder is at most .01 micro-seconds, a capacity of .001 microfarads in parallel with the cylinder will increase the time constant of the detection circuit to .05 micro-

one of concentric cylinders. The capacity per unit length of two concentric cylinders is given by:

$$C = 2\pi\epsilon_0 (\ln \frac{a}{b})^{-1} \quad \text{farad/meter} \qquad (1)$$

where ϵ_0 is the inductive capacitance of free space, b the radius of the outer cylinder, and a the radius of the inner cylinder, all given in the MKS rationalized system of units. Substituting the proper dimensions in the above formula, the capacity of the cylindrical detector is found to be:

$$C = (2\pi/4\pi)10^{-9}(\ln \frac{.0427}{.0156})^{-1} \quad \text{farad/meter}$$

$$= 49.7 \text{ micromicrofarad/meter.}$$

As the cylindrical detector was 15 centimeters in length, its capacity to ground is 4.97 micromicrofarads. The distributed capacity of the leads exterior to the detector must be approximately 15 micromicrofarads. The time constant of the total capacity in parallel with 50 ohms is 7.5 micro-micro-seconds. Since this time constant is much less than the length of a single pulse of the electron beam, it becomes necessary to parallel the detector with an additional capacity to increase the time constant. As the duration of a charge pulse on the cylinder is at most .01 micro-seconds, a capacity of .03 microfarads in parallel with the cylinder will increase the time constant of the detection circuit to .3 micro-

seconds, sufficient to prevent an appreciable amount of the induced charge from leaking off the detector.

From the 50-ohm concentric line, the signal is led into the tuning units. While these tuning units are conventional in superheterodyne construction, their physical construction, due to the frequencies involved, is of some interest. In the low-frequency tuning unit (TN-1B), the signal input circuit consists of a 30-megacycle trap filter. The detector and local oscillator are both "peanut" tubes, type 9002. The oscillatory L-C circuit of the local oscillator uses conventional condensers and coils.

In the higher frequency tuning units, (TN-2B, and TN-3B), the ordinary coil and condenser combinations are absent, being replaced by a so-called "butterfly" unit. This is really a modification of the split-stator condenser. The two "wings" of the "butterfly" capacitor represent the variable capacitor part of the circuit (rotor) while the inductance is formed as part of the construction of the stator. The signal voltage is fed from the input cable to the "butterfly" at a point where optimum coupling exists. The signal voltage is then applied to a type 1N-21 crystal, where it is mixed with the local oscillator frequency. A crystal is used as a mixer in these tuning units since the input capacity of a tube would be excessive at the frequencies involved.

From the tuning units, the intermediate frequency signal passes through five stages of amplification to the second de-

seconds, sufficient to prevent an appreciable amount of the
induced charge from leaking off the detector.

From the 50-ohm concentric line, the signal is fed into
the tuning units. While these tuning units are conventional
in superheterodyne construction, their physical construction,
due to the frequencies involved, is of some interest. In
the low-frequency tuning unit (TM-1B), the signal input cir-
cuit consists of a 30-megacycle trap filter. The detector
and local oscillator are both "peanut" tubes, type 9002. The
oscillatory L-C circuit of the local oscillator uses concen-
tional condensers and coils.

In the higher frequency tuning units,(TM-2B, and TM-3B),
the ordinary coil and condenser combinations are absent, be-
ing replaced by a so-called "butterfly" unit. This is really
a modification of the split-stator condenser. The two "wings"
of the "butterfly" capacitor represent the variable capacitor
part of the circuit (rotor) while the inductance is formed as
part of the construction of the stator. The signal voltage
is fed from the input cable to the "butterfly" at a point
where optimum coupling exists. The signal voltage is then ap-
plied to a type IN-21 crystal, where it is mixed with the
local oscillator frequency. A crystal is used as a mixer in
these tuning units since the input capacity of a tube would
be excessive at the frequencies involved.

From the tuning units, the intermediate frequency signal
passes through five stages of amplification in the second de-

tector. The second detector is one-half of a 6H6 tube. Its plate circuit is 20,200 ohms in series with a removable link switch. This link has been removed and a microammeter inserted in the circuit to permit measurement of the second detector diode current.

The sensitivity of the RDO receiver will be discussed later. Curves were obtained relating the input signal in microvolts to the output of the second detector in microamperes for 50 megacycles and harmonics.

Selectivity of a receiver is that characteristic which determines the extent to which it is capable of differentiating between the desired signal and signals of other frequencies. In the RDO receiver, the intermediate frequency amplifier has a bandwidth of 3 megacycles. Thus, as the frequencies at which measurements will be made are separated by 50 megacycles, the RDO receiver possesses sufficient selectivity.

3. 50-Megacycle Oscillator.

The source of electrons required to make the desired measurements of current in a pulsed electron beam is a modified 5RP cathode ray tube, and has been described previously. To group these electrons into bunches, the beam was modulated at 50 megacycles. This was done by applying a voltage at this frequency to the grid of the cathode ray tube. All conveniently available laboratory oscillators operating at 50 megacycles had a maximum output of about 1 volt. Since this is too small

tector. The second detector is one-half of a 6AL tube. The plate circuit is 20,000 ohms in series with a removable link switch. This link has been removed and a microammeter inserted in the circuit to permit measurement of the second detector diode current.

The sensitivity of the TRO receiver will be discussed later. Curves were obtained relating the input signal in microvolts to the output of the second detector in microamperes for 30 megacycles and harmonics.

Selectivity of a receiver is that characteristic which determines the extent to which it is capable of differentiating between the desired signal and signals of other frequencies. In the TRO receiver, the intermediate frequency amplifier has a bandwidth of 3 megacycles. Thus, at the frequencies at which measurements will be made are separated by 30 megacycles, the TRO receiver possesses sufficient selectivity.

3. 30-Megacycle Oscillator.

The source of electrons required to make the desired measurements of current in a pulsed electron beam in a modified 5AP cathode ray tube, and was been described previously. To group these electrons into bunches, the beam was modulated at 30 megacycles. This was done by applying a voltage at this frequency to the grid of the cathode ray tube. All conventionally available laboratory oscillators operating at 30 megacycles had a maximum output of about 1 volt. Since this is too small

a signal to provide sufficient grid drive for the formation of the pulsed beam, the signal source chosen was a Navy Model TBY-8 ultra-portable very high-frequency transmitter and receiver. It was obtained from the Boston Naval Shipyard. The output of this transmitter is .75 watts, and it has a frequency range of from 28 to 80 megacycles. (Reference 6).

The transmitter radio-frequency section consists of a conventional "Hartley" push-pull self-excited oscillator circuit using two acorn triode vacuum tubes, Navy Type-958A. The tank circuit consists of a tuning capacitor in parallel with a tuning inductance which may be made resonant at 50 megacycles.

A 5000 kilocycle crystal oscillator is provided in the equipment to furnish calibrating points throughout the tuning range.

To test the transmitter for the output voltage available, it was loaded with the input impedance of the Hewlett-Packard Type 410-A vacuum tube voltmeter about 1 micromicrofarad shunted with 6 megohms. The measured rms voltage of the output was 75 volts. Hence, this oscillator will provide sufficient signal to vary the grid potential of the cathode ray tube as desired, allowing the maximum current capacity of the tube to be realized. It is possible to estimate the number of electrons which can be expected in each bunch in the tube, for comparison with the expected charge in each bunch in the synchrotron. Manufacturing specifications indicate that cut-off bias for the

put meter on the panel and by setting the single calibrated and 20 millivolts and is determined by the reading of the out-

The output is continuously variable between 1 microvolt

high frequency electronic devices requiring a source of calibrated voltage". (Reference 7).

variable calibrated output voltage is obtained throughout the range. It is designed for testing radio receivers and other

range. It is designed for testing radio receivers and other

megacycles and is arranged and shielded that a continuously

megacycles and is arranged and shielded that a continuously

radio frequency oscillations over a frequency band between 7.5

radio frequency oscillations over a frequency band between 7.5

Signal Generator. (Reference 7).

oscillator is a Federal Type 304-CS2 Ultra-High-Frequency

oscillator is a Federal Type 304-CS2 Ultra-High-Frequency

School at the Parker Building, Boston, Massachusetts. The

School at the Parker Building, Boston, Massachusetts. The

tory test oscillator was obtained from the U. S. Navy Radio

tory test oscillator was obtained from the U. S. Navy Radio

between the receiver second-detector grid circuit and the

between the receiver second-detector grid circuit and the

input signal. To make this comparison, a calibrated labora-

input signal. To make this comparison, a calibrated labora-

4. Receiver Calibration Oscillator.

4. Receiver Calibration Oscillator.

As stated previously, a comparison must be obtained

As stated previously, a comparison must be obtained

between the receiver second-detector grid circuit and the

between the receiver second-detector grid circuit and the

input signal. To make this comparison, a calibrated labora-

input signal. To make this comparison, a calibrated labora-

tory test oscillator was obtained from the U. S. Navy Radio

tory test oscillator was obtained from the U. S. Navy Radio

School at the Parker Building, Boston, Massachusetts. The

School at the Parker Building, Boston, Massachusetts. The

oscillator is a Federal Type 304-CS2 Ultra-High-Frequency

oscillator is a Federal Type 304-CS2 Ultra-High-Frequency

Signal Generator. (Reference 7).

Signal Generator. (Reference 7).

The Federal Signal Generator is a device for producing

The Federal Signal Generator is a device for producing

radio frequency oscillations over a frequency band between 7.5

radio frequency oscillations over a frequency band between 7.5

megacycles and is arranged and shielded that a continuously

megacycles and is arranged and shielded that a continuously

variable calibrated output voltage is obtained throughout the

variable calibrated output voltage is obtained throughout the

range. It is designed for testing radio receivers and other

range. It is designed for testing radio receivers and other

high frequency electronic devices requiring a source of cali-

high frequency electronic devices requiring a source of cali-

brated voltage". (Reference 7).

brated voltage". (Reference 7).

The output is continuously variable between 1 microvolt

The output is continuously variable between 1 microvolt

and 20 millivolts and is determined by the reading of the out-

and 20 millivolts and is determined by the reading of the out-

put meter on the panel and by setting the single calibrated

put meter on the panel and by setting the single calibrated

drive characteristic and that the grid will be driven to

drive characteristic and that the grid will be driven to

zero bias from the cut-off bias by a pure sine wave, the

zero bias from the cut-off bias by a pure sine wave, the

average current will be found to be about 50 microamperes.

average current will be found to be about 50 microamperes.

For a period of .02 micro-seconds, the charge per unit is

For a period of .02 micro-seconds, the charge per unit is

equal to 1 microcoulomb, or about 10^{12} electrons. This

equal to 1 microcoulomb, or about 10^{12} electrons. This

is the same number of electrons per unit that is expected

is the same number of electrons per unit that is expected

in the thyratron.

in the thyratron.

4. Receiver Calibration Oscillator.

4. Receiver Calibration Oscillator.

As stated previously, a comparison must be obtained

As stated previously, a comparison must be obtained

between the receiver second-detector grid circuit and the

between the receiver second-detector grid circuit and the

input signal. To make this comparison, a calibrated labora-

input signal. To make this comparison, a calibrated labora-

tory test oscillator was obtained from the U. S. Navy Radio

tory test oscillator was obtained from the U. S. Navy Radio

School at the Parker Building, Boston, Massachusetts. The

School at the Parker Building, Boston, Massachusetts. The

oscillator is a Federal Type 304-CS2 Ultra-High-Frequency

oscillator is a Federal Type 304-CS2 Ultra-High-Frequency

Signal Generator. (Reference 7).

Signal Generator. (Reference 7).

The Federal Signal Generator is a device for producing

The Federal Signal Generator is a device for producing

radio frequency oscillations over a frequency band between 7.5

radio frequency oscillations over a frequency band between 7.5

megacycles and is arranged and shielded that a continuously

megacycles and is arranged and shielded that a continuously

variable calibrated output voltage is obtained throughout the

variable calibrated output voltage is obtained throughout the

range. It is designed for testing radio receivers and other

range. It is designed for testing radio receivers and other

high frequency electronic devices requiring a source of cali-

high frequency electronic devices requiring a source of cali-

brated voltage". (Reference 7).

brated voltage". (Reference 7).

The output is continuously variable between 1 microvolt

The output is continuously variable between 1 microvolt

and 20 millivolts and is determined by the reading of the out-

and 20 millivolts and is determined by the reading of the out-

put meter on the panel and by setting the single calibrated

put meter on the panel and by setting the single calibrated

drive characteristic and that the grid will be driven to

drive characteristic and that the grid will be driven to

zero bias from the cut-off bias by a pure sine wave, the

zero bias from the cut-off bias by a pure sine wave, the

average current will be found to be about 50 microamperes.

average current will be found to be about 50 microamperes.

For a period of .02 micro-seconds, the charge per unit is

For a period of .02 micro-seconds, the charge per unit is

equal to 1 microcoulomb, or about 10^{12} electrons. This

equal to 1 microcoulomb, or about 10^{12} electrons. This

is the same number of electrons per unit that is expected

is the same number of electrons per unit that is expected

in the thyratron.

in the thyratron.

attenuator dial. Output voltages are obtained across a 100 micromicrofarad condenser built into the attenuator housing in series with a 75-ohm resistor. A 75-ohm concentric shielded output cable was used to connect the test oscillator to the receiver for calibration. The calibration of the attenuator dial is given in terms of the open-circuit output voltages at the output jack of the equipment. Thus, since the input to the RDO receiver is a 50-ohm cable, a conversion factor is necessary to determine the signal actually received at the receiver in terms of the calibrated dial on the signal generator.

The circuit between the signal generator and the RDO receiver may be represented as follows:

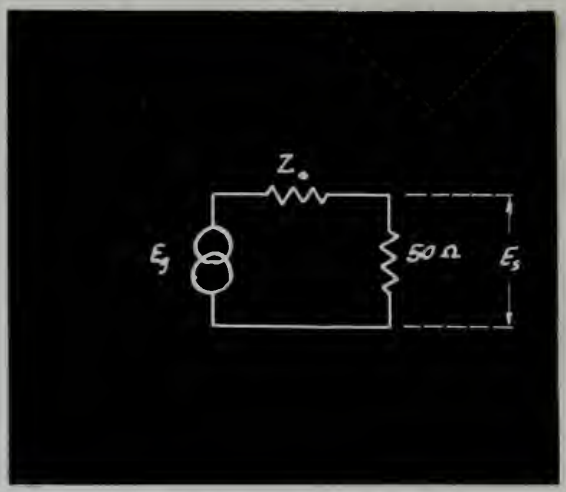

Fig. 5

where E_g is the voltage read on the calibrated dial of the generator, Z_o output impedance of the generator as given by a calibrated curve in the reference cited. The 50-ohm

attenuator dial. Output voltages are obtained across a 100 microcalibrated condenser built into the attenuator housing in series with a 75-ohm isolator. A 75-ohm concentric shielded output cable was used to connect the test oscillator to the receiver for calibration. The calibration of the attenuator dial is given in terms of the open-circuit output voltages at the output jack of the equipment. Thus, since the input to the RDO receiver is a 50-ohm cable, a conversion factor is necessary to determine the signal actually received at the receiver in terms of the calibrated dial on the signal generator.

The circuit between the signal generator and the RDO receiver may be represented as follows:

where E_g' is the voltage read on the calibrated dial of the generator, R_o output impedance of the generator as given by a calibrated curve in the reference cited. The 50-ohm

impedance is that of the RDO receiver input. The actual voltage appearing at the input terminals of the receiver is:

$$E_s = E_g \left[\frac{50}{50 + Z_o} \right] \qquad (2)$$

5. Receiver Calibration.

Using the Federal Signal Generator, runs were made at 50, 100, 150, 200, 250 and 300 megacycles and the receiver diode current compared with the calibrated output of the signal generator. These readings were corrected in accordance with equation (2). Since it is impossible to measure the phase of the voltage on the cylindrical detector with an RDO receiver, only the magnitude of the correction factor is necessary. These correction factors are given below:

Frequency	Z_o	Correction Factor
50 mcps	80 +j30	.374
100 "	60 -j8	.454
150 "	85 -j20	.369
200 "	72 +j10	.408
250 "	70 +j0	.416
300 "	80 +j8	.381

The corrected curves providing the desired calibration of the RDO receiver are given in Figure ~~4~~ 6. With these curves available, the harmonics of the voltage induced on the cylindrical detector as the bunch of electrons passes down the axis of the cylinder are immediately defined.

impedance is that of the RDO receiver input. The actual voltage appearing at the input terminals of the receiver is:

$$E_a = E_s \left[\frac{z_o}{z_o + Z_s} \right] \qquad (2)$$

3. Receiver Calibration.

Using the Federal Signal Generator, runs were made at 50, 100, 150, 200, 250 and 300 megacycles and the receiver diode current compared with the calibrated output of the signal generator. These readings were corrected in accordance with equation (2). Since it is impossible to measure the phase of the voltage on the cylindrical detector with an RDO receiver, only the magnitude of the correction factor is necessary. These correction factors are given below:

Frequency	E_s	Correction Factor
50 mcps	90 +130	.174
100 "	80 -18	.478
150 "	85 -120	.309
200 "	72 +130	.408
250 "	70 +18	.418
300 "	80 +18	.381

The corrected curves providing the desired calibration of the RDO receiver are given in Figure [illegible]. With these curves available, the harmonics of the voltage induced on the cylindrical detector at the mouth of electrons passing down the axis of the cylinder are immediately defined.

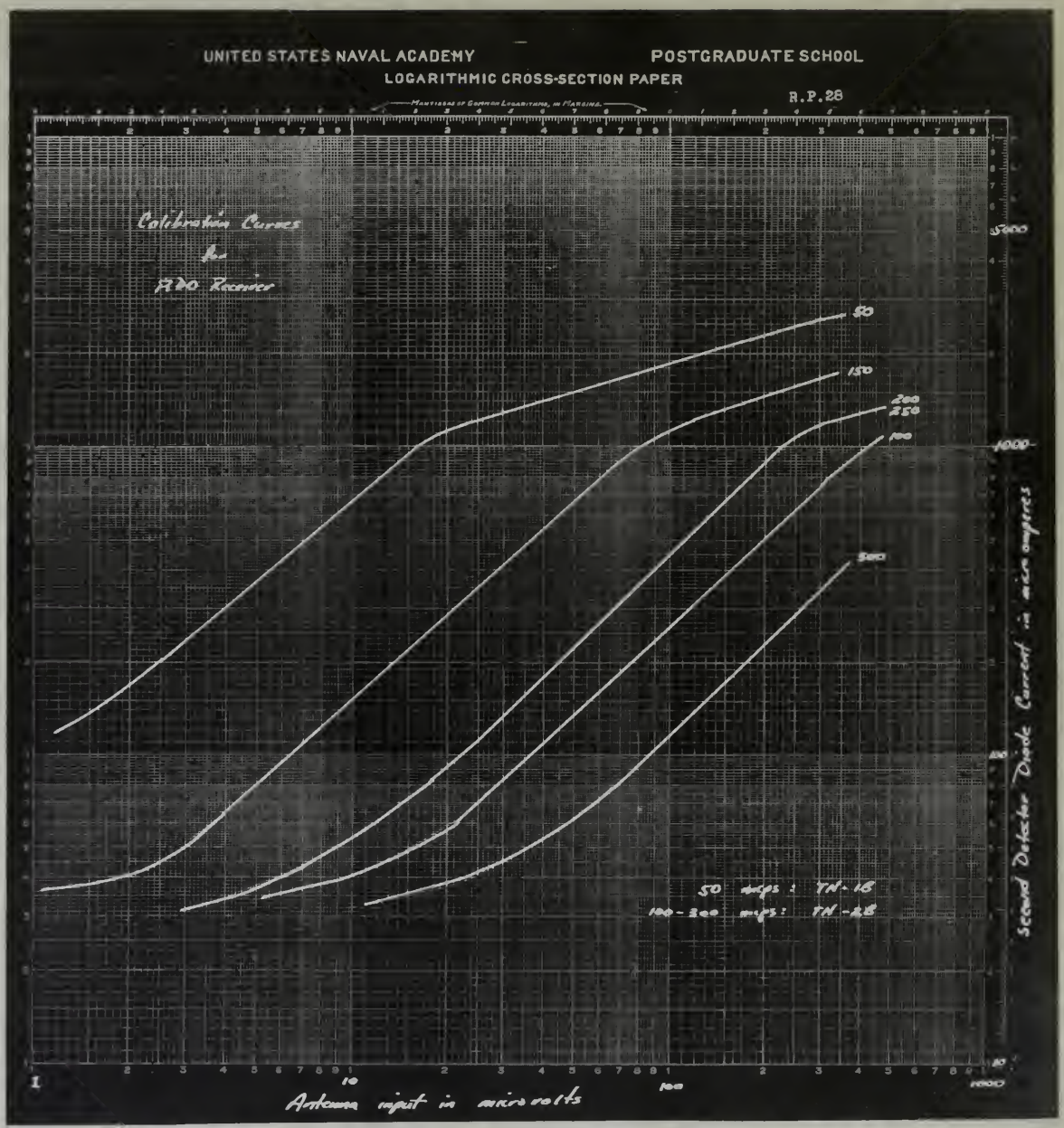
UNITED STATES NAVAL ACADEMY
POSTGRADUATE SCHOOL
LOGARITHMIC CROSS-SECTION PAPER
R.P.28
Calibration Curves
for
ARDO Receiver
50
150
200
250
100
300
50 mcps : TN-16
100-200 mcps : TN-28
Second Detector Diode Current in micro amperes
Antenna input in micro volts

Fig. 6

REFERENCES

1. The Science and Engineering of Nuclear Power, Vol. I, Chap. I, ADDISON-WESLEY PRESS, INC.

2. Reference Manual for Cathode-Ray Tubes and Instruments, ALLEN B. DUMONT LABORATORIES, INC.

3. History and Development of Circuital-Orbit Charged-Particle Accelerators, S. N. Anastasion, E. E. Seminar, Sept. 1947.

4. X-Rays in Theory and Experiment, Table II, p. 803, A. H. Compton and S. K. Allison, VAN NOSTRAND & CO., INC., 1947.

5. Preliminary Instruction Book for Radio Receiving Equipment, Model RDO, NAVSHIPS 900,527-IB, U. S. NAVY DEPARTMENT.

6. Instruction Book for Navy Model TBY-8 Ultra-Portable Very-High-Frequency Transmitting-Receiving Equipment, U. S. NAVY DEPARTMENT, BUREAU OF SHIPS.

7. Operating Instructions for Type 804-CS2 U-H-F Signal Generator, NAVAER 08-SS-129, 15 April 1944, U. S. NAVY DEPARTMENT.

8. The Mathematics of Physics and Chemistry, H. Margenau and G. M. Murphy, pp 74-76 and 216-218, D. VAN NOSTRAND CO., INC., 1943.

9. Special Theory of Relativity, Dr. I. A. Getting, Staff Seminar, Electrical Engineering Department, M.I.T., Dec. 3, 10, 17, 1947.

Bibliography

1. *The Volume and Distribution of Wayward Power*, Vol. I, Chap. 5, Adams-Smith Press, 1961.

2. *Reference Manual for Field Operators' Tools and Instruments*, Alcay W., Ludwig Laboratories, 1963.

3. *Wiring and Layout Diagrams of Circuit-Trial Panels*, Bartleby Associates, E. B. Annelson, S. S. Dentner, 1947.

4. *I-Beam in Theory and Construction*, Vol. II, pp. 803, A. B. Cooper and S. K. Gilman, Van Nostrand & Co., Inc., 1947.

5. *Installation Instructions Book for Radio Receiving Tubes*, Model 4000, Wireless 903,321-C, S. S. Kitz Corp., 1947.

6. *Instruction Book for Navy Model TBX-5 Ultra-Portable Test-Pilot-Structure Transmitter-Receiver Equipment*, U. S. Navy Department, Bureau of Ships.

7. *Operating Instructions for Type SCR-625 T-U-F Signal Generator*, Navship 36-430-12A, 15 April 1944, U. S. Navy Department.

8. *The Permeability of Cobalt and Chromium*, S. Berglund and O. S. Moseley, pp 74-76 and 218-219, N. Van Nostrand Co., Inc., 1943.

9. *Graphic Theory of Polarity*, Dr. I. A. Poeling, Staff Lecturer, Electrical Engineering Department, M.I.T., Dec. 3, 20, 17, 1941.

APPENDIX 1

THEORETICAL ANALYSIS OF THE PROBLEM

APPENDIX I

BIOCHEMICAL ANALYSIS OF THE PROCESS

APPENDIX I

MATHEMATICAL DEDUCTIONS

The problem under consideration is the calculation of the voltage, E(t), induced on a short cylinder by a group of electrons traveling along the axis of the cylinder at velocities which may approach the speed of light. The group of electrons will be in the shape of a line charge having a density variation determined by the grid drive characteristics of a cathode-ray tube. Each group will be separated from every other group at such a distance that the effects of only an individual bunch must be investigated.

The short cylinder, which will be called the detector, will have dimensions such that its length is greater than its diameter and very much less than the length of the electron group. The detector will be considered to present a pure capacitative load to the electron beam. This is possible because the time constants of the R-C networks of the detection and measurement circuit may be made very much longer than one period of the electron beam modulation frequency.

The solution of this problem involves several steps. First, it is necessary to calculate the charge density induced on an infinite cylinder by a single electron at the origin of the cylindrical coordinate system. A segment of

APPENDIX I

MATHEMATICAL DERIVATIONS

length L will then be cut from the infinite cylinder and allowed to move along the axis with a velocity v. The total charge on this segment as a function of time divided by the capacity of the detection circuit is the answer required.

Since the electrons may approach the speed of light, relativistic effects cannot be ignored and must be included in the calculations of the above paragraph.

It is then necessary to extend the case of a point charge to the more general case of a line charge whose density varies according to a prescribed function. The function used was derived by assuming a pure sine wave impressed on the grid of a cathode-ray tube biased to cut-off. The grid drive characteristic of the tube may be represented by a parabola.

length L will then be cut from the infinite cylinder and allowed to move along the axis with a velocity v. The total charge on this segment as a function of time thus required.

Since the electrons may approach the speed of light, relativistic effects cannot be ignored and must be included in the calculations of the above paragraph.

It is then necessary to extend the case of a point charge to the more general case of a line charge whose density varies according to a prescribed function. The function used was obtained by examining a pure sine wave impressed on the grid of a cathode-ray tube biased to cut-off. The grid drive characteristic of the tube may be represented by a parabola.

TABLE OF SYMBOLS

a = Radius of cylindrical segment (detector).

A_r = A constant, which is a function of r.

β = v/c.

C = A constant.

C_o = Capacity of the cylindrical detector to ground.

c = Velocity of light = 3×10^8 meters/second.

d = Grid drive of a Cathode-Ray Tube.

e = Electronic charge = 1.6×10^{-19} coulombs.

E_m = Peak volts.

ε_o = Inductive capacitance of free space = $(1/36)\times10^{-9}$ farad/meter.

ϵ = Base of natural logarithms = 2.71828.

f = Frequency.

i = Electric current in amperes.

j = $(-1)^{\frac{1}{2}}$

J_n = Bessel function of order n.

K = $(1 - \beta^2)^{-\frac{1}{2}}$

L = Length of cylindrical segment (detector).

λ = Wave length associated with the modulated electron beam.

Λ = Linear charge density in coulombs/meter.

μ = A constant.

μ_r = Roots of zero order Bessel Function divided by a, e.g., $J_0(\mu_r a) = 0$.

n = A constant.

ω = Angular frequency = $2\ f$.

TABLE OF SYMBOLS

ω = angular frequency = $2\pi\nu$.

u = a constant.

H_ν = Hankel of zero order Bessel function divided by x.
$x^{-1} J_0(H_\nu x) = 0$.

h = a constant.

V = linear charge density in coulombs/meter.

y = wave length associated with the conducted electron beam.

T = length of cylindrical resonant cavity.

ϵ = $(1 - \beta^2)^{-\frac{1}{2}}$

J_n = Bessel function of order n.

i = $(-1)^{\frac{1}{2}}$

I = Electric current in amperes.

f = frequency.

e = Base of natural logarithms = 2.7182.

ϵ_0 = Inductive capacitance of free space = $(1/36)\times10^{-9}$ farad/meter.

E_p = Peak volts.

e = Electronic charge = 1.6×10^{-19} coulombs.

d = grid drive of a Heacock-Ray tube.

σ = Velocity of light = 3×10^8 meters/second.

C_g = Capacity of the cylindrical detector to ground.

δ = A constant.

β = v/σ.

λ_p = A constant, which is a function of r.

ε = Inertia of cylindrical magnets (detector).

TABLE OF SYMBOLS
(Cont'd)

φ = Polar angle of a cylindrical coordinate system.

Φ = $\Phi(\varphi)$ = A function of φ.

q = Charge (in coulombs).

Q = Q(t) = Charge on the cylindrical segment (antenna).

r = Summation subscript.

R = $R(\rho)$ = A function of ρ.

ρ = Radial distance of a cylindrical coordinate system.

ρ = Charge density per unit volume = coulombs/meter^3.

s = Summation subscript.

dS = Element of surface.

σ = Surface charge density = coulombs/meter^2.

t = Time variable.

$d\tau$ = dx dy dz jedt = A four dimensional volume element.

V = A potential function satisfying LaPlace's equation.

dV = Element of volume.

dV = Element of potential.

v = Velocity of electrons in an electron beam.

x = vt

x = One axis of a Cartesian coordinate system.

ξ = Linear charge density variable.

y = One axis of a Cartesian coordinate system.

z = One axis of either a Cartesian coordinate system, or a Cylindrical coordinate system.

Z = Z(z) = A function of z.

Note 1: All duplications of symbols will become clear from the context.

Note 2: The MKS rationalized system of units is used throughout the following discussion.

Table of Symbols
(cont'd)

φ = Polar angle of a cylindrical coordinate system.

Φ = $\Phi(\varphi)$ = A function of φ.

q = Charge (in coulombs).

Q = Q(t) = Charge on the cylindrical segment (antenna).

r = Summation subscript.

R = R(ρ) = A function of ρ.

ρ = Radial distance of a cylindrical coordinate system.

ρ_c = Charge density per unit volume = coulomb/meter^3.

s = Summation subscript.

dS = Element of surface.

σ = Surface charge density = coulomb/meter^2.

t = Time variable.

dT = dx dy dz in Joule = A four dimensional volume element.

V = A potential function satisfying Laplace's equation.

dV = Element of volume.

dV = Element of potential.

v = Velocity of electrons in an electron beam.

x = vt

X = One axis of a Cartesian coordinate system.

$\bar{X}$ = Linear charge density variable.

y = One axis of a Cartesian coordinate system.

z = One axis of either a Cartesian coordinate system, or a Cylindrical coordinate system.

Z = Z(z) = A function of z.

Note 1) All applications of symbols will become clear from the context.

First, it is necessary to calculate the charge density on an infinite cylinder due to a point charge, an electron, at the origin.

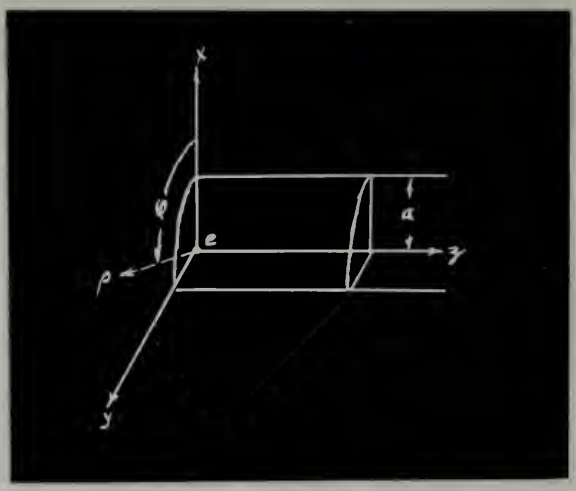

Fig. 1—Cylinder of radius a extending to infinity in both directions, with a charge e at the center.

To do this, the potential field within the cylinder must be found. The normal derivative of this electrostatic field evaluated at $\rho = a$, will define the charge density at any point on the cylinder. Proceeding from LaPlace's equation in cylindrical coordinates:

$$\frac{\partial^2 V}{\partial \rho^2} + \frac{1}{\rho}\frac{\partial V}{\partial \rho} + \frac{1}{\rho^2}\frac{\partial^2 V}{\partial \varphi^2} + \frac{\partial^2 V}{\partial z^2} = 0, \qquad (1)$$

which must be satisfied by the potential field everywhere inside the cylinder except at the origin. A solution of the type:

$$V = R\,\Phi\,Z \qquad (2)$$

First, it is necessary to calculate the charge density on an infinite cylinder due to a point charge, an electron, at the origin.

Fig. 1--Cylinder of radius a extending to infinity in both directions, with a charge e at the center.

To do this, the potential field within the cylinder must be found. The normal derivative of this electrostatic field evaluated at $\rho = a$, will define the charge density at each point on the cylinder. Proceeding from Laplace's equation in cylindrical coordinates:

$$\frac{\partial^2 \lambda}{\partial \rho^2} + \frac{1}{\rho}\frac{\partial \lambda}{\partial \rho} + \frac{1}{\rho^2}\frac{\partial^2 \lambda}{\partial \phi^2} + \frac{\partial^2 \lambda}{\partial z^2} = 0. \qquad (1)$$

which must be satisfied by the potential field everywhere inside the cylinder except at the origin. A solution of the type:

$$\lambda = R\Phi Z \qquad (2)$$

must be found. Here R, Φ, and Z are functions of r, φ, and z alone. Substituting into LaPlace's equation and dividing by $R\Phi Z\rho^{-2}$, the variables may be separated to give:

$$\frac{\rho}{R}\frac{d}{d\rho}\left[\frac{dR}{d\rho}\right] + \frac{1}{\Phi}\frac{d^2\Phi}{d\varphi^2} + \frac{\rho^2}{Z}\frac{d^2Z}{dz^2} = 0. \qquad (3)$$

Then, by making the following definitions:

$$\frac{1}{\Phi}\frac{d^2\Phi}{d\varphi^2} = -n^2, \qquad (4)$$

and:

$$\frac{1}{Z}\frac{d^2Z}{dz^2} = \mu^2, \qquad (5)$$

where n and μ are real constants, R must satisfy the equation:

$$\rho^2\frac{d^2R}{d\rho^2} + \rho\frac{dR}{d\rho} + (\mu^2\rho^2 - n^2)R = 0. \qquad (6)$$

If the change of variable $\mu\rho = u$ is made, equation (6) becomes Bessel's differential equation.

The potential function satisfying LaPlace's equation is then of the form: (Reference 8)

$$V_{\mu,n} = C_{\mu,n} J_n(\mu\rho)\epsilon^{\pm(\mu z \pm jn\varphi)} \qquad (7)$$

$$\Lambda^{hv} = e^{hv} \int_0^\infty (hb)\, e^{i(h\xi + v\eta)} \qquad (4)$$

where ξ is the former (reference 8).

The horizontal Laplacian multiplied Taylor's solution is Bessel's differential equation.

If the absolute value of $\lambda = i\kappa$ above, equation (4) becomes

$$b \frac{q^2 b}{q\xi^2} + b \frac{qb}{q\xi} + (h^2 b^2 - \kappa^2) R = 0 \qquad (5)$$

where Σ and Φ are real constants, Λ must satisfy the equation:

$$\frac{\Sigma}{1} \frac{q^2}{q\xi^2} = -\kappa^2 \qquad (6)$$

and:

$$\frac{\Phi}{1} \frac{q^2}{q\varphi^2} = -\nu^2 \qquad (7)$$

Then, by moving the following relationship:

$$\frac{\nu}{b} \frac{qb}{q\xi} \left[\frac{qb}{q\xi} \right] + \frac{\Phi}{1} \frac{q^2 b}{q\varphi^2} + \frac{\Sigma}{b} \frac{q^2 b}{q\xi^2} = 0. \qquad (8)$$

Multiplying by $b\Phi^{-1}\Sigma^{-1}$, the multipliers may be substituted to find and a close. Substituting into Taylor's equation and Φ must be found. Here ν^2, Φ, and Σ are functions of ξ^2 and

This solution, however, is more general than will be needed to solve the problem. If the point charge creating the potential field is placed at the origin, the required potential function will be symmetrical about the origin and V will be independent of φ .

From equation (7), a solution must be found which will vanish when z approaches ∞, is symmetrical about the origin and gives $V = 0$ when $\rho = a$. Such a solution will be of the form:

$$V = \sum_{r=1}^{\infty} A_r \epsilon^{-\mu_r |z|} J_0(\mu_r \rho) \quad , \qquad (8)$$

where $J_0(\mu_r a) = 0$. A_r must now be determined from the boundary conditions of the problem.

Since by symmetry the plane $z = 0$ is formed by lines of force except at the point charge itself, $\left[\frac{\partial V}{\partial z}\right]_0$ must equal zero on this plane except for a small area ΔS at the origin. Hence:

$$\left[\frac{\partial V}{\partial z}\right]_{z=0} = -\sum_{r=1}^{\infty} \mu_r A_r J_0(\mu_r \rho) \quad . \qquad (9)$$

Multiplying both sides of this equation by $\rho J(\mu_s \rho)\, d\rho\, d\varphi$ and integrating from $\rho = 0$ to $\rho = a$, and from $\varphi = 0$ to $\varphi = 2\pi$, all the terms under the summation sign dis-

$\phi = \delta\psi^0$ will now clearly obtain the modification sign discontinuity $\Delta\phi = 0$ as $b = 0$ to $b = a^+$ and multiplied both sides of this equation by $b\,J_1(k'b)\,dq\,dq$

$$\left[\frac{\partial g}{\partial \lambda}\right]_{\lambda=0} = -\sum_{k=1}^{\infty} k' A'_k J_1^0(k'b) \quad . \tag{9}$$

and integrating from $b = 0$ to $b = a^+$ remembering that $\phi = 0$ at $\theta = 0$ and $\theta = \pi$ and that $\Delta\phi = 0$ at the origin. Hence:

$$\left[\frac{\partial g}{\partial \lambda}\right]_{\lambda=0} \text{ must equal } \left[\frac{\partial g}{\partial \lambda}\right]_{\lambda=0} \text{ except at the point charge itself.}$$

Since $\beta\lambda$ eliminates the plane $z = 0$ is formed $\Delta\lambda$ lines of force except at the point charge itself. $\left[\frac{\partial g}{\partial \lambda}\right]_{\lambda=0}$ must equal zero and fixes $\lambda = 0$ where $b = a$. Such a solution will be of the form:

$$\lambda = \sum_{k=1}^{\infty} A'_k \varepsilon^{-k'|z|} J_1^0(k'b) \quad ; \tag{8}$$

where $g^0(k', a) = 0$. k' must now be determined from the boundary conditions of the problem.

Since $\beta\lambda$ eliminates the plane $z = 0$ is formed $\Delta\lambda$ lines of force except at the point charge itself. $\left[\frac{\partial g}{\partial \lambda}\right]_{\lambda=0}$ must equal zero on the plane plane except for a small area ΔS at the origin. Hence:

$$\left[\frac{\partial g}{\partial \lambda}\right]_{\lambda=0} = -\sum_{k=1}^{\infty} k' A'_k J_1^0(k'b) \quad . \tag{9}$$

$\phi = \delta\psi^0$ will now clearly obtain the modification sign discontinuity $\Delta\phi = 0$ as $b = 0$ to $b = a^+$ and multiplied both sides of this equation by $b\,J_1(k'b)\,dq\,dq$

appear except for the term in which r = s. Solving for A_s:

$$A_s = \frac{\int\int \rho \left[\frac{\partial V}{\partial z}\right]_0 J_0(\mu_s \rho)\, d\rho\, d\varphi}{-\int\int \rho\, \mu_s \left[J_0(\mu_s \rho)\right]^2 d\rho\, d\varphi},$$

$$\cdot \frac{J_0(\mu_s \cdot 0) \int\int \left[\frac{\partial V}{\partial z}\right]_0 dS}{-\mu_s \left\{\frac{a^2}{2}\left[\left[J_0(\mu_s a)\right]^2 + \left[J_1(\mu_s a)\right]^2\right] 2\pi\right\}},$$

$$A_s = \frac{e}{2\pi \varepsilon_0 a^2 \mu_s \left[J_1(\mu_s a)\right]^2} . \tag{10}$$

Here, the numerator has been evaluated by means of Gauss's theorem, remembering that only half of the flux from the electron passes in a positive z direction. Thus, the potential inside the cylinder is found to be:

$$V = \sum_{n=1}^{\infty} \frac{e\, \epsilon^{-\mu_r |z|}\, J_0(\mu_r \rho)}{2\pi \varepsilon_0 a^2 \mu_r \left[J_1(\mu_r a)\right]^2} . \tag{11}$$

The charge density on the cylinder may be calculated from the formula:

from the formula:

$$V = \sum_{n=1}^{\infty} \frac{2\pi\varepsilon_0 a_s^2 h^2 \left[J_1'(h'a)\right]^2}{J_0(h'b)} e^{-h'|z|} \cdot \tag{17}$$

The energy density on the cylinder may be evaluated

potential inside the cylinder is found to be:

$$A = \frac{2\pi\varepsilon_0 a_s h^2 \left[J_1'(h'a)\right]^2}{c} \cdot \tag{101}$$

there, the numerator has been evaluated by means of Neumann's theorem, remembering that only part of the flux from the electrons passes in a positive $\hat{a}$ direction. Thus, the

$$V^2 = \frac{-h^2 \left\{ \frac{s}{q_e} \left[J_0(h'a) \right]^2 + \left[J_1'(h'a) \right]^2 \right\} \pi a}{2\pi (h'a) \left| \frac{g_s}{g_A} \right|^2 q^2} \cdot$$

$$V^2 = \frac{-\int\int b\, h^2 \left[J_0'(h'b) \right]^2 dq\, dq}{\int\int b \left| \frac{g_s}{g_A} \right|^2 J_0'(h'b)\, dq\, dq} \cdot$$

above example for the case in which $\lambda = s$. Solving for V^2,

$$\sigma = -\epsilon_0 \left[\frac{\partial V}{\partial \rho} \right]_{\rho = a} , \tag{12}$$

giving:

$$\sigma = \frac{e}{2\pi a^2} \sum_{r=1}^{\infty} \frac{\epsilon^{-\mu_r |z|}}{J_1(\mu_r a)} . \tag{13}$$

If this charge density is integrated over the infinite cylinder, the value of the integral must converge to the value e:

$$\int\int \sigma \, dS = \frac{e}{2\pi a^2} \sum_{r=1}^{\infty} \frac{1}{J_1(\mu_r a)} \int_{-\infty}^{+\infty} \epsilon^{-\mu_r |z|} \, 2\pi a \, dz ,$$

$$e = \frac{2e}{a} \sum_{r=1}^{\infty} \frac{1}{\mu_r J_1(\mu_r a)} .$$

From which,

$$\frac{1}{2} = \sum_{r=1}^{\infty} \frac{1}{(\mu_r a) J_1(\mu_r a)} . \tag{14}$$

From equation (13) the charge on a finite section cut from the infinite cylinder may be calculated. This cylin-

$$\frac{\pi}{l} = \sum_{k=1}^{\infty} \frac{(k'a)\,\eta'(k'a)}{l} \,. \qquad (12)$$

Thus eqn. (12) the charge on a single section one

$$\sigma = \frac{a}{2\varepsilon} \sum_{k=1}^{\infty} \frac{k'\,\eta'(k'a)}{l} \,.$$

$$\int_{-\infty}^{\infty} e^{-k'|\beta|} \cos q\rho \,,$$

$$\int e\,q\,2 = \frac{2\pi a_r}{\varepsilon} \sum_{k=1}^{\infty} \frac{\eta'(k'a)}{l}$$

mains at

ality factor, the ratio of the figures just converge to the

If this charge density is integrated over the infinite

$$c = \frac{\pi\, a_r}{\varepsilon} \sum_{k=1}^{\infty} \frac{\eta'(k'a)}{\varepsilon^{-k'|\beta|}} \,. \qquad (13)$$

Hence:

$$c = -\varepsilon' \left[\frac{\partial \beta}{\partial \lambda} \right]_{b=a} , \qquad (13a)$$

drical section is moving toward the point charge with a velocity v which is less than c (relativistic corrections will be included later in this analysis).

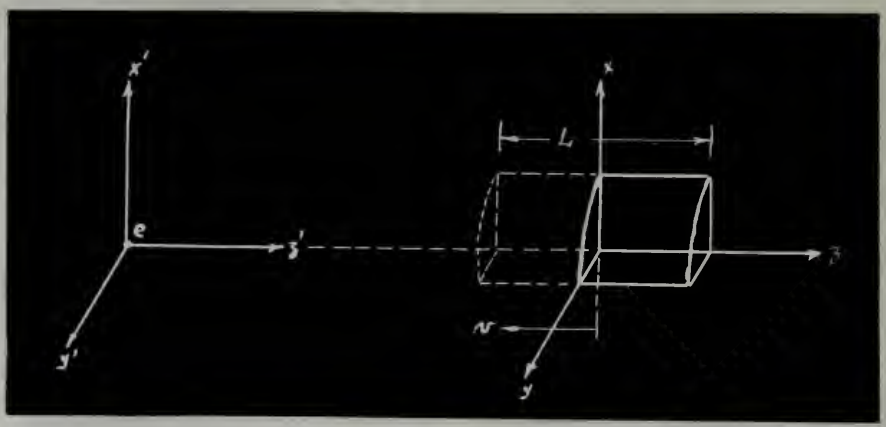

Fig. 2--Electron, and moving cylinder.

Consider a primed coordinate system with the electron at the origin and an unprimed system moving with the cylinder. The length of the cylinder is L units.

The first solution, a non-relativistic one, will illustrate the method and will be followed by an analysis valid for all velocities.

Integrating over the cylinder of length L:

$$Q = \int_L \sigma\, ds = \int_{v'-\frac{L}{2}}^{v'+\frac{L}{2}} \frac{e}{2\pi a^2} \sum_{n=1}^{\infty} \frac{\epsilon^{-\mu_r |z'|}\, 2\pi a\, dz}{J_1(\mu_r a)} \quad ; \qquad (15)$$

drical section is moving toward the point charge with a velocity v which is less than c (relativistic corrections will be included later in this analysis).

Fig. 5--Electron, and moving cylinder.

Consider a primed coordinate system with the electron at the origin and an unprimed system moving with the cylinder. The length of the cylinder is L units.

The first solution, a non-relativistic one, will illustrate the method and will be followed by an analysis valid for all velocities.

Integrating over the cylinder of length L

$$\phi = \int_0^r \frac{\rho \, 2\pi a \, da}{\sqrt{a^2 + z'^2}} = \frac{\rho}{c} \sum_{z'=1}^{z'=L} 2\pi a \int_{a=0}^{a=r} \frac{da}{\sqrt{a^2 + z'^2}} \; ; \qquad (13)$$

$$Q = \frac{e}{a} \sum_{r=1}^{\infty} \frac{1}{J_1(\mu_r a)} \int_{x'-\frac{L}{2}}^{x'+\frac{L}{2}} \epsilon^{-\mu_r |z'|} dz' \quad . \qquad (16)$$

The integral of equation (16) must be examined in detail. As the integrand contains the absolute value of z, it must be broken up into parts in which the absolute value sign may be ignored. The integration may then be completed.

When $x' > \frac{L}{2}$

$$\int_{x'-\frac{L}{2}}^{x'+\frac{L}{2}} \epsilon^{-\mu_r z'} dz' = 2 \frac{\epsilon^{-\mu_r v t'}}{\mu_r} \sinh(\mu_r \tfrac{L}{2}) \quad . \qquad (17)$$

Then, when $-\frac{L}{2} < x' < \frac{L}{2}$

$$\int_{x'-\frac{L}{2}}^{x'+\frac{L}{2}} \epsilon^{-\mu_r |z'|} dz' = \int_{x'-\frac{L}{2}}^{0} \epsilon^{\mu_r z'} dz' + \int_{0}^{x'+\frac{L}{2}} \epsilon^{-\mu_r z'} dz' \quad ,$$

$$= \frac{2}{\mu_r} \left[1 - \epsilon^{-\mu_r \frac{L}{2}} \cosh(\mu_r v t') \right] . \qquad (18)$$

When $x' < -\frac{L}{2}$, the sign of the exponential term changes in equation (17) above:

$$Q = \frac{\sigma}{\varepsilon} \sum_{k=1}^{\infty} \frac{2(k\pi\sigma)}{1} \int_{x_1-\frac{\pi}{2}}^{x_1+\frac{\pi}{2}} e^{-k\pi\beta_1 q_1} q_1 \qquad (16)$$

The integral of equation (16) must be examined in detail. We can integrate and obtain the absolute value of x_1 if must be proven at this point in which the absolute value sign may be ignored. The integration can then be completed.

When $x_1 > \frac{\pi}{2}$

$$\int_{x_1-\frac{\pi}{2}}^{x_1+\frac{\pi}{2}} e^{-k\pi\beta_1 q_1} = \frac{2}{\varepsilon^{k\pi}} \sinh(k\pi\tfrac{\pi}{2}) \cdot e^{-k\pi x_1} \qquad (17)$$

When $-\frac{\pi}{2} < x_1 < \frac{\pi}{2}$

$$\int_{x_1-\frac{\pi}{2}}^{x_1+\frac{\pi}{2}} e^{-k\pi\beta_1 q_1} = \int_{x_1-\frac{\pi}{2}}^{0} e^{k\pi\beta_1 q_1} + \int_{0}^{x_1+\frac{\pi}{2}} e^{-k\pi\beta_1 q_1} ,$$

When $x_1 < -\frac{\pi}{2}$, the sign of the exponent is changed in equation (17) above.

$$= \frac{k\pi}{2}\left[1 - e^{-k\pi\frac{\pi}{2}} \cos(k\pi x_1)\right] . \qquad (18)$$

$$\int_{x'-\frac{L}{2}}^{x'+\frac{L}{2}} \epsilon^{+\mu_r z'} dz' = 2 \frac{\epsilon^{\mu_r v t'}}{\mu_r} \sinh\left(\mu_r \frac{L}{2}\right) . \qquad (19)$$

With these results, the charge Q(t') on the cylinder of length L may be determined. Q will be defined only in the positive region of vt'. The curve, Q(t), is an even function and independent of the direction of the electron's motion.

When $0 < x' < \frac{L}{2}$,

$$Q = \frac{2e}{a} \sum_{r=1}^{\infty} \frac{1 - \epsilon^{-\mu_r \frac{L}{2}} \cosh(\mu_r v t)}{\mu_r J_1(\mu_r a)} , \qquad (20)$$

and when $\frac{L}{2} < vt < \infty$,

$$Q = \frac{2e}{a} \sum_{r=1}^{\infty} \frac{\epsilon^{-\mu_r v t} \sinh(\mu_r \frac{L}{2})}{\mu_r J_1(\mu_r a)} . \qquad (21)$$

Q(t) is shown in Fig. 3. The change in time variable t' (in the electron's coordinate system) to t (in the cylinder's coordinate system) is possible as non-relativistic conditions have been assumed.

Relativistic corrections must now be entered in equations (20) and (21). This is due to the fact that the field

tions (30) and (31). This is due to the fact that the field

Derivatives normal to the surface may be obtained in volume-

coordinate systems is possible on non-relativistic conditions

have been assumed.

(In the slow motion's coordinate system) as a (in the cylinder's

$\phi(s)$ is shown in fig. 3. The change in time variable s,

$$\Phi = \frac{a}{2\pi c} \sum_{n=1}^{\infty} \frac{h_n J_1'(h_n a)}{e^{-h_n s_1} \sinh(h_n \frac{s}{r})} \cdot \tag{31}$$

and since $\frac{s}{r} < s_1 < \infty$,

$$\Phi = \frac{a}{2\pi c} \sum_{n=1}^{\infty} \frac{h_n J_1'(h_n a)}{1 - e^{-h_n \frac{s}{r}} \cosh(h_n s_1)} \cdot \tag{30}$$

Also $0 < s_1 < \frac{s}{r}$;

motion.

Inversion and independence of the direction of the electron's

the positive region of s_1'. The curve $\phi(s)$ is an even

of length r may be considered. ϕ will be defined only in

s_1 three cases result: the change $\phi(s_1)$ on the cylinder

$$\Phi = \sum \frac{h_n}{e} \sinh(h_n \frac{s}{r}) \cdot \tag{19}$$

APPENDIX I

of the electron changes at relativistic velocities. It is quite simple to predict what will happen as the electron approaches the speed of light. The field of the electron is contracted toward a plane perpendicular to the direction of motion of the electron. Then, the induced charge on the cylinder approaches zero whenever the electron is outside the cylinder (detector) as v approaches c. When the charge is inside the detector, however, the induced charge will approach -e. This effect results in a square wave of induced charge response, Q(t), when v = c.

It is now necessary to examine the charge density under the above conditions, e.g., when the electron velocity approaches the speed of light. As the electron's field is transformed to a plane, the induced charge density on the cylinder must be infinite where the plane of the field of the electron intersects the cylinder. This infinite charge density, however, is only over an infinitesimal section of the cylinder, and the product of the infinite charge density and the infinitesimal width must converge to the charge on the electron.

To enable the calculation of the charge density on the cylindrical detector, it is necessary to turn to the mathematical theory of relativity. (Reference 9). If it is assumed that electric charge is conserved in transformations from stationary to moving coordinate systems, then:

$$dq = dq' \qquad (22)$$

$$dq = dq_1 \qquad (20)$$

from electrostatic to moving coordinate systems, then assumed that electric charge is conserved in transformations between inertial systems of relativity, (Reference 3). If it is quite simple to predict what will happen as the electron approaches the speed of light. The field of the electron is constricted toward a plane perpendicular to the direction of motion of the electron. Then, the induced charge on the cylinder (detector) as a approaches c. When the charge is inside the detector, however, the induced charge will approach -e. This effect results in a square wave of induced charge response, $G(x)$, when $\lambda = 0$.

It is now necessary to examine the charge density under the above conditions, e.g., when the electron velocity approaches the speed of light. As the electron's field is transformed to a plane, the induced charge density on the cylinder must be infinite where the plane of the field of the electron intersects the cylinder. This infinite charge density, however, is only over an infinitesimal section of the cylinder, and the product of the infinite charge density and the infinitesimal width must converge to the charge on the electron.

To examine the polarization of the charge density on the cylindrical detector, it is necessary to turn to the mathematical theory of relativity, (Reference 3). If it is assumed that electric charge is conserved in transformations

Here:

$$dq = \rho\, dx\, dy\, dz,$$

$$dq' = \rho' dx' dy' dz',$$

where dx dy dz, and dx'dy'dz' are volume elements in the stationary and moving coordinate systems respectively, and ρ and ρ' are the charge densities in the two coordinate systems. The charge densities and the volume elements are not invarient in the transformation:

$$\rho \neq \rho' ,$$

$$dV \neq dV'.$$

Suppose a four-dimensional volume element be introduced:

$$d\tau = dxdydz\, jcdt,$$

which must be invarient in the coordinate system transformations. In the four-dimensional frame of reference, such transformations are merely rotations of an axis; hence:

$$d\tau = dxdydzjcdt = dx'dy'dz'jcdt' = d\tau' \qquad (23)$$

In this frame of reference, charge density can be shown to be the fourth component of a four vector representation of current, or:

$$i_4 = jc\rho \qquad (24)$$

In terms of the primed and unprimed coordinate systems previously defined, the charge density on the cylindrical

positively defined, the charge density on the ellipsoid

In terms of the retard and advanced potentials

$$\phi = \tfrac{1}{2}(\phi_r + \phi_a) \qquad (24).$$

centred, or:

the fourth component of a four vector representation of

In this frame of reference, charge density can be shown to

$$\rho' = \text{density factor} \times d\tau/d\tau_0' \times \rho = \rho_0' \qquad (23)$$

transformations are merely rotations of an axial vector

tions. In the four-dimensional frame of reference, such

which must be invariant in the coordinate system transforma-

$$\rho' = \text{density factor}.$$

Suppose a two-dimensional volume element be intro-

duced:

$$d\tau = d\tau_0'.$$

$$\rho = \rho_0'.$$

are not invariant in the transformation:

ρ and ρ_0' are the charge densities in the two coordi-

nate systems. The charge densities and the volume elements

stationary and moving coordinate systems respectively, and

where $d\tau$ $d\tau_0'$, and $d\tau'$ $d\tau_0'$ are volume elements in the

$$d\tau' = \rho_0' d\tau_0' d\tau_0',$$

$$d\tau = \rho\, dx\, dy\, dz.$$

Here:

detector becomes, in tensor form:

$$i_4 = j\rho \quad = \sum_i \; a_{4i} i'. \tag{25}$$

Where a_{4i} are tensor components given by:

$$a_{ij} = \begin{vmatrix} K & 0 & 0 & j\beta K \\ 0 & 1 & 0 & 0 \\ 0 & 0 & 1 & 0 \\ -j\beta K & 0 & 0 & K \end{vmatrix} \tag{26}$$

(of which only the bottom row are of interest), and i' is a four vector representing the current as seen from the electron's coordinate system, a simple static problem. (In equation (26), $K = [1-\beta^2]^{-\frac{1}{2}}$ and $\beta = \frac{v}{c}$.) Thus:

$$i_1' = 0$$

$$i_2' = 0$$

$$i_3' = 0$$

$$i_4' = j\rho\rho'.$$

From which:

$$i_4 = a_{41} i_1' + a_{42} i_3' + a_{43} i_3' + a_{44} i_4' \tag{25}$$

$$= jK\rho\rho',$$

giving:

$$\rho = K\rho' \tag{27}$$

The following Lorentz transformation equations will also be required:

be rederived.

The coefficient tensor L_{ijkl} is symmetrical with respect to the

$$L = \tfrac{1}{2} L_{ijkl} \tag{51}$$

first:

$$= \tfrac{1}{2} L_{ijkl} \delta_{ik} \delta_{jl} .$$

$$T^{ik} = \tfrac{1}{2} L_{ijkl} \left(\delta_{ik} \delta_{jl} + \delta_{il} \delta_{jk} \right) \tag{53}$$

Also write:

$$T^{ik}_{jl} = \tfrac{1}{2} L_{ijkl} .$$

$$T^{23}_{23} = 0$$

$$T^{31}_{31} = 0$$

$$T^{12}_{12} = 0$$

$$T^{11} = 0$$

Equation (52) $\varepsilon = \left[1 - (\xi_2)^2 \right]^{\frac{1}{2}}$ and $\xi_2 = \frac{c}{a}$ [1] Hunter, Proc. Royal Society A, "A simple effective Rayleigh problem." (In a long radius ellipsoid the overload is near that on the equator only the factor can take of influence), and T_{ik} is

$$T^{11} = \begin{vmatrix} -\frac{1}{2} L_{1k} & 0 & 0 & \varepsilon \\ 0 & 1 & 0 & 0 \\ 0 & 0 & 1 & 0 \\ \varepsilon & 0 & 0 & \frac{1}{2} L_{1k} \end{vmatrix} \tag{52}$$

Since T^{ik} has tensor characteristics:

$$T^{ik} = \sum_{r}^{1} \quad \text{with} \quad T_{ik} . \tag{53}$$

determ proceeds, in tensor form:

$$z' = K(z + vt) \tag{28}$$

$$t' = K(t + \frac{\beta}{c} z) \tag{29}$$

$$y' = y \tag{30}$$

$$x' = x \tag{31}$$

If equations (27) to (31) are substituted into equation (13), an expression valid for relativistic electron velocities will be obtained:

$$\sigma = \frac{1}{\sqrt{1-\beta^2}} \frac{e}{2\pi a^2} \sum_{n=1}^{\infty} \frac{\epsilon^{-\mu_n \left| \frac{z + vt}{\sqrt{1-\beta^2}} \right|}}{J_1(\mu_n a)} \quad . \tag{32}$$

This expression must now be integrated over the length of the cylindrical detector, thus defining the total charge Q(t). As equation (32) is in the coordinate system of the cylinder, the limits of integration are $-\frac{L}{2}$ and $+\frac{L}{2}$. This integration process must be handled cautiously since the charge density becomes infinite as β approaches 1.

$$Q = K \frac{e}{a} \sum_{n=1}^{\infty} \frac{1}{J_1(\mu_n a)} \int_{-\frac{L}{2}}^{+\frac{L}{2}} \epsilon^{-\mu_n K |z + vt|} dz \quad . \tag{33}$$

Again, it is necessary to divide the integral into several special cases to permit the removal of the absolute value signs around $|z + vt|$. Thus, when $vt > \frac{L}{2}$:

$$Q = \frac{2e}{a} \sum_{n=1}^{\infty} \frac{\epsilon^{-\mu_n K vt} \sinh \mu_n K \frac{L}{2}}{\mu_n J_1(\mu_n a)} \quad . \tag{34}$$

$$\Omega = \frac{\omega}{2c} \sum_{k=1}^{\infty} \frac{h^2 \tau'(h^2 a)}{\tau(h^2 a)} \, e^{-h^2 K a t} \sin \pi h^2 K \frac{\pi}{2} \quad . \tag{34}$$

since $\sin \pi n = 0$ if n is an integer. Then, upon $at > \frac{\pi}{2}$:

$$\Omega = K \frac{\omega}{2c} \sum_{k=1}^{\infty} \frac{\tau'(h^2 a)}{\tau(h^2 a)} \int_{-\frac{\pi}{2}}^{+\frac{\pi}{2}} e^{-h^2 K |p + q_1|^2} \, dp \quad . \tag{35}$$

the circle property becomes initially $\sqrt{3}$ multicomplex I. This integration process must be pursued analytically since $\frac{\pi}{2}$ and $+\frac{\pi}{2}$. $\eta(s)$. An addition (35) is in the coordinate system of the elliptical detector, thus omitting the usual circle of the cylindrical detector, thus omitting the usual circle

This expression must also be integrated over the length

$$C = \frac{1}{4^{1-\beta_2}} \frac{\pi \omega_0}{c} \sum_{k=1}^{\infty} \frac{\tau'(h^2 a)}{\tau(h^2 a)} \, e^{-h^2 \left| \frac{\lambda^{1-\beta_2}}{\beta + \omega_2} \right|} \quad . \tag{36}$$

(33)' an expression valid for relativistic elevation velocities will be obtained:

If equations (31) to (37) are modified into dimensionless

$$x_1 = x \tag{37}$$

$$\lambda_1 = \lambda \tag{38}$$

$$\beta_1 = \beta(\beta + \frac{c}{\omega}) \tag{39}$$

$$\gamma_1 = \beta(\beta + \lambda \beta) \tag{40}$$

Examining equation (34) in detail, it will be noted that Q approaches 0 for all x's greater than L/2 when K approaches ∞. This was predicted previously from physical reasoning.

The second part of the integration of equation (32) is the case when $-\frac{L}{2} < vt < \frac{L}{2}$. This gives:

$$Q = K \frac{e}{a} \sum_{n=1}^{\infty} \frac{1}{J_1(\mu_n a)} \left[\int_{-\frac{L}{2}}^{-x} \epsilon^{\mu_n K (z+vt)} dz + \int_{-x}^{\frac{L}{2}} \epsilon^{-\mu_n K (z+vt)} dz \right] \quad (35)$$

$$Q = \frac{2e}{a} \sum_{n=1}^{\infty} \frac{(1 - \epsilon^{-\mu_n K \frac{L}{2}} \cosh \mu_n K vt)}{\mu_n J_1(\mu_n a)} . \quad (36)$$

Examining equation (36) as K approaches ∞, it will be noted that between the given limits for vt the value of Q converges to unity.

This provides some substantiation for the validity of equations (34) and (36), which have as a limit the square wave of Q(t) deduced from physical reasoning.

It is now necessary to extend the above calculations to include the case of a distributed charge having a characteristic linear charge density. The charge density of the electron beam will be calculated assuming that a pure sinusoidal

[illegible] there will be uniformly convergent over a finite simultaneous Laplace domain $\mathcal{D}$. The double integral of the right-hand member of a significant circle around a singularity of $\Phi(s)$ [illegible] the case of a significant circle around a singularity of $\Phi(s)$ [illegible] the case of a significant circle around a singularity of $\Phi(s)$ [illegible] the case

driving voltage is impressed upon the grid of a cathode-ray tube. Specifications of the ALLEN B. DuMONT LABORATORIES, INC. indicate that the average cathode-ray tube grid drive characteristics may be represented by a parabola of the form:

$$i = Cd^2, \tag{37}$$

where i is the beam current, C, a constant of proportionality, and d, the grid drive (i.e., the grid voltage above cut-off). If the tube is biased to cut-off and a sinusoidal driving voltage applied, for a single period the form of the driving function will be:

$$d = 0 \quad : \quad -\pi < \omega t < -\frac{\pi}{2}$$

$$d = E_m \cos \omega t \quad : \quad -\frac{\pi}{2} < \omega t < \frac{\pi}{2}$$

$$d = 0 \quad : \quad \frac{\pi}{2} < \omega t < \pi$$

or the positive part of a cosine wave. Then, since the current may be expressed as:

$$i = \Lambda v,$$

where Λ is the linear charge density of the electron beam and v the electron velocity, the charge density of the cathode-ray tube electron beam is:

$$\Lambda = \frac{C}{v} \frac{E_m^2}{2} (1 + \cos 2\omega t); \tag{38}$$

and zero over the remainder of the cycle.

The linear charge density function given in equation (38) may be used as follows from the determination of the

(38) may be seen to follow from the requirements of the one-to-one electron beam tube:

$$V = \frac{h}{e}\frac{\omega}{2\pi}(1 + \cos 2\pi\theta); \tag{38}$$

where V is the Linear charge density of the electron beam and θ the electron velocity, the charge density of the beam must vary as:

$$\rho = \rho_0(1 + \cos 2\pi\theta);$$

or the positive half of a cosine wave. Then, using the current must vary as:

$$i = \rho_0 v;$$

$$i = \rho_0 v_0(1 + \cos 2\pi\theta);$$

$$i = i_0(1 + \cos 2\pi\theta); \tag{39}$$

where i is the beam current, i_0 a constant of proportionality, and θ, the grid drive (i.e., the grid voltage above cut-off). If the tube is biased to cut-off and a sinusoidal driving voltage applied, for a single period the flow of the varying function will be:

$$\theta = 0 \qquad -\tfrac{1}{4} < \omega t < \tfrac{1}{4}$$

$$\theta = \cos \omega t \qquad \tfrac{1}{4} < \omega t < \tfrac{3}{4}$$

$$\theta = 0 \qquad \tfrac{3}{4} < \omega t < \tfrac{5}{4}$$

potential inside an infinite cylinder due to the line charge at the origin. This will require that $|z-\xi|$* be substituted for $|z|$ in equation (11). An integral of this function over ξ gives a potential function which may be treated as already described. This method may be indicated symbolically for the non-relativistic case as follows:

The element of potential dV due to an element of charge $\Lambda\, d\xi$ is:

$$dV = \frac{\Lambda\, d\xi}{2\pi\varepsilon_0 a^2} \sum_{r=1}^{\infty} \frac{\epsilon^{-\mu_r |z-\xi|}}{\mu_r [J_1(\mu_r a)]^2} J_0(\mu_r \rho) \,. \tag{11a}$$

If the total charge is integrated from $-\infty$ to $+\infty$ (considering a single bunch of electrons only, defined as above), the total potential at any point inside the infinite cylinder will be given by:

$$V = \frac{1}{2\pi\varepsilon_0 a^2} \sum_{r=1}^{\infty} \frac{J_0(\mu_r \rho)}{\mu_r [J_1(\mu_r a)]^2} \int_{-\infty}^{+\infty} \Lambda(\xi)\, \epsilon^{-\mu_r |z-\xi|}\, d\xi \,. \tag{11b}$$

The normal derivative of this function will give the surface charge density on the cylinder. Applying equation (12), the charge density is found to be:

$$\sigma = \frac{1}{2\pi a^2} \sum_{r=1}^{\infty} \frac{1}{J_1(\mu_r a)} \int_{-\infty}^{+\infty} \Lambda(\xi)\, \epsilon^{-\mu_r |z-\xi|}\, d\xi \,. \tag{13a}$$

---

* ξ indicates the location of an element of charge $\Lambda\, d\xi$. The time variable of equation (38) must be changed to a space variable.

$$Q = \frac{2\pi\sigma_0}{l}\sum_{h=1}^{\infty}\frac{1}{\tau'(h^2\alpha)}\int_{-\infty}^{+\infty} V(z)\, e^{-h'|\beta-z|}\, dz\,. \qquad (12a)$$

(12), the charge density is found to be

then charge density on the cylinder. Applying notation

The normal derivative of this function will give the sur-

$$\Lambda = \frac{2\pi\sigma_0}{l}\sum_{h=1}^{\infty}\frac{h'[\tau'(h'\alpha)]^2}{\tau(h'\alpha)}\int_{-\infty}^{+\infty} V(z)\, e^{-h'|\beta-z|}\, dz\,. \qquad (12b)$$

Limits of this number will be given by:

$$\frac{2\pi\sigma_0}{l}\sum_{h=1}^{\infty}\frac{h'[\tau'(h'\alpha)]^2}{\tau(h'\alpha)}\int_{-\infty}^{+\infty} V(z)\, e^{-h'|\beta-z|}\, dz\,. \qquad (12b)$$

If the total charge is integrated from $-\infty$ to $+\infty$ (generating a single number of electrons only, defined as above), the total potential at any point inside the interval $V\equiv 1$ is:

$$dA = \frac{2\pi\sigma_0}{V}\sum_{h=1}^{\infty}\frac{h'[\tau'(h'\alpha)]^2}{\tau(h'\alpha)}\, e^{-h'|\beta-z|}\,. \qquad (12c)$$

The element of potential dA due to an element of charge $V\,dz$ is:

follows:

modified slightly from the non-relativistic case as

$$dA = \frac{2\pi\sigma_0}{V}\sum_{h=1}^{\infty}\frac{h'[\tau'(h'\alpha)]^2}{\tau(h'\alpha)}\, e^{-h'|\beta-z|}\,. \qquad (12c)$$

If the total charge is integrated from $-\infty$ to $+\infty$ (generating a single number of electrons only, defined as above), the total potential at any point inside the interval $V\equiv 1$ is:

Limits of this number will be given by:

$$\frac{2\pi\sigma_0}{l}\sum_{h=1}^{\infty}\frac{h'[\tau'(h'\alpha)]^2}{\tau(h'\alpha)}\int_{-\infty}^{+\infty} V(z)\, e^{-h'|\beta-z|}\, dz\,. \qquad (12b)$$

The normal derivative of this function will give the surface charge density on the cylinder. Applying notation (12), the charge density is found to be:

$$Q = \frac{2\pi\sigma_0}{l}\sum_{h=1}^{\infty}\frac{\tau'(h'\alpha)}{l}\int_{-\infty}^{+\infty} V(z)\, e^{-h'|\beta-z|}\, dz\,. \qquad (12a)$$

---

* z indicates the location of an element of charge $V\,dz$.
The first derivative of equation (12) must be changed in a
minus direction.

The charge on a segment of the infinite cylinder is found by summing over z from $-\frac{L}{2}$ to $+\frac{L}{2}$:

$$Q(x) = \int_{x-\frac{L}{2}}^{x+\frac{L}{2}} \sigma\, 2\pi a\, dz = \frac{1}{a} \sum_{r=1}^{\infty} \frac{1}{J_1(\mu_r a)} \int_{x-\frac{L}{2}}^{x+\frac{L}{2}} \int_{-\infty}^{+\infty} \epsilon^{-\mu_r |z-\xi|} \Lambda(\xi)\, d\xi\, dz \,. \qquad (16a)$$

An alternate method of calculation would start with the charge function for a point charge given by equation (16), and apply this function as a weighing function to the linear charge density as follows:

$$Q(x) = \int_{-\infty}^{+\infty} \frac{\Lambda(\xi)\, d\xi}{a} \sum_{r=1}^{\infty} \frac{1}{J_1(\mu_r a)} \int_{(x-\xi)-\frac{L}{2}}^{(x-\xi)+\frac{L}{2}} \epsilon^{-\mu_r |z|}\, dz \,, \qquad (39)$$

where the x of equation (16) has been replaced by $(x - \xi)$ since the line charge extends symmetrically from x in the ξ direction.

By a change of variable $z = z_1 - \xi$, equation (39) can be shown to become identical with (16a). Hence, the determination of the induced charge on a cylindrical detector when a linearly distributed charge passes down its axis involves only the evaluation of the integral:

$$\int_{x-\frac{L}{2}}^{x+\frac{L}{2}} \int_{-\infty}^{+\infty} \epsilon^{-\mu_r |z-\xi|} \Lambda(\xi)\, d\xi\, dz \qquad (40)$$

$$\int_{x-\frac{1}{2}}^{x+\frac{1}{2}} \int_{-\infty}^{+\infty} V(\xi)\, q\xi\, q\rho\, e^{-h^2\beta\,|\xi|} \tag{35}$$

solves only the solution of the Poisson:

$$\Delta\varphi = \frac{1}{\varepsilon_0}\rho$$

where Δ denotes the Laplacian operator. Hence, the derivation of the induced charge by a dielectric sphere in uniform field will be given in Section 4. Here, the derivation of the ε dependence of capacity $c = 4\pi\varepsilon_0 r$, equation (39) may be given.

ε dielectric.

Since the Ewald-Kornfeld formulation (12) has been replaced by ($\varepsilon = \varepsilon$) above the x of equation (12) has been replaced by ($\varepsilon - \varepsilon$)

$$\sigma(x) = \int_{-\infty}^{+\infty} \frac{a}{V(\xi)\, q\xi} \sum_{h=1}^{\infty} \frac{1}{1} \int_{(x-\xi)-\frac{1}{2}}^{(x-\xi)+\frac{1}{2}} e^{-h\beta|\xi|}\, q\rho \,, \tag{38}$$

where convert is follows:

We alternate method of calculation would start with the simple Ewald solution for a point charge given by equation (12),

$$\sigma(x) = \int_{x-\frac{1}{2}}^{x+\frac{1}{2}} a\, \varepsilon a\, aq\rho = \frac{a}{1} \sum_{h=1}^{\infty} \frac{1}{1} (h^2 a) \int_{x-\frac{1}{2}}^{x+\frac{1}{2}} \int_{-\infty}^{+\infty} V(\xi)\, q\xi\, q\rho \cdot e^{-h^2\beta-\xi|} \tag{12e}$$

It remains to be shown that $-\frac{5}{r}$ as $+\frac{5}{r}$:

and its modification as the electron velocity approaches relativistic speeds.

Changing variables of equation (38) from those of time to ξ, the space variable associated with the density distribution of the electron beam, $2\omega t$ becomes $\frac{4\pi}{\lambda}\xi$, where λ is the distance between adjacent maximum density points of the electron beam and is a function of the electron velocity. Thus, integral (40) becomes:

$$\int_{x-\frac{\ell}{2}}^{x+\frac{\ell}{2}} \int_{-\frac{\lambda}{4}}^{\frac{\lambda}{4}} \epsilon^{-\mu_r |z-\xi|} \Lambda_0 \left(1 + \cos \frac{4\pi}{\lambda}\xi\right) d\xi\, dz \quad . \tag{40a}$$

To perform the operation indicated above, the absolute value signs must be removed. This changes integral (40) to:

$$\int_{x-\frac{\ell}{2}}^{x+\frac{\ell}{2}} \left[\int_{-\frac{\lambda}{4}}^{z} \epsilon^{-\mu_r (z-\xi)} \Lambda_0 \left(1 + \cos \frac{4\pi}{\lambda}\xi\right) d\xi \; + \right.$$

$$\left. \int_{z}^{\frac{\lambda}{4}} \epsilon^{-\mu_r (\xi - z)} \Lambda_0 \left(1 + \cos \frac{4\pi}{\lambda}\xi\right) d\xi \right] dz \quad , \tag{40b}$$

where $-\frac{\lambda}{4} < z < \frac{\lambda}{4}$. In the integrals (40a) and (40b), the limits of integration of ξ are $-\frac{\lambda}{4}$ and $+\frac{\lambda}{4}$ since only a single pulse is defined between these limits. Actually,

a single bump is derived between zero and infinity. Adamsii's limits of integration of π were $-\frac{\phi}{2}$ and $+\frac{\phi}{2}$ minus only minus $-\frac{\phi}{2} < \vartheta < \frac{\phi}{2}$. In the relativity (1928) case (1924)' the

$$\int_{-\frac{\phi}{2}}^{\frac{\phi}{2}} \epsilon^{-h'(\frac{\pi}{2}-\frac{\vartheta}{2})} V^{\circ}(1+\cos^2\frac{\vartheta}{2})\, q\epsilon \, dq \quad + \quad (1928)$$

$$\int_{\frac{\pi}{2}}^{\frac{3\pi}{2}} \epsilon^{-h'(\vartheta-\frac{\pi}{2})} V^{\circ}(1+\cos^2\frac{\vartheta}{2})\, q\epsilon \, dq \quad +$$

$$\int_{\frac{3\pi}{2}}^{\frac{5\pi}{2}} \epsilon^{-h'(\frac{5\pi}{2}-\vartheta)} V^{\circ}(1+\cos^2\frac{\vartheta}{2})\, q\epsilon \, dq$$

either must be removed. Into standard integral (1924) so: to perform the integration indicated above, the upsilon axis

$$\int_{\frac{\pi}{2}}^{\frac{5\pi}{2}} \epsilon^{-h'(\vartheta-\frac{\pi}{2})} V^{\circ}(1+\cos^2\frac{\vartheta}{2})\, q\epsilon \, dq \quad . \quad (1928)$$

time velocity. Then, integral (1924) becomes:

$$V \quad \text{is the distance between adjacent minima caused}$$

by the electron beam and is a function of the elec-

tron velocity. Adamsii's [1924] derivation of the diffraction pattern, $\sin\vartheta = \frac{V}{\phi_{\mu}}\pi$, where ϑ is the phase angle associated with the density

Compiling derivation of equation (321 from Phase of relativistic change.

any its modification -- the significant material difference

in a cathode-ray tube modulated at 50 megacycles, the pulses will be repeated at intervals of λ . Despite these repetitions, interaction effects may be assumed negligible.

Performing the integration of (40b):

$$F(x) = \int_{x-\frac{L}{2}}^{x+\frac{L}{2}} \Lambda_0 \left[\frac{2}{\mu_r} \left(1 - \epsilon^{-\mu_r \frac{\lambda}{4}} \cosh \mu_r z\right) \right. \tag{41}$$

$$\left. + \frac{2}{\mu_r} \frac{\mu_r^2}{\mu_r^2 + \left(\frac{4\pi}{\lambda}\right)^2} \left(\cos \frac{4\pi}{\lambda} z + \epsilon^{-\mu_r \frac{\lambda}{4}} \cosh \mu_r z \right) \right] dz .$$

As F(x) is defined only for $-\frac{\lambda}{4} < z < \frac{\lambda}{4}$, the region of definition for x is:

$$-\frac{\lambda}{4} + \frac{L}{2} < x < \frac{\lambda}{4} - \frac{L}{2}$$

Performing the indicated operations of equation (41), F(x) is found to be:

$$F(x) = \Lambda_0 \frac{\mu_r}{2} \left[L - \epsilon^{-\mu_r \frac{\lambda}{4}} \left(\sinh \mu_r \frac{L}{2} \cosh \mu_r x \right) \left(1 - \frac{1}{1 + \left(\frac{4\pi}{\mu_r \lambda}\right)^2}\right) \right. \tag{42}$$

$$\left. + \frac{1}{1 + \left(\frac{4\pi}{\mu_r \lambda}\right)^2} \frac{\lambda}{2\pi} \sin \frac{2\pi}{\lambda} L \cos \frac{4\pi}{\lambda} x \right] .$$

$$+\frac{1+\left(\frac{h_r y}{\pi a}\right)^2}{1}\cdot\frac{\pi a}{y}\sin\frac{y}{\pi a}\pi\cos^2\frac{y}{d a}x\Bigg]\,.$$

(B3)

$$F(x)=V_0\frac{5}{h_r}\left[\Gamma-\epsilon^{-h_r\frac{d}{y}}\left(\sinh h_r\tfrac{5}{\Gamma}\cos p\, h_r x\right)\left(1-\frac{1}{1+\left(\frac{h_r y}{a a}\right)^2}\right)\right.$$

Furthermore the indicated operations of equation (A2)"

$F(x)$ is found to be

$$-\frac{d}{y}+\frac{5}{\Gamma}<x<\frac{d}{y}-\frac{5}{\Gamma}$$

Performing the integration of $(A2)$:

$$F(y)=\int_{x-\frac{5}{\Gamma}}^{x+\frac{5}{\Gamma}}V_0\left[\frac{h_r}{5}\left(1-\epsilon^{-h_r\frac{d}{y}}\cos p\, h_r\beta\right)\right.$$

(A2)

$$+\frac{h_r}{5}\frac{h_r+\left(\frac{y}{a a}\right)^2}{h_r^2}\left(\cos\frac{y}{a a}\beta+\epsilon^{-h_r\frac{d}{y}}\cos p\, h_r\beta\right)\Big]d\beta\,.$$

We $F(x)$ is defined only for $-\frac{d}{y}<x<\frac{d}{y}$. the region of

integration for x is:

Thus, the desired function, Q, is:

$$Q(vt) = \frac{1}{a} \sum_{n=1}^{\infty} \frac{1}{J_1(\mu_n a)} F(x) \quad . \tag{43}$$

If λ may be assumed large enough to make the term $(\frac{4\pi}{\mu_n \lambda})^2$ small compared to one, the quantity $\left[1 - \frac{1}{1+(\frac{4\pi}{\mu_n \lambda})^2}\right]$ in equation (42) will become essentially negligible. The wave length of the electron beam will become large enough to fulfill the above conditions for electron velocities greater than 0.1 c, or for acceleration voltages greater than 3 kv. (These conditions will be fulfilled in the experimental section of this thesis.) Thus, equation (43) reduces to:

$$Q(vt) = \Lambda \left[L + \frac{\lambda}{2\pi} \sin \frac{2\pi}{\lambda} L \cos \frac{4\pi}{\lambda} x \right] \sum_{n=1}^{\infty} \frac{2}{\mu_n a J_1(\mu_n a)} \quad . \tag{44}$$

The term $\sum_{n=1}^{\infty} \frac{2}{\mu_n a J_1(\mu_n a)}$ has been found equal to unity by equation (14), giving for the induced charge function:

$$Q(t) = \Lambda_0 \left[L + \frac{\lambda}{2\pi} \sin \frac{2\pi}{\lambda} L \cos \frac{4\pi}{\lambda} vt \right]. \tag{45}$$

To understand the implications of equation (45), consider the following simplified method of computing the charge function when the electron beam is traveling at the velocity of light. The field of the electrons is everywhere perpendicular to the axis of the beam and the induced charge on

$$\eta(x) = \frac{b}{\pi} \sum_{k=1}^{\infty} \frac{1}{J_1(k'_0)} L(x) \,. \qquad (23)$$

Thus, the desired function, η, is

dimple to the axis of the beam and the induced charge on of light. The field of the electron is axisymmetric- function when the electron beam is traveling at the velocity the following simplified method of computing the charge to understand the implications of equation (19), consider

$$\mathcal{Q}(t) = V_0 \left[\Gamma + \frac{y}{z_0} \sin \frac{z_0}{d_0} \Gamma \cos \frac{y}{d_0} \omega t \right]. \qquad (25)$$

equation (24), giving for the induced charge function

The term $\sum_{k=1}^{\infty} \frac{k_0 \, J_1(k'_0)}{2}$ has been found equal to unity by

$$\mathcal{Q}(\omega t) = V \left[\Gamma + \frac{z_0}{y} \sin \frac{y}{z_0} \Gamma \cos \frac{y}{d_0} x \right] \sum_{k=1}^{\infty} \frac{k_0 \, J_1(k'_0)}{2} \,. \qquad (27)$$

parimental section of this study.) Then, equation (23) reduces to:

$$\eta(x) = \frac{b}{\pi} \sum_{k=1}^{\infty} \frac{1}{J_1(k'_0)} L(x) \,. \qquad (23)$$

If y may be assumed large enough to make the term $\left(\frac{k'_0 y}{d_0}\right)^2$ small compared to one, the quantity $\left[1 - \frac{1}{1 + \left(\frac{k'_0 y}{d_0}\right)^2}\right]$ in equation (25) will become essentially unity. The same length of the electron beam will become large enough to fulfill the above conditions for electron velocities greater than 0.1c, or for accelerating voltages greater than 3 MV. (These conditions will be fulfilled in the ex- perimental section of this study.) Then, equation (23) reduces to:

the cylinder is just equal to the charge contained within the cylinder. The charge function will be of the form:

$$Q(t) = \int_{\omega t - \frac{L}{2}}^{\omega t + \frac{L}{2}} \Lambda_0 \left(1 + \cos \frac{4\pi}{\lambda} \xi\right) d\xi \tag{46}$$

$$Q(t) = \Lambda_0 \left[L + \frac{\lambda}{2\pi} \sin \frac{2\pi}{\lambda} L \cos \frac{4\pi}{\lambda} \omega t \right] . \tag{45}$$

This relation is identical to equation (45) derived previously. The term in equation (42):

$$\epsilon^{-\mu_r \frac{\lambda}{4}} \left(\sinh \mu_r \frac{L}{2} \cosh \mu_r x\right) \left(1 - \frac{1}{1 + \left(\frac{4\pi}{\mu_r \lambda}\right)^2}\right)$$

must then contain the correction for the fringing field of the electron bunch at non-relativistic velocities. Any corrections made to equation (43) to account for relativistic contraction of the electron's field must take place in this term. It must approach zero as K approaches ∞.

Suppose that λ is much greater than L. For this condition $\sin \frac{2\pi}{\lambda} L$ will almost equal $\frac{2\pi}{\lambda} L$, reducing equation (45) to:

$$Q(t) = L\Lambda_0 \left(1 + \cos \frac{4\pi}{\lambda} \omega t\right) = L\Lambda_0 (1 + \cos \omega t) . \tag{45a}$$

But equation (45a) is exactly the shape of the charge density of the electron beam multiplied by L. This proves that the

of the electron beam multiplied by E. This proves that the equation (45a) is exactly the shape of the charge density distribution $\sin\frac{y}{z_m}r$ will almost equal $\frac{y}{z_m}r$, reducing equation (45) to:

$$Q(t) = rV^o(1+\cos\tfrac{y}{d_m}vt) = rV^o(1+\cos\omega t) \quad . \tag{45a}$$

Suppose that y is much greater than L. For this condition the capacitance is just equal to the capacitance combined with the cavities. The charge variation will be of the form:

$$Q(t) = \int_{vt-\frac{s}{2}}^{vt+\frac{s}{2}} V^o(1+\cos\tfrac{y}{d_m}\xi)\,q\,\xi \tag{46}$$

$$Q(t) = V^o\left[r + \tfrac{z_m}{y}\sin\tfrac{y}{z_m}r\cos\tfrac{y}{d_m}vt\right] \quad . \tag{47}$$

This relation is identical to equation (45) derived previously. One term in equation (47):

$$e^{-W\frac{d}{y}}\left(\sinh W\tfrac{s}{2}\cosh Wx\right)\left(1-\frac{1+\left(\frac{Wy}{d_m}\right)^2}{1}\right)$$

must then contain the correction for the fringing field of the electron bunch at non-relativistic velocities. Any corrections made to equation (47) to account for relativistic contraction of the electron's field must take place in this term. It must approach zero as β approaches 1.

induced charge on the cylindrical detector almost exactly reproduces the charge density passing through it along its axis providing that the assumptions made in the above derivation continue to be valid. The constant L is present because only the charge within the cylinder contributes to the induced charge at the velocities considered in this derivation.

It must be emphasized that the above conclusion is correct only with the assumptions given when the linear charge is long compared with the cylindrical detector and when the charge density is a smooth curve tailing off on the ends.

If the impedance the detection circuit presents to the electron beam is assumed a pure capacitative reactance equal to $\frac{1}{j\omega C_o}$, the induced voltage function on the cylindrical detector becomes:

$$E(t) = \frac{L V_o}{C_o} (1 + \cos \omega t) . \qquad (47)$$

This function is shown in Fig. 4.

If these pulses are considered to be repeated with a definite period T, a Fourier analysis may be obtained of the function. The Fourier expansion will contain a constant term and cosine terms, as E(t) is an even function:

$$E(t) = \frac{a_o}{2} + \sum_{n=1}^{\infty} a_n \cos n\omega t , \qquad (48)$$

where a_o and a_n are given by:

where a_0 and a_n are given by:

$$E(t) = \frac{a_0}{2} + \sum_{n=1}^{\infty} a_n \cos n\omega t \ , \qquad (46)$$

time and noting terms, as $E(t)$ is an even function:

$$E(t) = \frac{E_0}{2} (1 + \cos \omega t) \ . \qquad (47)$$

This function is shown in Fig. 4.

If these pulses are considered to be separated with a definite period T, a Fourier analysis may be obtained of the function. The Fourier expansion will contain a constant

and cosine terms, as $E(t)$ is an even function:

$$E(t) = \frac{a_0}{2} + \sum_{n=1}^{\infty} a_n \cos n\omega t \ ,$$

where a_0 and a_n are given by:

$$a_0 = \frac{\angle \Lambda_\bullet}{C_\bullet} \tag{49}$$

$$a_n = \frac{\angle \Lambda_\bullet}{C_\bullet} \frac{1}{\pi} \left[-\frac{8}{n(n^2-4)} \right] \sin \frac{n\pi}{2} \tag{50}$$

When $\angle \frac{\Lambda_\bullet}{C_0}$ is expressed as E_m, E(t) can be written:

$$E(t) = E_m \left[.5 + .85 \cos \omega t + .5 \cos 2\omega t + .17 \cos 3\omega t \right.$$

$$\left. -.0243 \cos 5\omega t + .00806 \cos 7\omega t \ldots\ldots\ldots \right. \tag{51}$$

An idea of the number of harmonics necessary to reproduce the detector voltage function may be had from Fig. 5, where the constant term and three harmonics of the Fourier series are plotted.

$$B_n = \frac{C_o}{LV_o} \frac{1}{n\pi} \left[\frac{6}{n(n-1)} \right] \sin \frac{n\pi}{2} \qquad (50)$$

$$B_o = \frac{C_o}{LV_o} \qquad (49)$$

Since $t \frac{V_o}{C_o}$ is proportional as B_n, $E(t)$ must be evaluated:

$$E(t) = E_m \left[.2 + .82 \cos \omega t + .2 \cos 2\omega t + .17 \cos 3\omega t \right.$$

$$\left. - .02 \cos 5\omega t + .00806 \cos 7\omega t \right. \qquad (51)$$

An idea of the number of harmonics necessary to reproduce the capacitor voltage function may be had from Fig. 5, where the constant term and first seven harmonics of the Fourier series are plotted.

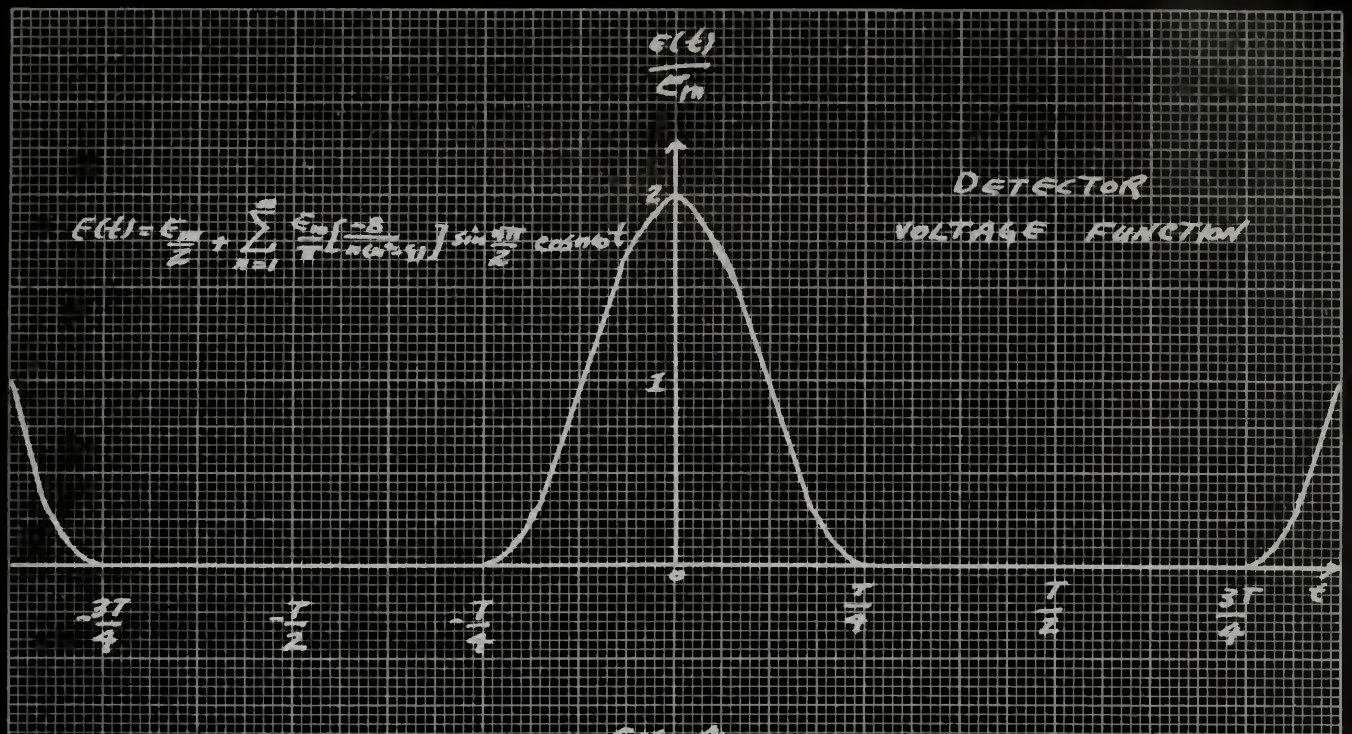
$\frac{e(t)}{E_m}$
$F(t) = \frac{E_m}{2} + \sum_{n=1}^{\infty} \frac{E_m}{\pi}\left[\frac{-\Delta}{n(\alpha-\gamma)}\right] \sin\frac{n\pi}{2} \cos n\omega t$
DETECTOR
VOLTAGE FUNCTION
2
1
0
$-\frac{3\pi}{4}$
$-\frac{\pi}{2}$
$-\frac{\pi}{4}$
$\frac{\pi}{4}$
$\frac{\pi}{2}$
$\frac{3\pi}{4}$
ωt

FIG. 4

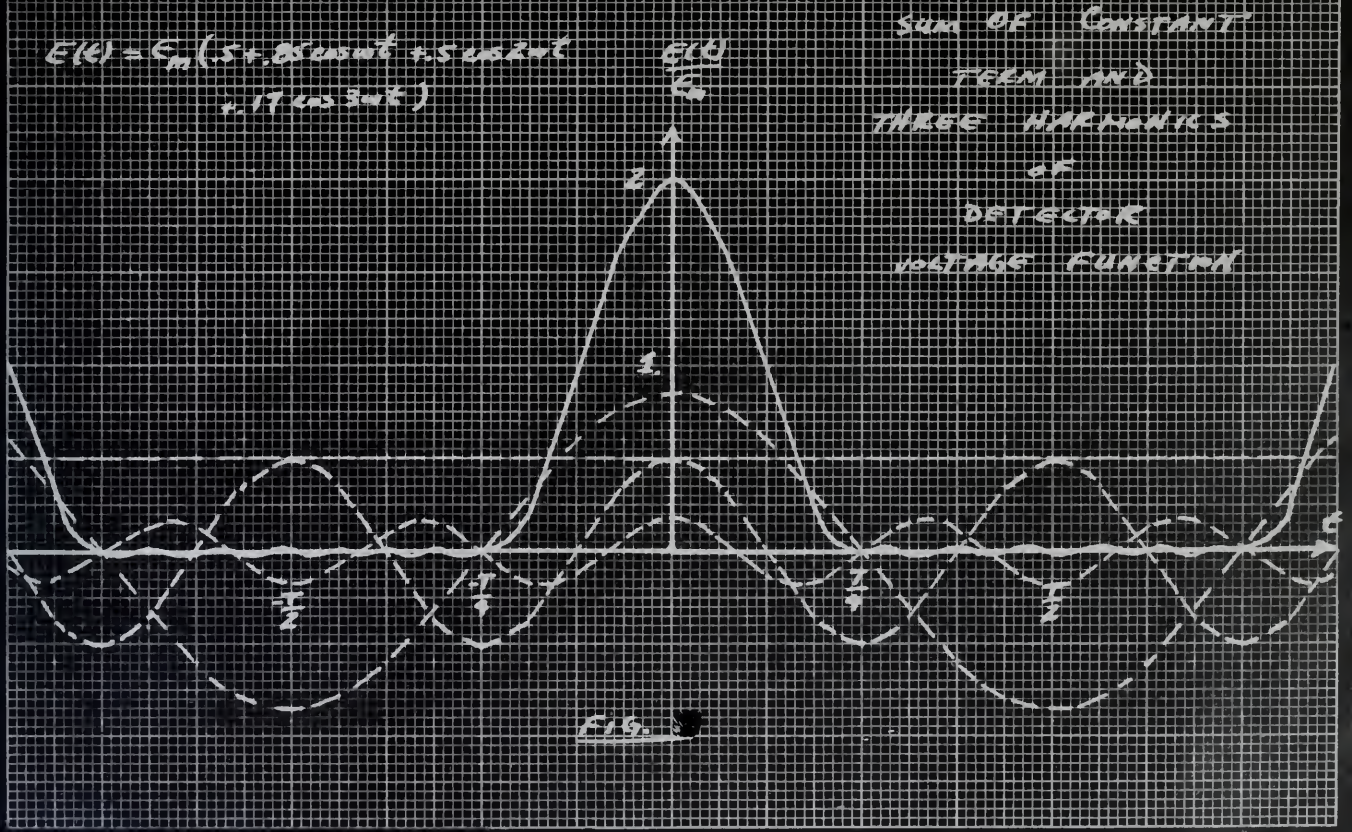
$E(t) = E_m(.5 + .85\cos\omega t + .5\cos 2\omega t + .17\cos 3\omega t)$
$\frac{e(t)}{E_m}$
SUM OF CONSTANT TERM AND THREE HARMONICS OF DETECTOR VOLTAGE FUNCTION
2
1
$-\frac{\pi}{2}$
$-\frac{\pi}{4}$
$\frac{\pi}{4}$
$\frac{\pi}{2}$
ωt

FIG. 5

APPENDIX 2

CONSTRUCTIONAL DRAWINGS OF DETECTOR HOUSING AND COLLECTOR PLATE

APPENDIX 2

CONSTRUCTIONAL DRAWINGS OF DEFLECTOR HOUSING
AND COLLECTOR PLATE

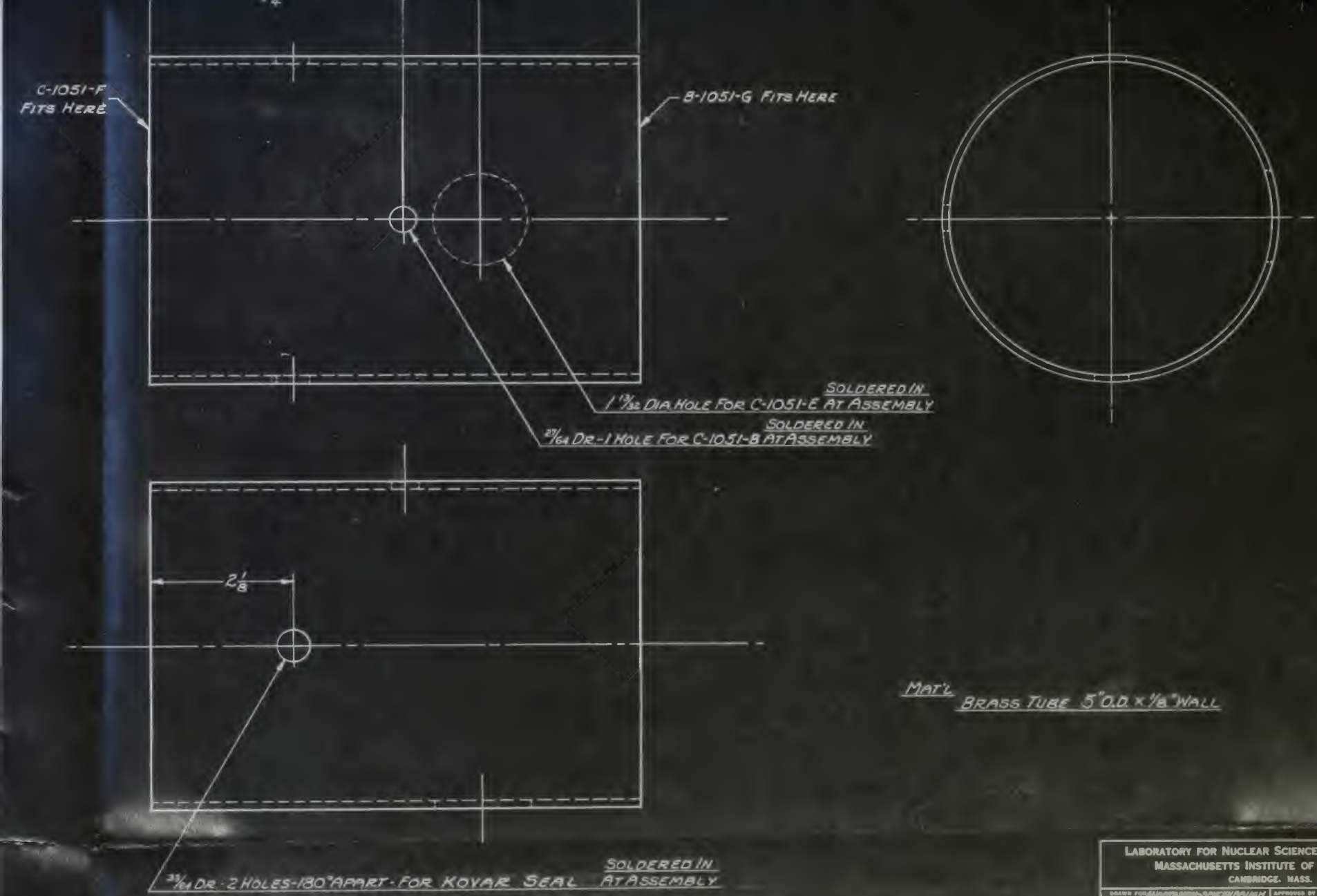

MAT'L BRASS TUBE 5" O.D. x 1/8" WALL

LABORATORY FOR NUCLEAR SCIENCE AND ENGINEERING
MASSACHUSETTS INSTITUTE OF TECHNOLOGY
CAMBRIDGE, MASS.

DRAWN FOR [illegible]	APPROVED BY
DRAWN BY SMITH	SCALE FULL SIZE
CHECKED BY A.M.D.	DATE NOV. 14 1947

TITLE:
DETECTOR HOUSING

DWG. NO. A-1051-A | FILE 6421

DWG. NO. C-1051-B

DWG. NO. C-1051-B

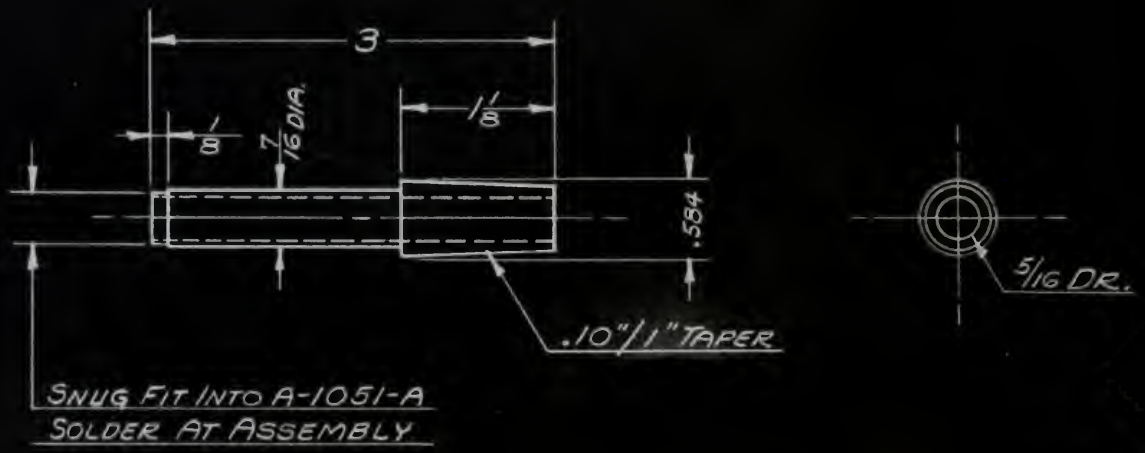

SNUG FIT INTO A-1051-A
SOLDER AT ASSEMBLY

MAT'L
BRASS

TOLERANCES ON MACHINING DIMENSIONS UNLESS OTHERWISE STATED:
FRACTIONAL ± 1/64" DECIMAL ± .005". ANGULAR ± 1/2°

LABORATORY FOR NUCLEAR SCIENCE AND ENGINEERING
MASSACHUSETTS INSTITUTE OF TECHNOLOGY
CAMBRIDGE, MASS.

DRAWN FOR ANASTASION-SENCENBAUGH	APPROVED BY
DRAWN BY SMITH	SCALE FULL SIZE
CHECKED BY	DATE DEC. 29, 1947

TITLE: IONIZATION GAUGE FITTING

DWG. NO. C-1051-B | FILE 6421

PRINTED BY BLUEPRINT SERVICE CO. BOSTON, MASS. RE ORDER NO A-220

DWG. NO. C-1051-C

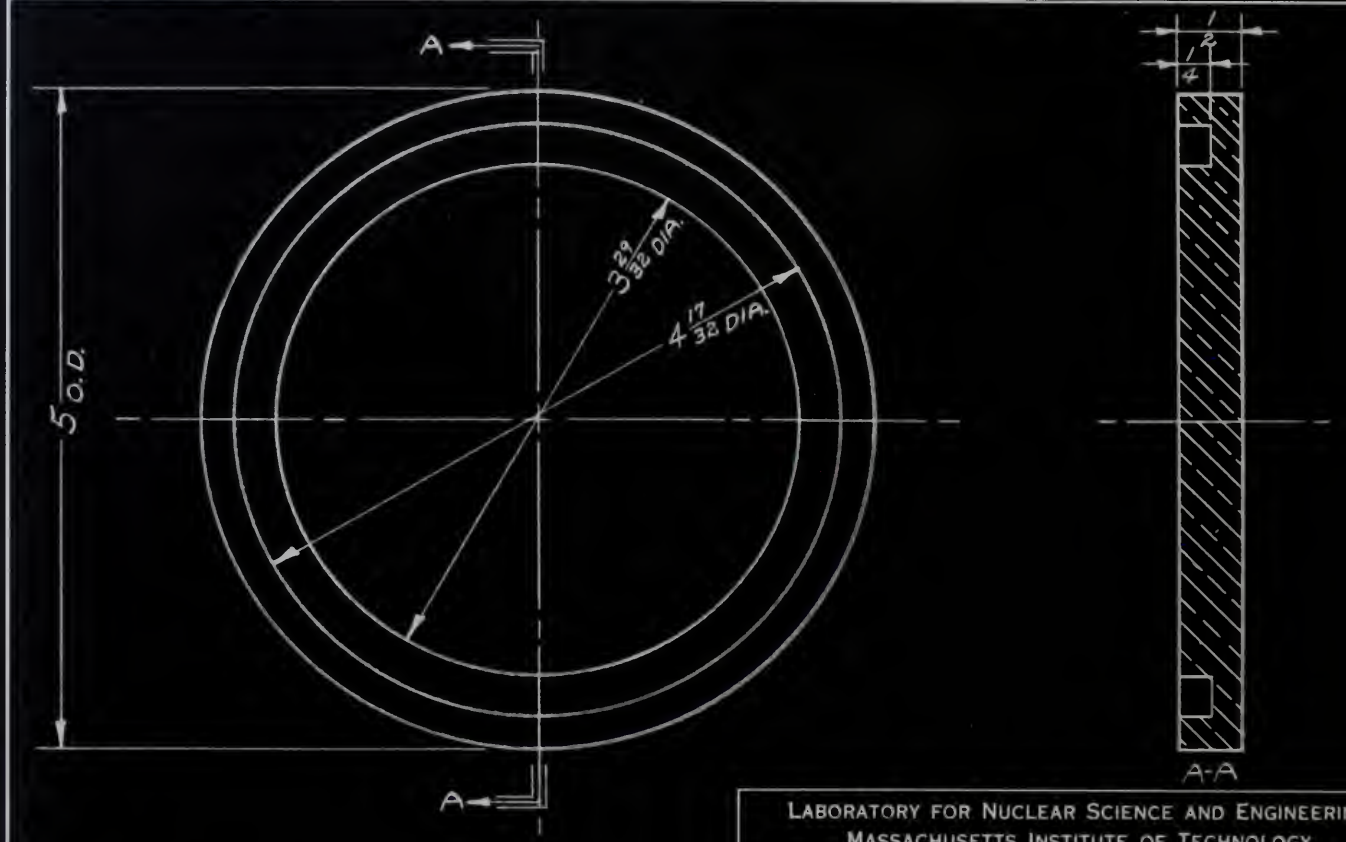

MAT'L BRASS

TOLERANCES ON MACHINING DIMENSIONS UNLESS OTHERWISE STATED:
FRACTIONAL ± 1/64". DECIMAL ± .005". ANGULAR ± 1/2°

PRINTED BY SPAULDING MOSS CO. BOSTON, MASS. RE ORDER NO. A-220

LABORATORY FOR NUCLEAR SCIENCE AND ENGINEERING
MASSACHUSETTS INSTITUTE OF TECHNOLOGY
CAMBRIDGE. MASS.

DRAWN FOR ANASTASION-SENCENBAUGH	APPROVED BY
DRAWN BY SMITH	SCALE FULL SIZE
CHECKED BY A.N.D.	DATE DEC. 29, 1947

TITLE: COLLECTOR PLATE

DWG. NO. C-1051-C | FILE 6421

DWG. NO. C-1051-C

C-1051-D ON 3MD

DWG. NO. C-1051-D

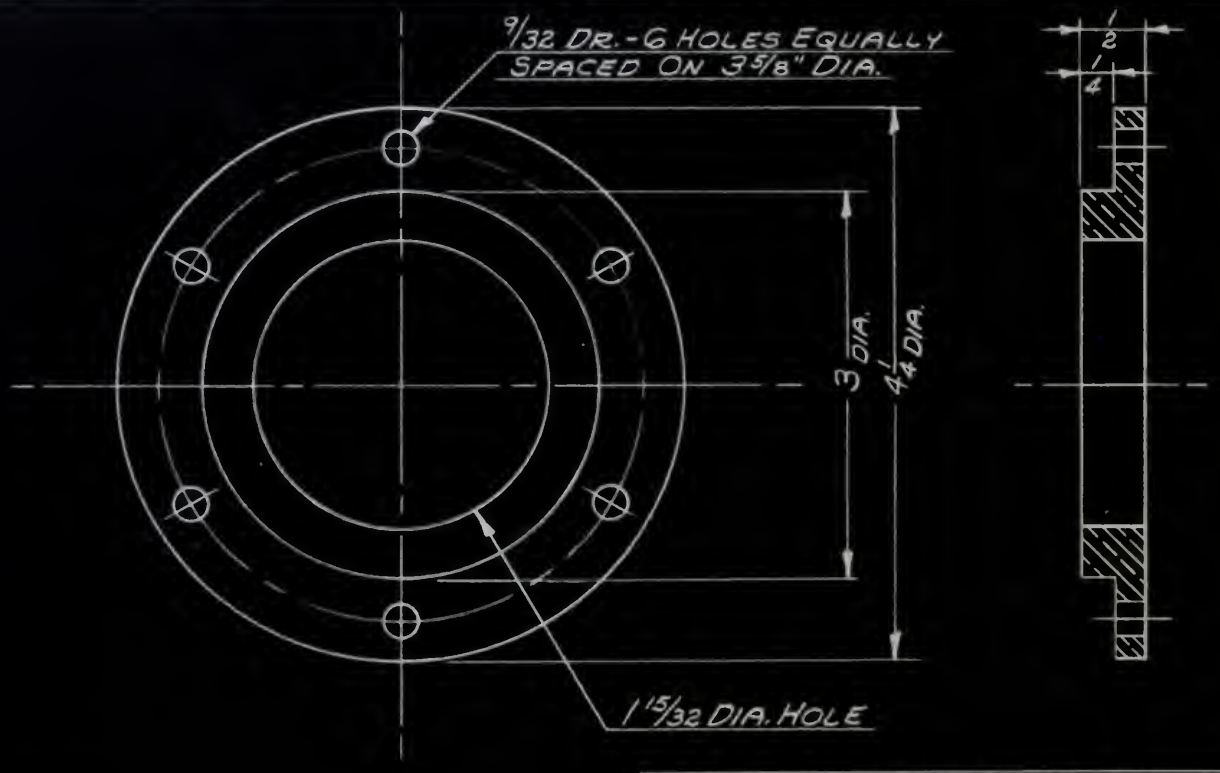

MAT'L BRASS

LABORATORY FOR NUCLEAR SCIENCE AND ENGINEERING
MASSACHUSETTS INSTITUTE OF TECHNOLOGY
CAMBRIDGE. MASS.

DRAWN FOR ANASTASION-SENCENBAUGH	APPROVED BY
DRAWN BY SMITH	SCALE FULL SIZE
CHECKED BY	DATE DEC. 29, 1947

TITLE: VACUUM SYSTEM COUPLING FLANGE

DWG. NO. C-1051-D | FILE 6421

TOLERANCES ON MACHINING DIMENSIONS UNLESS OTHERWISE STATED:
FRACTIONAL ± 1/64". DECIMAL ± .005". ANGULAR ± 1/2°

PRINTED BY SPAULDING-MOSS CO. BOSTON, MASS. RE ORDER NO. A-220

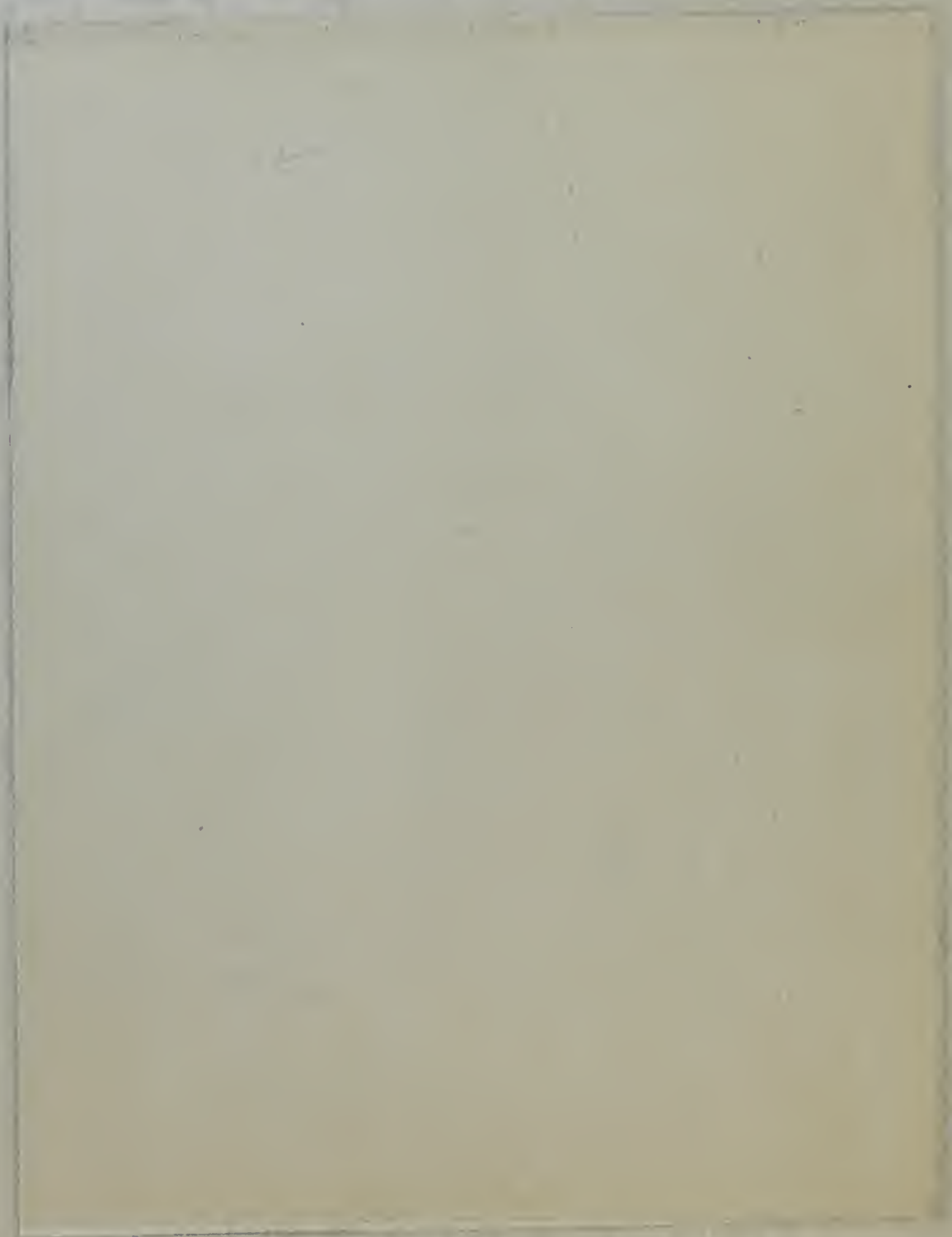

DWG. NO. C-1051-E

DWG. NO. C-1051-E

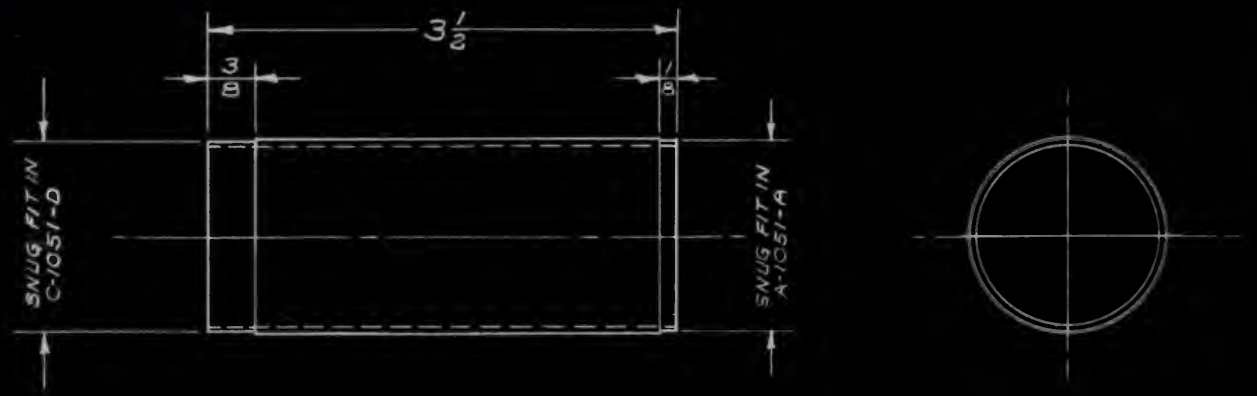

MAT'L BRASS TUBE - 1½ O.D. x 1/16 WALL

LABORATORY FOR NUCLEAR SCIENCE AND ENGINEERING
MASSACHUSETTS INSTITUTE OF TECHNOLOGY
CAMBRIDGE. MASS.

DRAWN FOR ANASTASION-SENCENBAUGH	APPROVED BY
DRAWN BY SMITH	SCALE FULL SIZE
CHECKED BY	DATE NOV. 14, 1947

TITLE: VACUUM INLET TO DETECTOR HOUSING

DWG. NO. C-1051-E | FILE 6421

TOLERANCES ON MACHINING DIMENSIONS UNLESS OTHERWISE STATED:
FRACTIONAL ± 1/64", DECIMAL ± .005", ANGULAR ± ½°

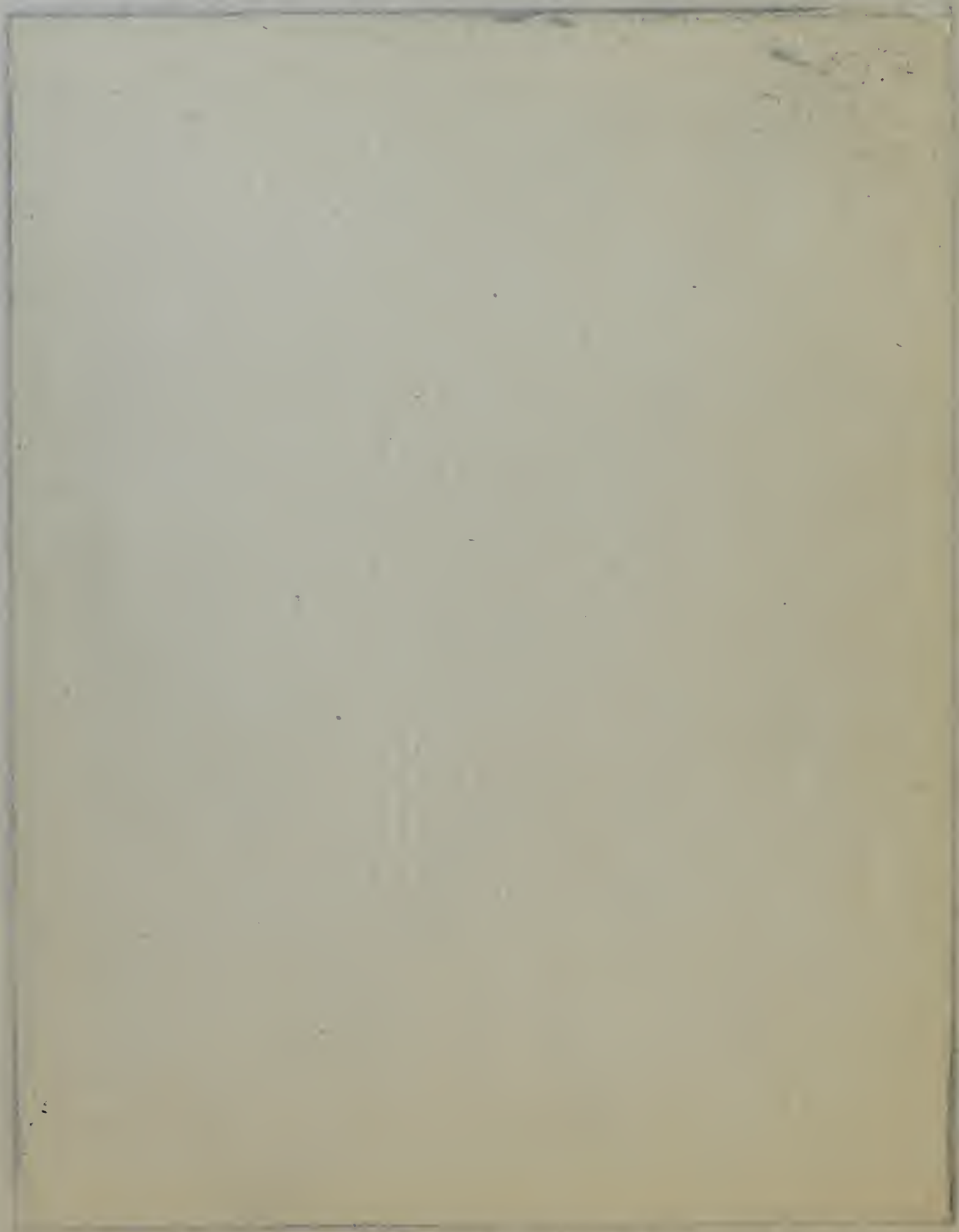

DWG. NO. C-1051-F

NOTE
CUT GROOVES AFTER ASSEMBLY WITH A-1051-A

MAT'L BRASS

LABORATORY FOR NUCLEAR SCIENCE AND ENGINEERING
MASSACHUSETTS INSTITUTE OF TECHNOLOGY
CAMBRIDGE, MASS.

DRAWN FOR ANASTASION-SENCENBAUGH	APPROVED BY
DRAWN BY SMITH	SCALE FULL SIZE
CHECKED BY	DATE NOV. 14, 1947

TITLE: FLANGE #1

DWG. NO. C-1051-F | FILE 6421

TOLERANCES ON MACHINING DIMENSIONS UNLESS OTHERWISE STATED:
FRACTIONAL ± 1/64", DECIMAL ± .005", ANGULAR ± 1/2°

PRINTED BY SPAULDING-MOSS CO. BOSTON MASS. RE ORDER NO. A-220

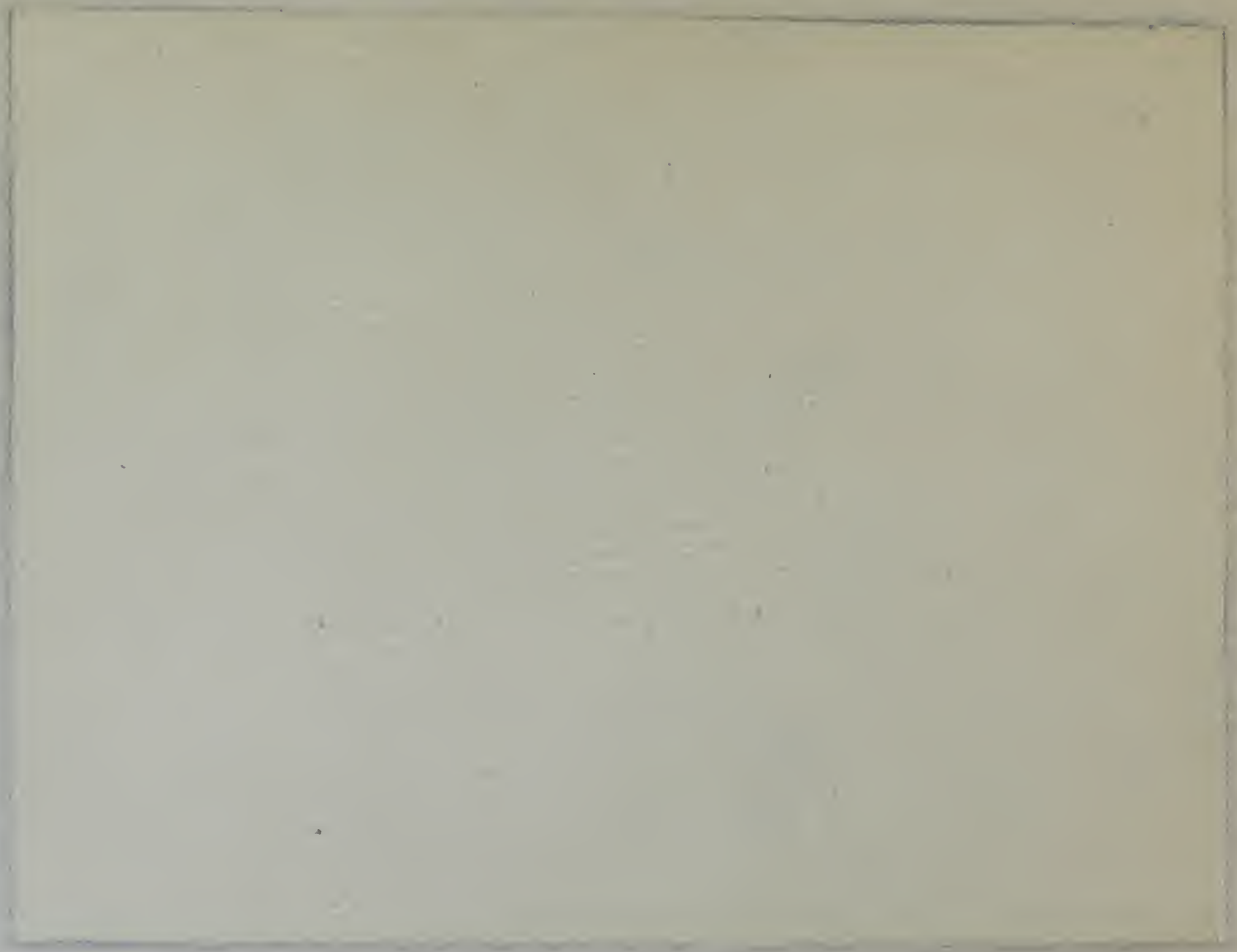

DWG. NO. B-1051-G

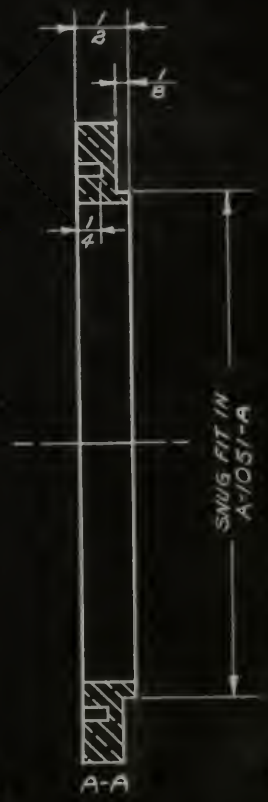

NOTE
CUT GROOVES AFTER ASSEMBLY WITH A-1051-A

MAT'L BRASS

TOLERANCES ON MACHINING DIMENSIONS UNLESS OTHERWISE STATED: FRACTIONAL ± 1/64", DECIMAL ± .005", ANGULAR ± 1/2°

LABORATORY FOR NUCLEAR SCIENCE AND ENGINEERING
MASSACHUSETTS INSTITUTE OF TECHNOLOGY
CAMBRIDGE, MASS.

DRAWN FOR ANASTASION-SENCENBAUGH	APPROVED BY
DRAWN BY SMITH	SCALE FULL SIZE
CHECKED BY AMD.	DATE NOV. 14, 1947

TITLE: FLANGE #2

DWG. NO. B-1051-G | FILE 6421

PRINTED BY SPAULDING-MOSS CO., BOSTON, MASS. RE-ORDER NO B-1051

APPENDIX 3

SCHEMATIC DRAWINGS OF THE ACCELERATING SYSTEM TOGETHER WITH CIRCUIT DETAILS

APPENDIX 3

SCHEMATIC DIAGRAMS OF THE ACCELEROMETER SYSTEM

POSITIVE SIGN CIRCUIT DETAILS

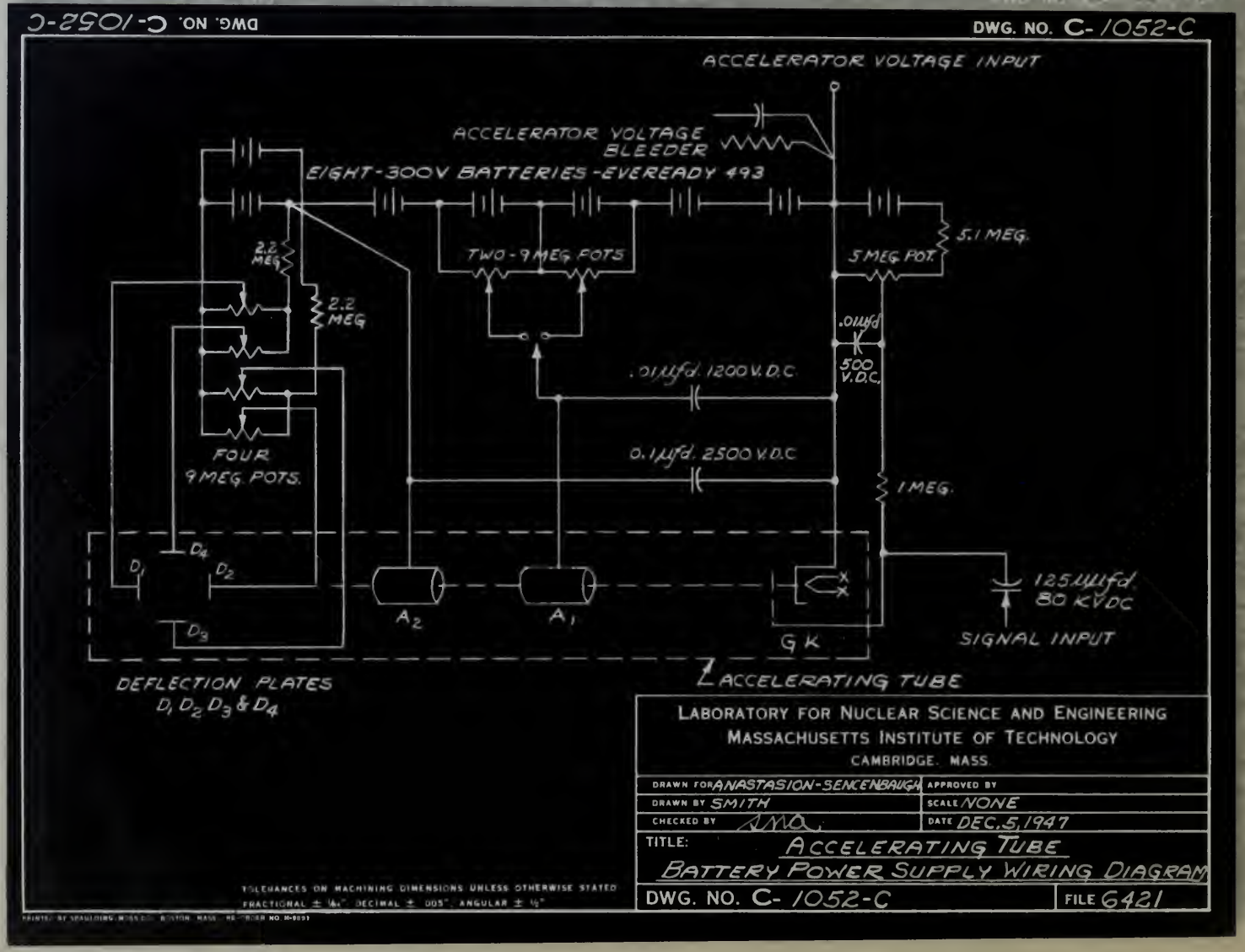
DWG. NO. C-1052-C
ACCELERATOR VOLTAGE INPUT
ACCELERATOR VOLTAGE BLEEDER
EIGHT-300V BATTERIES-EVEREADY 493
2.2 MEG
2.2 MEG
TWO-9 MEG POTS
5 MEG POT.
5.1 MEG.
.01μfd
500 V.D.C.
.01μfd. 1200 V.D.C.
0.1μfd. 2500 V.D.C
FOUR 9 MEG POTS.
1 MEG.
D4
D1
D2
D3
A2
A1
G
K
125 μμfd 80 KV DC
SIGNAL INPUT
DEFLECTION PLATES D1 D2 D3 & D4
ACCELERATING TUBE
LABORATORY FOR NUCLEAR SCIENCE AND ENGINEERING
MASSACHUSETTS INSTITUTE OF TECHNOLOGY
CAMBRIDGE. MASS.
DRAWN FOR ANASTASION-SENCENBAUGH
APPROVED BY
DRAWN BY SMITH
SCALE NONE
CHECKED BY
DATE DEC. 5, 1947
TITLE: ACCELERATING TUBE
BATTERY POWER SUPPLY WIRING DIAGRAM
DWG. NO. C-1052-C
FILE 6421
TOLERANCES ON MACHINING DIMENSIONS UNLESS OTHERWISE STATED
FRACTIONAL ± 1/64". DECIMAL ± .005". ANGULAR ± 1/2°

DWG. NO. C-1052-D

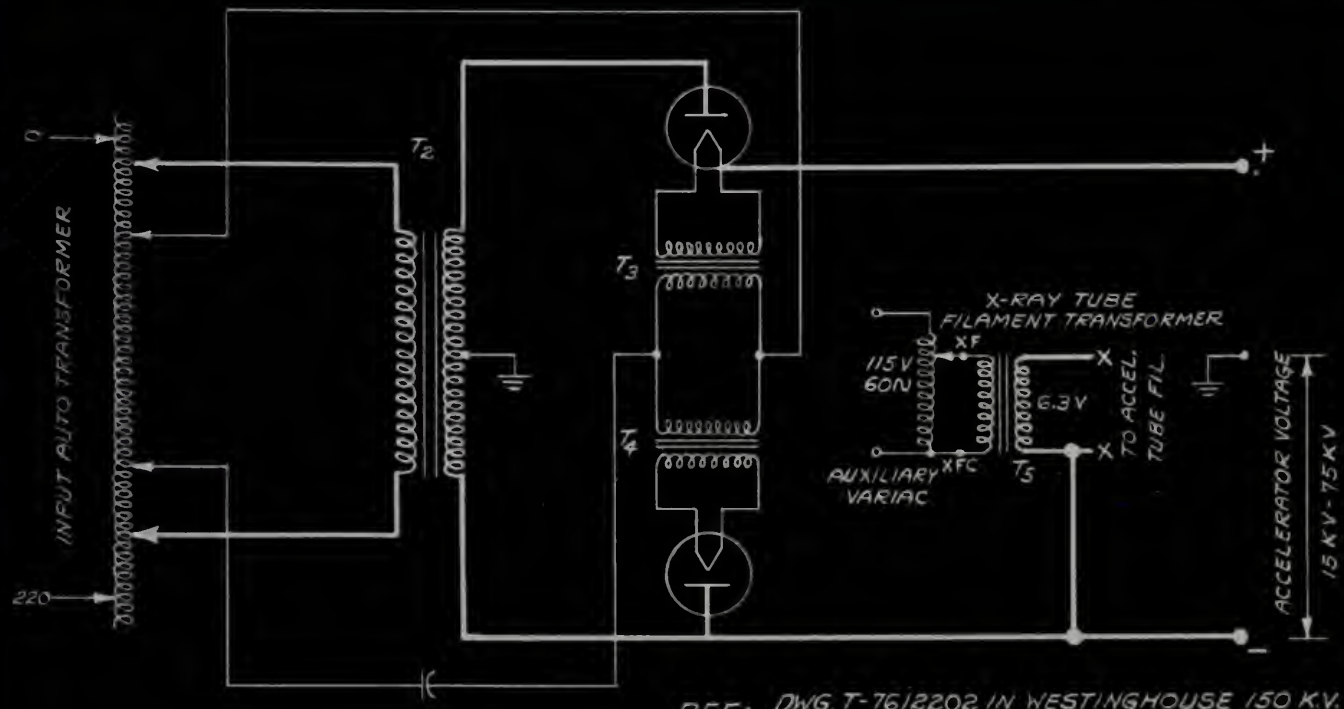

REF: DWG. T-7612202 IN WESTINGHOUSE 150 K.V. X-RAY UNIT LABORATORY INSTRUCTIONS

LABORATORY FOR NUCLEAR SCIENCE AND ENGINEERING
MASSACHUSETTS INSTITUTE OF TECHNOLOGY
CAMBRIDGE, MASS.

DRAWN FOR ANASTASION-SENCENBAUGH	APPROVED BY
DRAWN BY SMITH	SCALE NONE
CHECKED BY AMQ	DATE DEC. 8, 1947

TITLE: * SCHEMATIC WIRING DIAGRAM OF WESTINGHOUSE 150 K.V. X-RAY EQUIPMENT

DWG. NO. C-1052-D | FILE 6421

* SIMPLIFIED & MODIFIED TO PROVIDE ACCELERATING VOLTAGE & ISOLATED FILAMENT VOLTAGE FOR THE ACCELERATING TUBE

TOLERANCES ON MACHINING DIMENSIONS UNLESS OTHERWISE STATED
FRACTIONAL ± 1/64" DECIMAL ± .005" ANGULAR ± 1/2°

PRINTED BY SPAULDING-MOSS CO. BOSTON, MASS. RE ORDER NO. M-8093

DWG. NO. C-1052-D

DWG. NO. C-1052-E

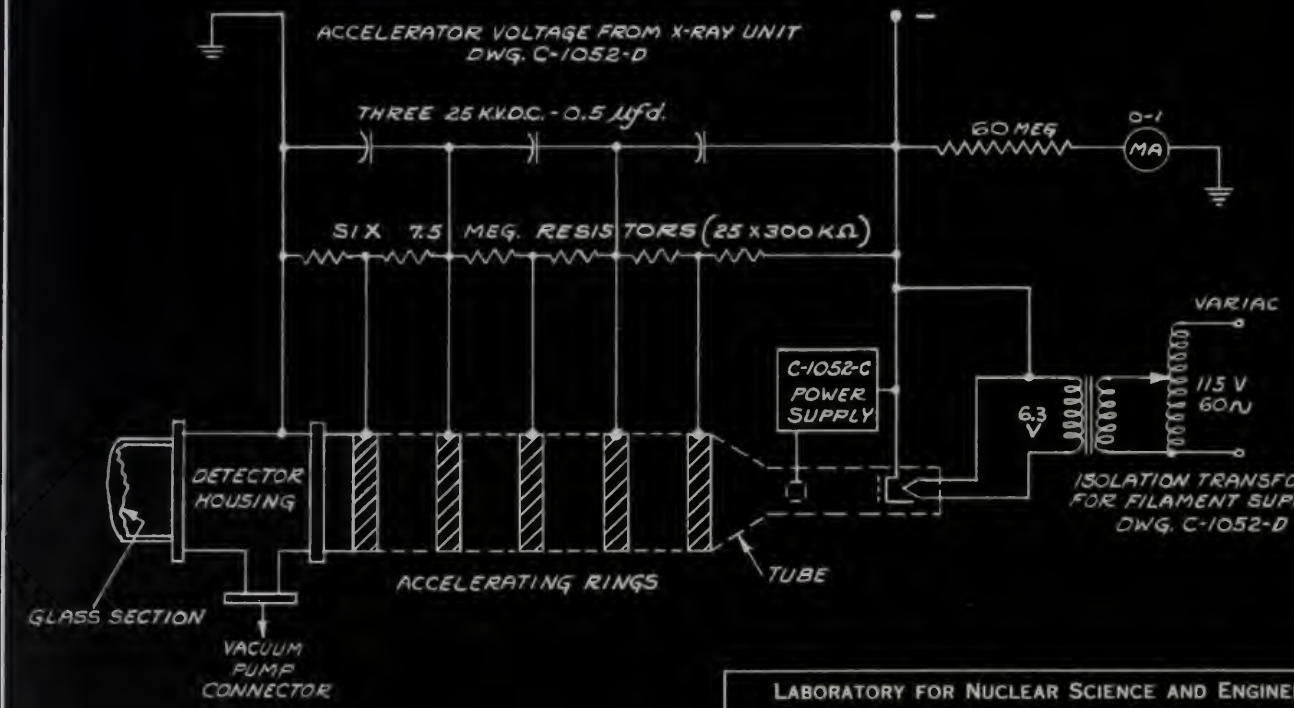

LABORATORY FOR NUCLEAR SCIENCE AND ENGINEERING
MASSACHUSETTS INSTITUTE OF TECHNOLOGY
CAMBRIDGE. MASS.

DRAWN FOR ANASTASION-SENCENBAUGH	APPROVED BY
DRAWN BY SMITH	SCALE NONE
CHECKED BY AMD.	DATE DEC. 5, 1947

TITLE: ACCELERATING VOLTAGE DETAIL

DWG. NO. C-1052-E | FILE 6421

TOLERANCES ON MACHINING DIMENSIONS UNLESS OTHERWISE STATED:
FRACTIONAL ± 1/64". DECIMAL ± .005". ANGULAR ± 1/2°

PRINTED BY SPAULDING-MOSS CO. BOSTON, MASS. RE-ORDER NO. M-9091

DWG. NO. C-1052-E

DWG. NO. C-1052-F

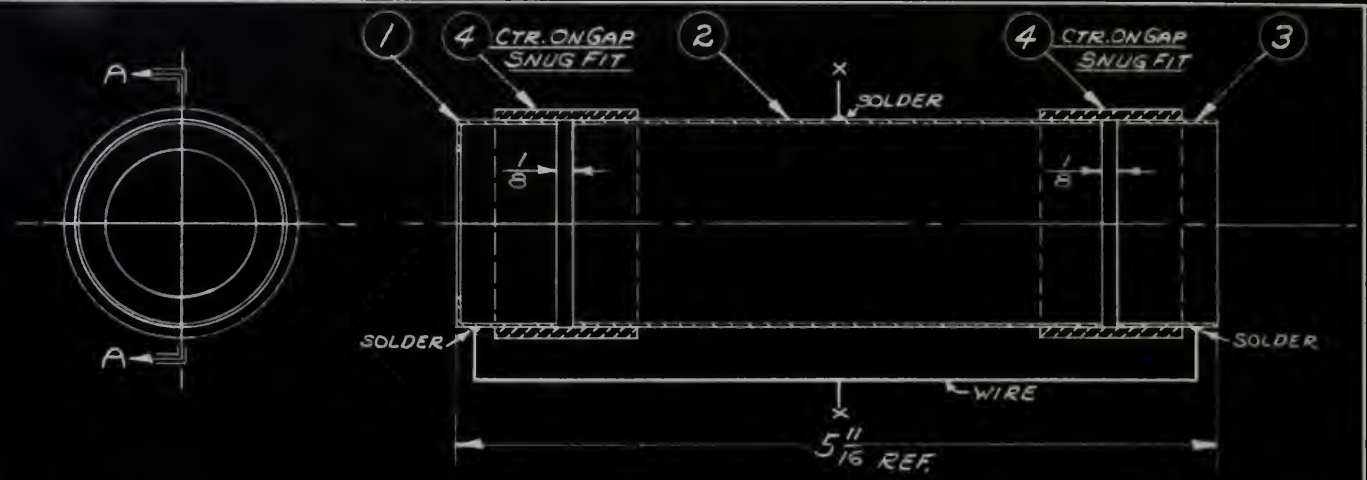

X = CONNECTION TO HOUSING TERMINAL

DETAIL "A"
MAT'L - BRASS

REF. DWG. C-1052-G

PT NO.	NO. REQ.	PART
4	2	1 25/32 O.D. x 3/32 WALL - PYREX GLASS - 1 1/16" LG
3	1	1 9/32 O.D. x 1/64 WALL - BRASS TUBING - 3/4" LG
2	1	1 9/32 O.D. x 1/64 WALL - BRASS TUBING - 3.937" LG
1	1	DETAIL "A"

LABORATORY FOR NUCLEAR SCIENCE AND ENGINEERING
MASSACHUSETTS INSTITUTE OF TECHNOLOGY
CAMBRIDGE. MASS.

DRAWN FOR ANASTATION-SENCENBAUGH	APPROVED BY
DRAWN BY SMITH	SCALE FULL SIZE
CHECKED BY	DATE DEC. 18, 1947

TITLE: CYLINDRICAL DETECTOR ASSEMBLY

DWG. NO. C-1052-F FILE 6421

TOLERANCES ON MACHINING DIMENSIONS UNLESS OTHERWISE STATED:
FRACTIONAL ± 1/64" DECIMAL ± .005" ANGULAR ± 1/2°

PRINTED BY SARGENT-WILES CO., BOSTON, MASS. BE-GRUES NO. M-9891

DWG. NO. C-1052-F

DWG. NO. C-1052-G

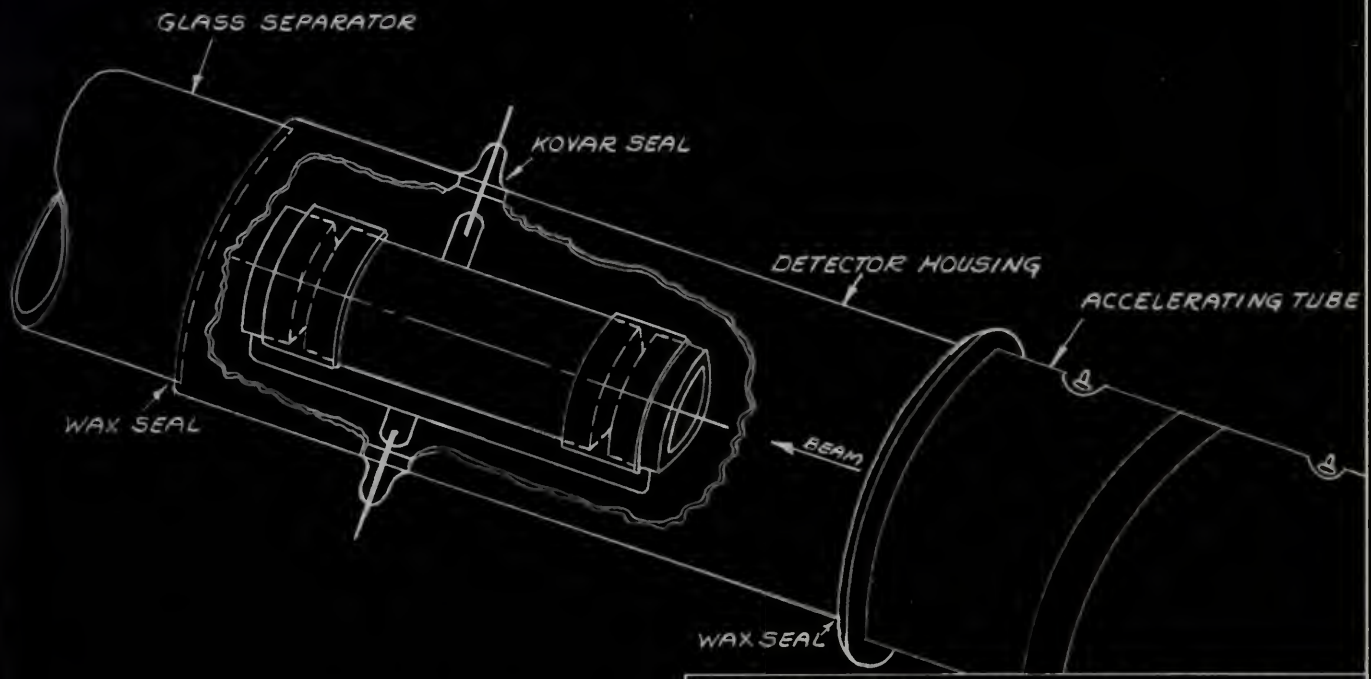

REF. DWGS. C-1052-E & C-1052-F

TOLERANCES ON MACHINING DIMENSIONS UNLESS OTHERWISE STATED
FRACTIONAL ± 1/64" DECIMAL ± .005", ANGULAR ± 1/2°

LABORATORY FOR NUCLEAR SCIENCE AND ENGINEERING
MASSACHUSETTS INSTITUTE OF TECHNOLOGY
CAMBRIDGE, MASS.

DRAWN FOR ANASTASION-SENCENBAUGH	APPROVED BY
DRAWN BY SMITH	SCALE NONE
CHECKED BY AMO.	DATE DEC. 18, 1947

TITLE:
ISOMETRIC SKETCH OF DETECTOR IN HOUSING

DWG. NO. C-1052-G | FILE 6421

DWG. NO. C-1052-G

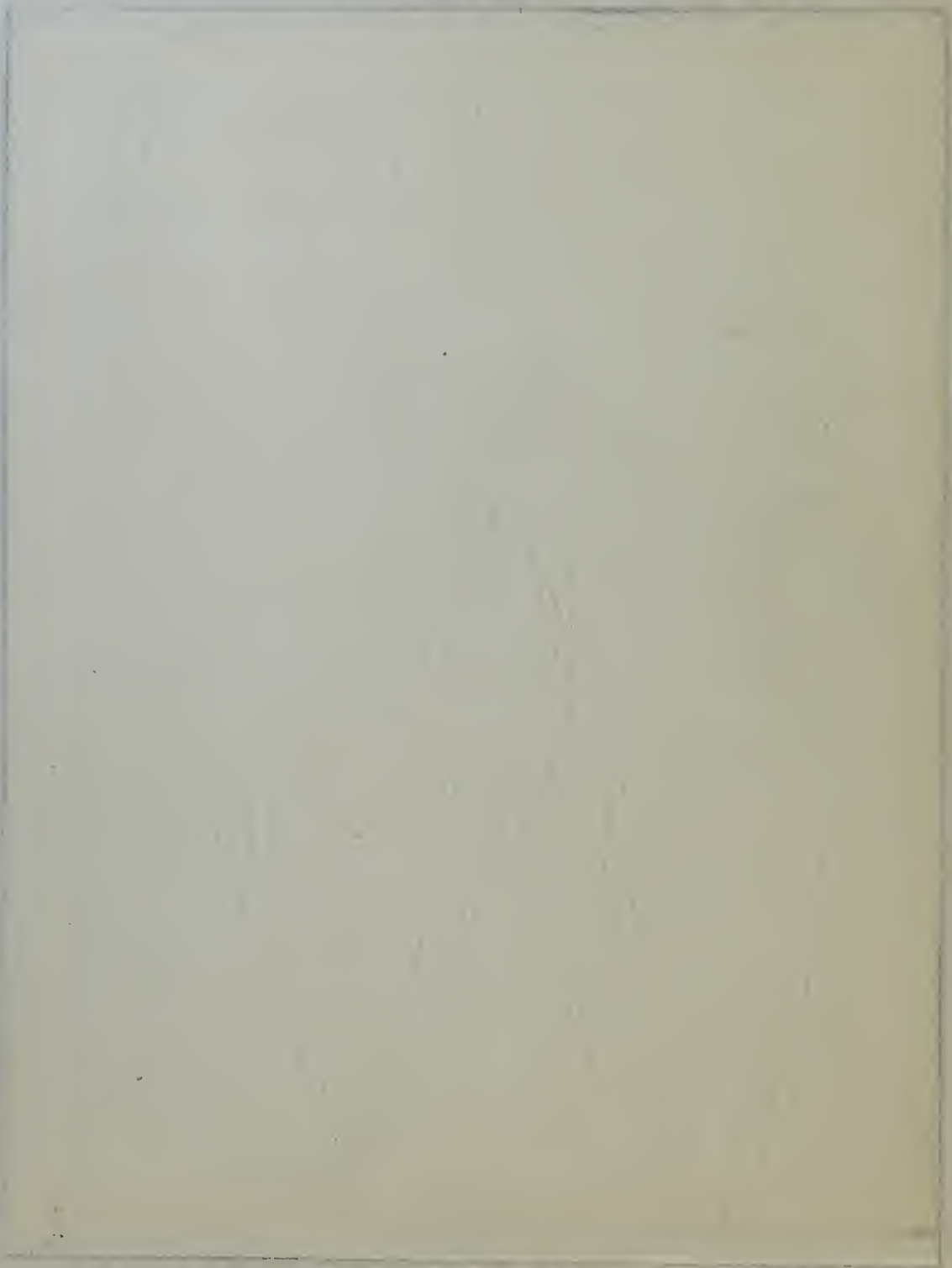

DWG. NO. C-1052-H

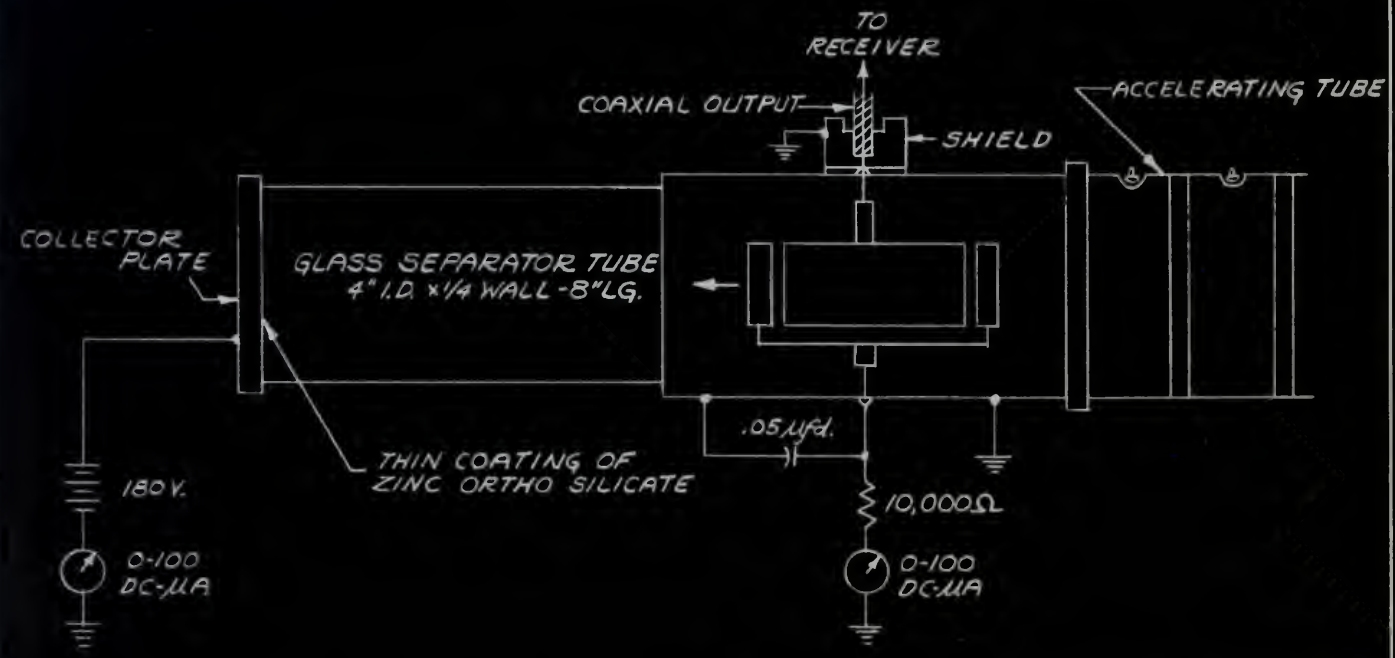

REF. DWGS - C-1052-E, F & G

LABORATORY FOR NUCLEAR SCIENCE AND ENGINEERING
MASSACHUSETTS INSTITUTE OF TECHNOLOGY
CAMBRIDGE. MASS.

DRAWN FOR ANASTASION-SENCENBAUGH	APPROVED BY
DRAWN BY SMITH	SCALE NONE
CHECKED BY [illegible]	DATE JAN. 15, 1948

TITLE: COLLECTOR END CIRCUIT DETAILS

DWG. NO. C-1052-H | FILE 6421

TOLERANCES ON MACHINING DIMENSIONS UNLESS OTHERWISE STATED:
FRACTIONAL ± 1/64", DECIMAL ± .005", ANGULAR ± 1/2°

PRINTED BY STANDARD MODELLO BOSTON MASS. RE ORDER NO A-220

DWG. NO. C-1052-H

DWG. NO. C-1052-I

DWG. NO. C-1052-I

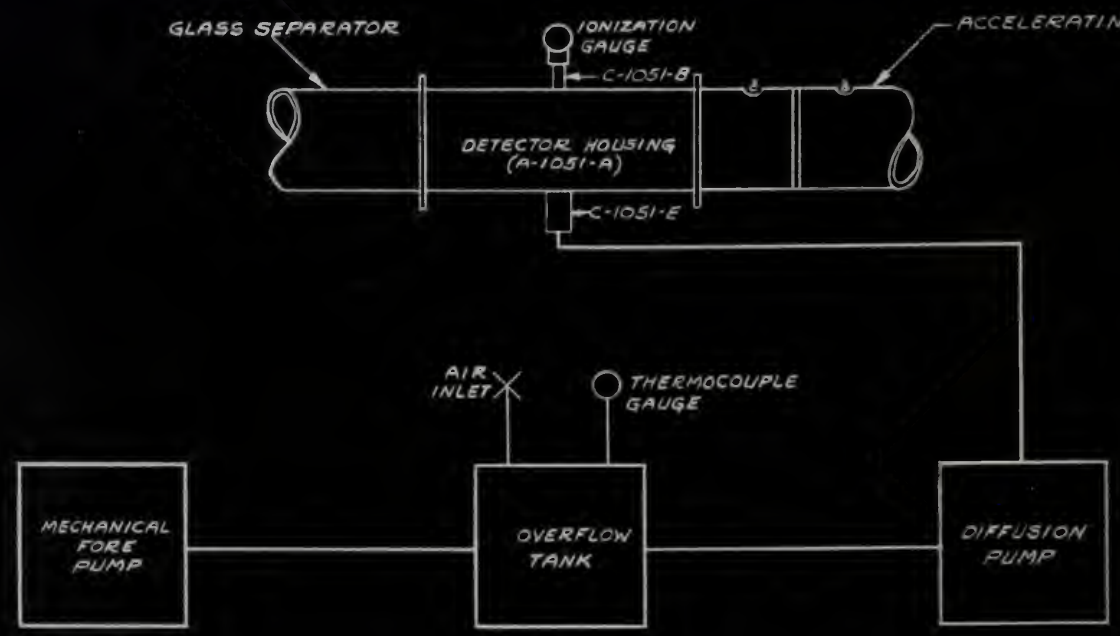

REF. DWG. C-1052-E

LABORATORY FOR NUCLEAR SCIENCE AND ENGINEERING
MASSACHUSETTS INSTITUTE OF TECHNOLOGY
CAMBRIDGE. MASS.

DRAWN FOR ANASTASION-SENCENBAUGH	APPROVED BY
DRAWN BY SMITH	SCALE NONE
CHECKED BY A.M.Q.	DATE DEC. 30, 1947

TITLE: VACUUM SYSTEM BLOCK DIAGRAM

DWG. NO. C-1052-I | FILE 6421

TOLERANCES ON MACHINING DIMENSIONS UNLESS OTHERWISE STATED:
FRACTIONAL ± 1/64", DECIMAL ± .005", ANGULAR ± 1/2°

PRINTED BY STANDARD BLUE CO. BOSTON MASS. NO. ORDER NO A-220

APPENDIX 4

PHOTOGRAPHS OF THE SYSTEM

APPENDIX A

PHOTOGRAPHS OF THE SYSTEM

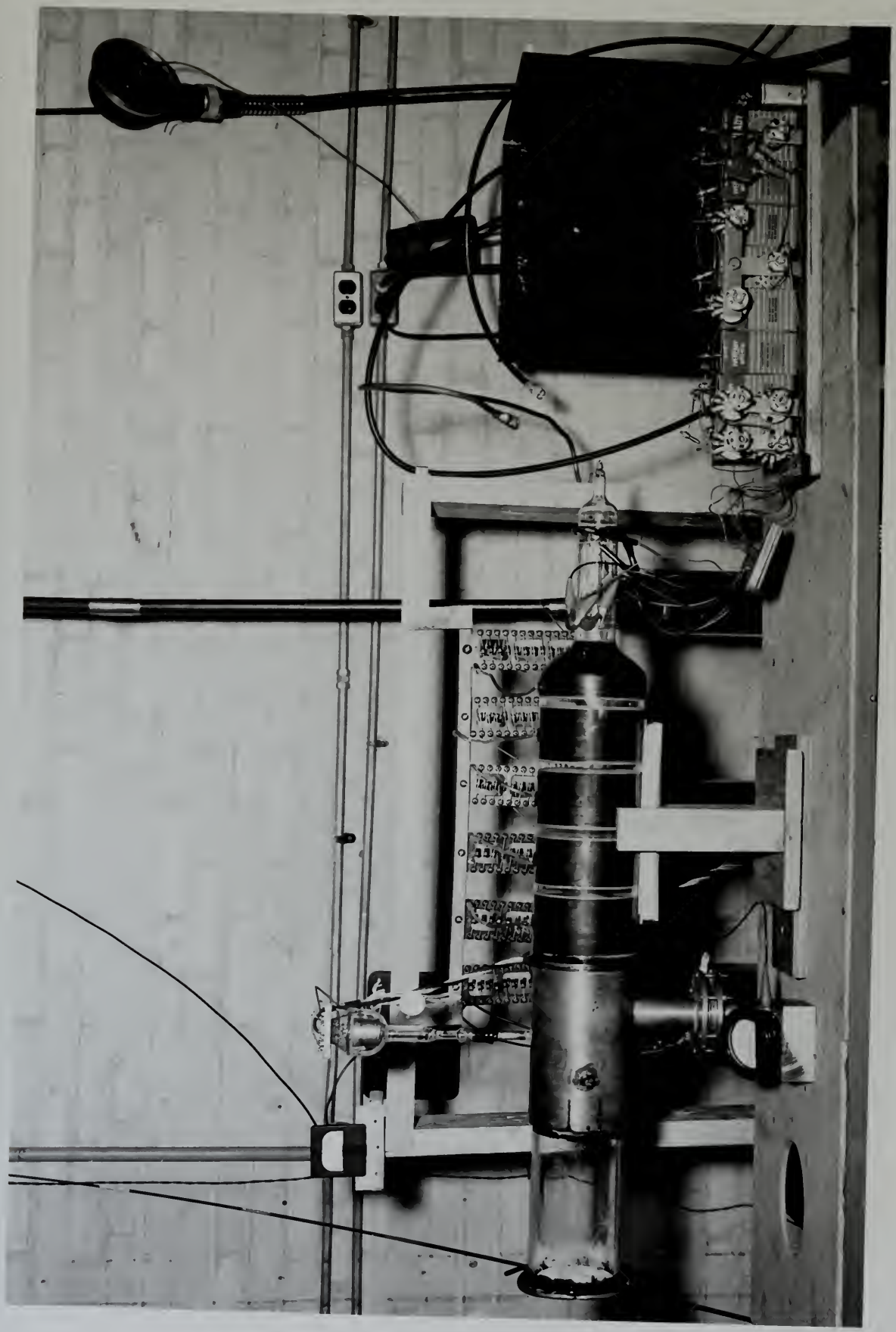

DANGER

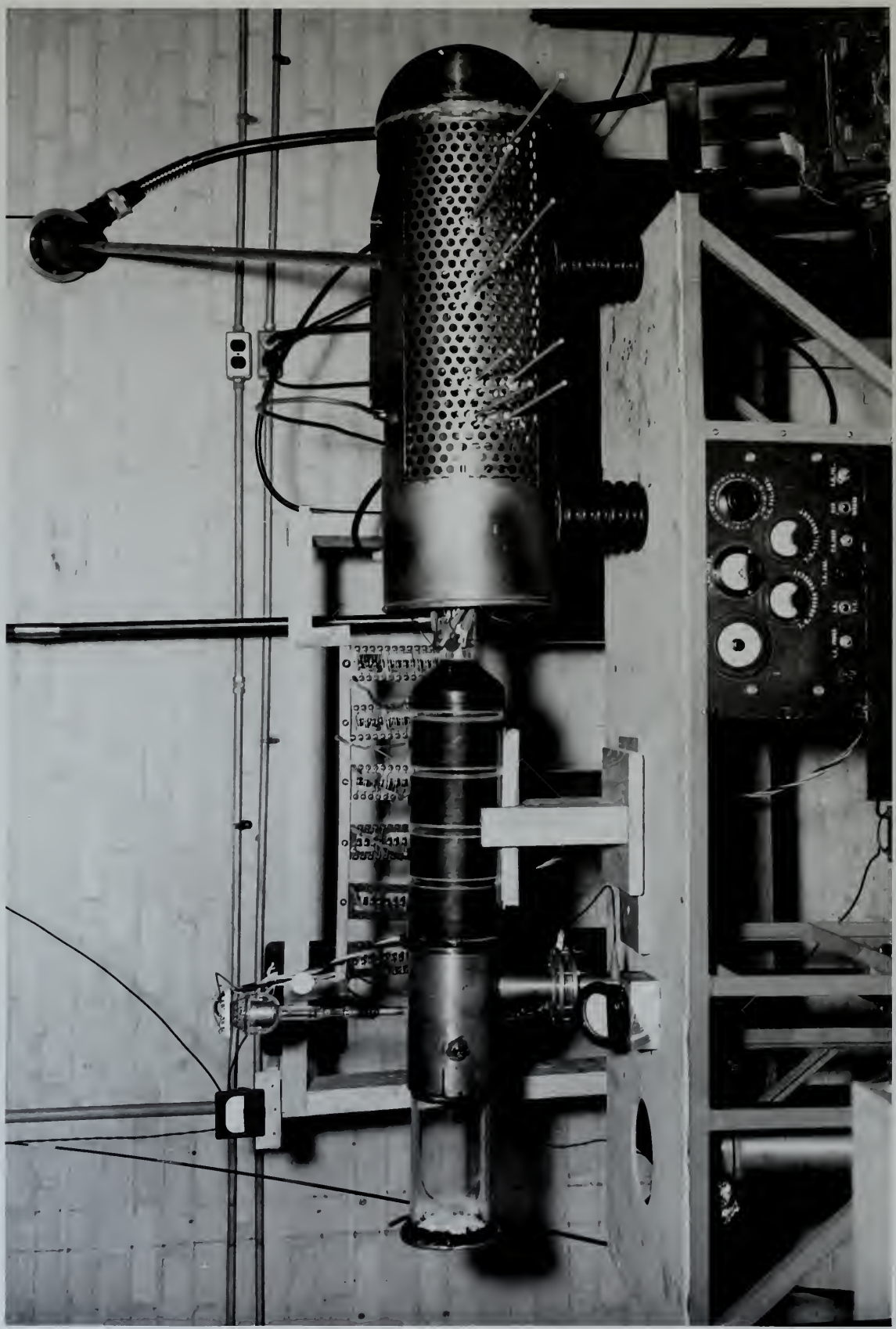

KEEP
AWAY
DANGER
HIGH VOLTAGE

APPENDIX 5

ACTIVATION SCHEDULE

APPENDIX 5

ACTIVATION SCHEDULE

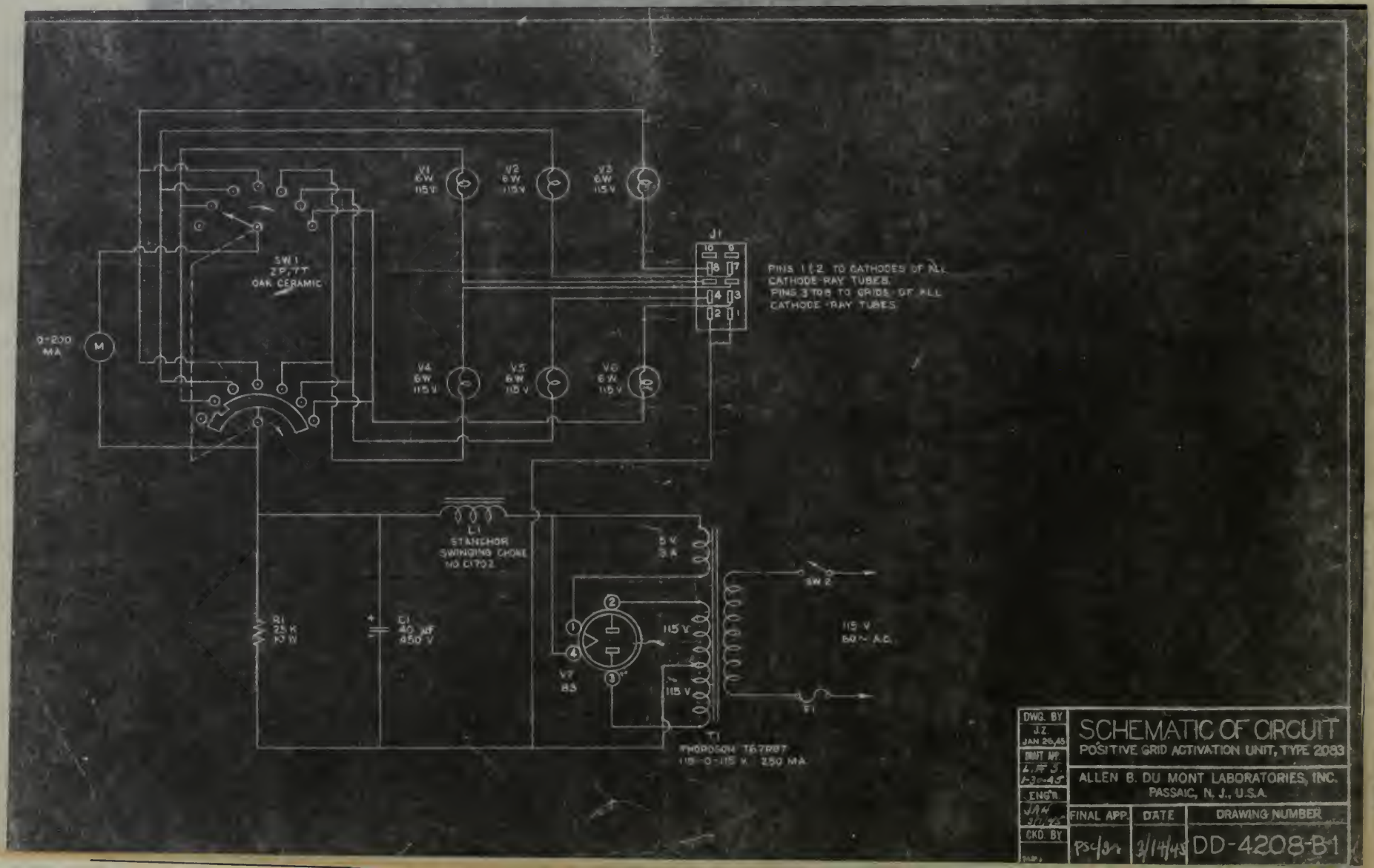

DWG. BY J.Z. JAN 28,45	SCHEMATIC OF CIRCUIT POSITIVE GRID ACTIVATION UNIT, TYPE 2083		
DRAFT MP. L.F.S. 1-30-45	ALLEN B. DU MONT LABORATORIES, INC. PASSAIC, N. J., U.S.A.		
ENG'R. JAH 2/1/45	FINAL APP.	DATE	DRAWING NUMBER
CK'D. BY	PSC/JR	3/14/45	DD-4208-B1

DWG. NO. C-1052-A

DWG. NO. C-1052-A

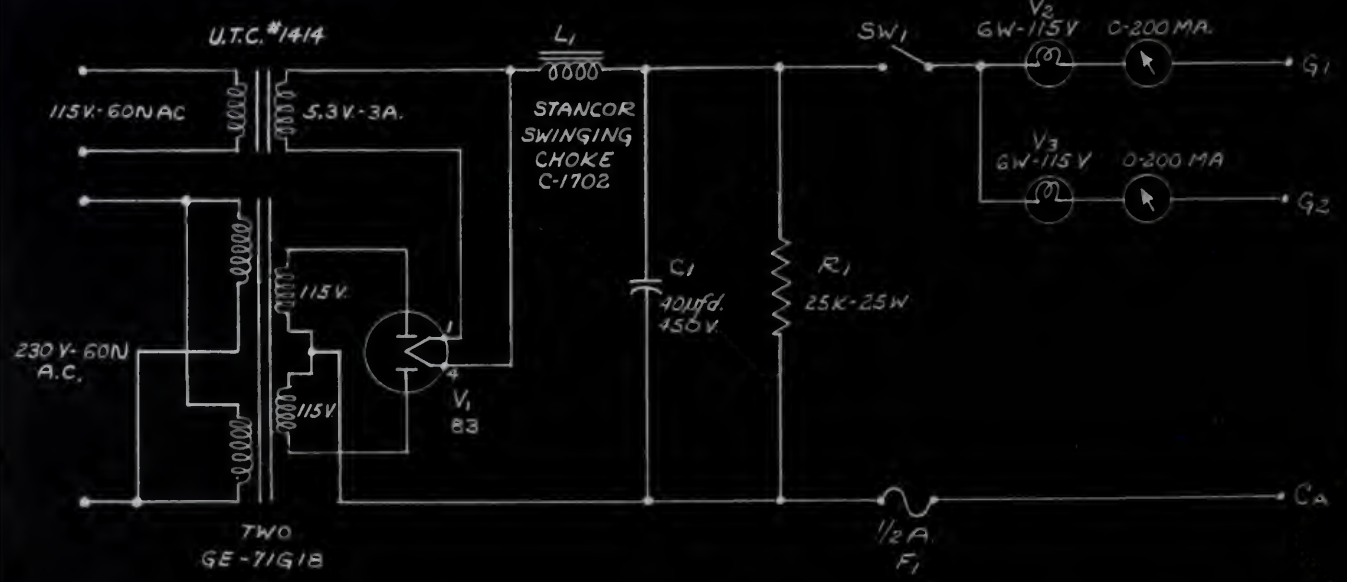

ACCELERATING TUBE CATHODE ACTIVATION UNIT #1

REF.
A.B. DUMONT DWG. # DD-4208-B-1

LABORATORY FOR NUCLEAR SCIENCE AND ENGINEERING
MASSACHUSETTS INSTITUTE OF TECHNOLOGY
CAMBRIDGE. MASS.

DRAWN FOR ANASTASION-SENCENBAUGH	APPROVED BY
DRAWN BY SMITH	SCALE NONE
CHECKED BY AMO.	DATE NOV. 17, 1947

TITLE: MODIFIED POSITIVE GRID ACTIVATION UNIT WIRING DIAGRAM

DWG. NO. C-1052-A | FILE 6421

TOLERANCES ON MACHINING DIMENSIONS UNLESS OTHERWISE STATED:
FRACTIONAL ± 1/64", DECIMAL ± .005", ANGULAR ± 1/2°

PRINTED BY ARTHUR WEISS CO., BOSTON, MASS. BY ORDER NO. A-220

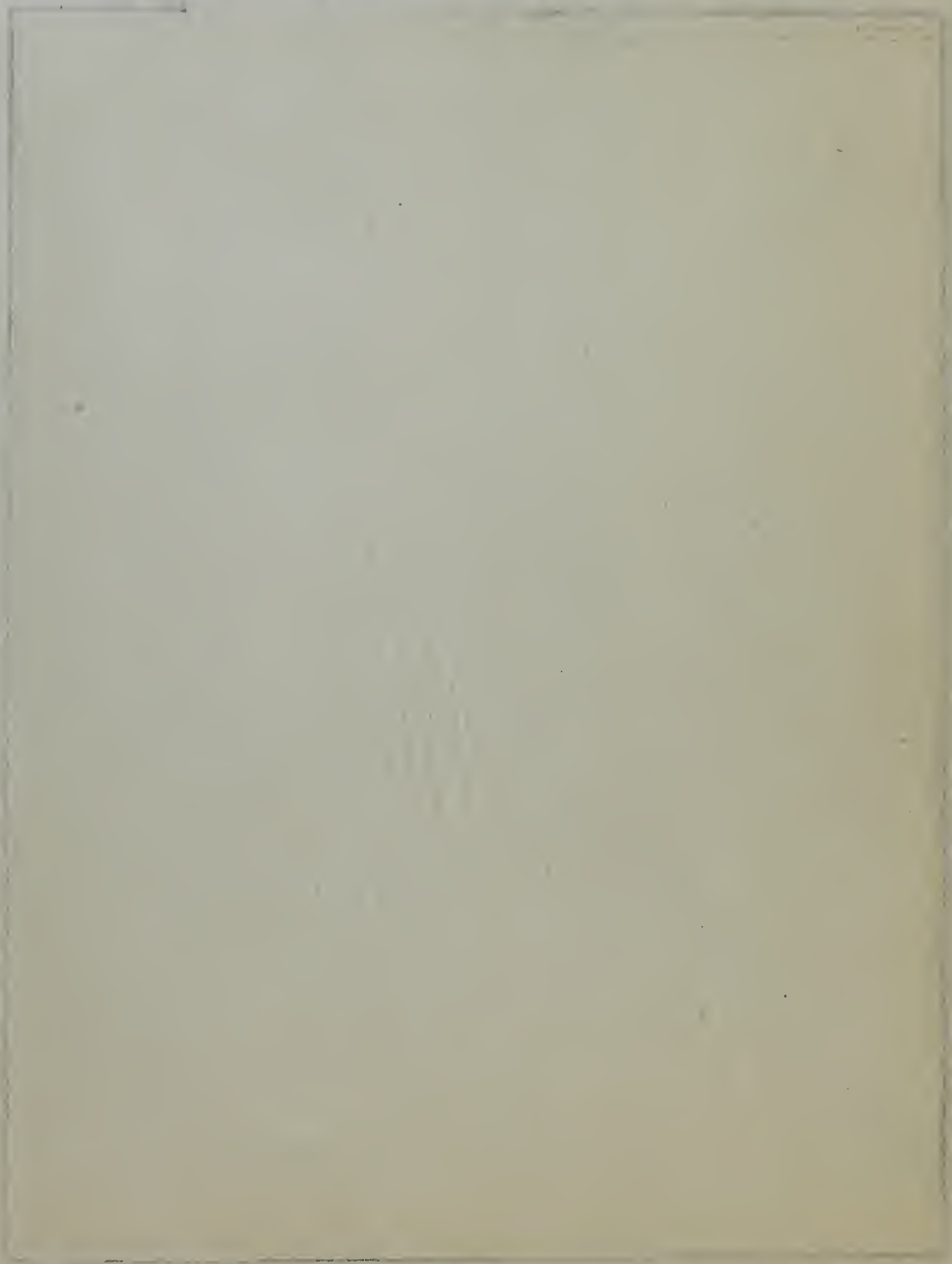

DWG. NO. C-1052-B

DWG. NO. C-1052-B

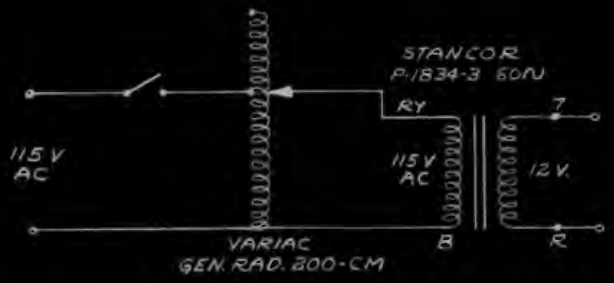

ACCELERATING TUBE CATHODE ACTIVATION - UNIT 2

LABORATORY FOR NUCLEAR SCIENCE AND ENGINEERING
MASSACHUSETTS INSTITUTE OF TECHNOLOGY
CAMBRIDGE, MASS.

DRAWN FOR ANASTASION-SENCENBAUGH	APPROVED BY
DRAWN BY SMITH	SCALE NONE
CHECKED BY AMO	DATE NOV. 15, 1947

TITLE: VARIABLE HEATER VOLTAGE UNIT WIRING DIAGRAM

DWG. NO. C-1052-B | FILE 6421

TOLERANCES ON MACHINING DIMENSIONS UNLESS OTHERWISE STATED:
FRACTIONAL ± 1/64", DECIMAL ± .005", ANGULAR ± 1/2°

PRINTED BY SPAULDING MOSS CO. BOSTON, MASS. RE ORDER NO. A-220

Allen B. DuMont Laboratories, Inc.
Passaic, N. J., U. S. A.

Cathode Breakdown for Synchrotron Tube

The following cathode processing schedule is to be applied 2 or 3 minutes after the parts have cooled off after bombarding. Emission readings are to be taken for each tube on types where positive voltage is applied and recorded opposite that tube at the end of the schedule.

a. Heater is operated at 5.5 volts for 5 minutes.

b. Heater is operated at 7.5 volts for 5 minutes.

c. Heater is operated at 9.0 volts for 5 minutes.

d. Heater is operated at 12.5 volts for 20 seconds.

e. Heater is operated at 9.0 volts and the grid heated to 1000°C. and held at this temperature for 15 seconds.

f. Heater is operated at 12.5 volts for 20 seconds.

g. Heater is operated at 9.0 volts for 5 minutes.

h. Heater is operated at 9.0 volts for 7 minutes with grid maintained positive by circuit of Drawing No. DD-4208-B.

i. Lower heater to 7.5 volts for 3 minutes with grid voltage still applied.

j. Cut grid voltage only and flash getter (one only).

k. Apply 9.0 volts to heater for 1 minute.

l. With heater at 9.0 volts apply grid voltage for 3 minutes.

m. Lower heater to 7.5 volts with grid voltage applied for 3 minutes.

n. Remove connections. Check ionization gauge reading (3×10^{-6} or better).

o. Tip off.

Allen B. Du Mont Laboratories, Inc.
Passaic, N. J., U. S. A.

Cathode Treatment for Evacuation Line

The following cathode processing schedule is to be applied 2 or 3 minutes after the parts have cooled off after bombarding. Emission readings are to be taken for each tube on types where position voltage is applied and recorded opposite that tube at the end of the schedule.

a. Heater in operated at 7.5 volts for 5 minutes.

b. Heater is operated at 7.5 volts for 5 minutes.

c. Heater is operated at 9.0 volts for 5 minutes.

d. Heater is operated at 12.5 volts for 20 seconds.

e. Heater is operated at 9.0 volts and the grid heated to 1000°C. and held at this temperature for 15 seconds.

f. Heater is operated at 12.5 volts for 20 seconds.

g. Heater is operated at 9.0 volts for 5 minutes.

h. Heater is operated at 9.0 volts for 7 minutes with grid maintained positive by circuit of Drawing No. DD-4239-B.

i. Lower heater to 7.5 volts for 3 minutes with grid voltage still applied.

j. Cut grid voltage only and flash heater (one only).

k. Apply 9.0 volts to heater for 1 minute.

l. With heater at 9.0 volts apply grid voltage for 3 minutes.

m. Lower heater to 7.5 volts with grid voltage applied for 3 minutes.

n. Remove connections. Check ionization gauge reading (3×10^{-6} or better).

o. Tip off.

Cathode Activation Schedule as used in this thesis.

a. Heater is operated at 5.5 volts for 5 minutes.

b. Heater is operated at 7.5 volts for 5 minutes.

c. Heater is operated at 9.0 volts for 5 minutes.

d. Heater is operated at 12.5 volts for 20 seconds.

e. Heater is operated at 9.0 volts for 15 seconds.

f. Heater is operated at 12.5 volts for 20 seconds.

g. Heater is operated at 9.0 volts for 5 minutes.

h. Heater is operated at 10.0 volts for 7 minutes with grid maintained positive by circuit of Drawing C-1052-A.

i. Lower heater to 7.5 volts for 3 minutes with grid voltage still applied.

j. Cut grid voltage only.

k. Apply 9.0 volts to heater for 1 minute.

l. With heater at 10.0 volts apply grid voltage for 3 minutes.

m. Lower heater to 7.5 volts with grid voltage applied for 3 minutes.

n. Remove connections. Check ionization gauge reading.

Repeat (f) to (m) until emission reading on positive-grid activation unit is satisfactory.

Cathode Activation Schedule
as used in this study.

a. Heater is operated at 5.5 volts for 5 minutes.

b. Heater is operated at 7.5 volts for 5 minutes.

c. Heater is operated at 9.0 volts for 5 minutes.

d. Heater is operated at 12.5 volts for 20 seconds.

e. Heater is operated at 9.0 volts for 15 seconds.

f. Heater is operated at 12.5 volts for 20 seconds.

g. Heater is operated at 9.0 volts for 5 minutes.

h. Heater is operated at 10.0 volts for 7 minutes with grid emission positive by current of Steering E-10?-A.

i. Lower heater to 7.5 volts for 3 minutes with grid voltage still applied.

j. Cut grid voltage only.

k. Apply 9.0 volts to heater for 1 minute.

l. With heater at 10.0 volts apply grid voltage for 3 minutes.

m. Lower heater to 7.5 volts with grid voltage applied for 3 minutes.

n. Remove connections. Check ionization gauge reading.

Repeat (l) to (m) until emission reading on positive grid exceeds limit as specified.

Emission Readings During Activation

Item	Emission Reading in Milliamperes	
	1st run	2nd run
h	12	42
i	2	15
l	20	42
m	6	15

Relative Reading Ratio Analysis

Item	Relative Reading in Millisecs.	
	Jar One	Jar Two
h	12	42
i	2	15
j	20	42
m	6	19

APPENDIX 6

CHARACTERISTICS OF EVEREADY BATTERY 493

APPENDIX B

CHARACTERISTICS OF STANDARD BATTERY 493

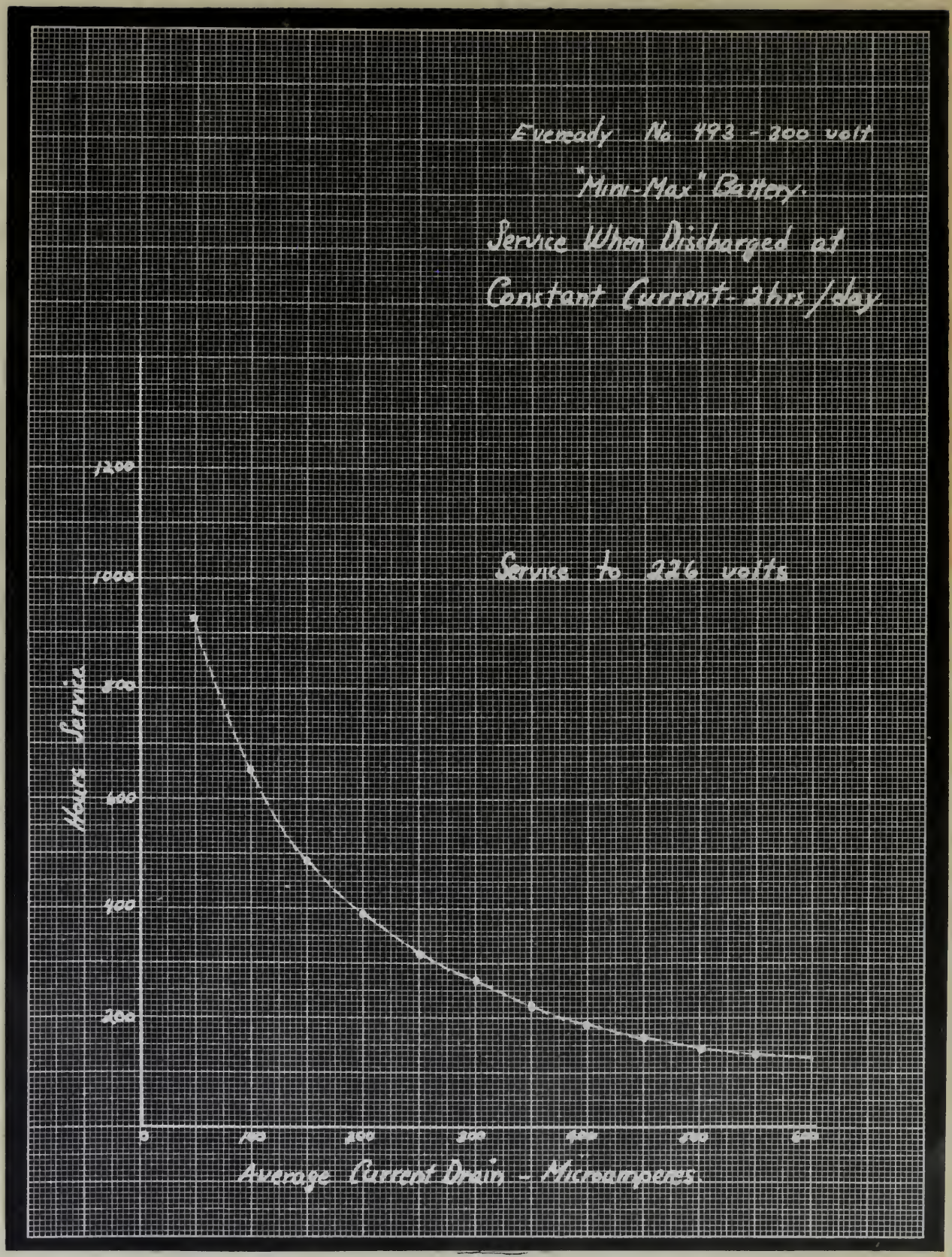
Eveready No. 493 - 300 volt
'Mini-Max' Battery.
Service When Discharged at
Constant Current - 2 hrs/day
Service to 226 volts
Hours Service
1200
1000
800
600
400
200
0
100
200
300
400
500
600
Average Current Drain - Microamperes

DATE DUE

AUG 31 BINDERY

Thesis 11254
A44 Anastasion
AUTHOR Measurement of current in pulsed electron beams
TITLE

DATE LOANED	BORROWER'S NAME	DATE RETURNED

Thesis 11254
A44 Anastasion
Measurement of current in pulsed electron beams.

Library
U. S. Naval Postgraduate School
Monterey, California

ARTISAN GOLD LETTERING AND SMITH BINDERY OAKLAND, CALIF

thesA44
Measurement of current in pulsed electro
3 2768 001 91464 1
DUDLEY KNOX LIBRARY